

# Magnetic Nanocomposite Hydrogels for Tissue Engineering: Design Concepts and Remote Actuation Strategies to Control Cell Fate

Alberto Pardo, Manuel Gómez-Florit, Silvia Barbosa, Pablo Taboada, Rui M. A. Domingues,\* and Manuela E. Gomes\*

Cite This: *ACS Nano* 2021, 15, 175–209

Read Online

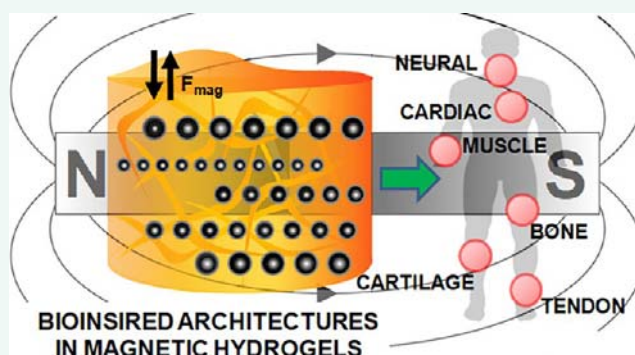
ACCESS |

Metrics & More

Article Recommendations

**ABSTRACT:** Most tissues of the human body are characterized by highly anisotropic physical properties and biological organization. Hydrogels have been proposed as scaffolding materials to construct artificial tissues due to their water-rich composition, biocompatibility, and tunable properties. However, unmodified hydrogels are typically composed of randomly oriented polymer networks, resulting in homogeneous structures with isotropic properties different from those observed in biological systems. Magnetic materials have been proposed as potential agents to provide hydrogels with the anisotropy required for their use on tissue engineering. Moreover, the intrinsic properties of magnetic nanoparticles enable their use as magnetomechanic remote actuators to control the behavior of the cells encapsulated within the hydrogels under the application of external magnetic fields. In this review, we combine a detailed summary of the main strategies to prepare magnetic nanoparticles showing controlled properties with an analysis of the different approaches available to their incorporation into hydrogels. The application of magnetically responsive nanocomposite hydrogels in the engineering of different tissues is also reviewed.

**KEYWORDS:** magnetic nanoparticles, nanocomposite hydrogels, magnetically responsive hydrogels, magnetic field configuration, anisotropy, remote actuation, magnetomechanical stimulation, regenerative medicine, tissue engineering



## INTRODUCTION

The final aim of tissue engineering (TE) is to fully restore damaged tissues to their preinjured state, while reducing the healing time and the medical complications. For this purpose, the field has relied on the development of artificial composites (scaffolds) capable of providing structural support during the initial stages of tissue formation. These engineered scaffolds should present the following features: (i) mimic the complex structure of the native tissues from nano- to macroscale; (ii) meet the mechanical, electrical, and structural properties of the tissues, which in almost all cases are largely heterogeneous; (iii) provide the required biophysical and biochemical cues to induce the desired growth, proliferation, and differentiation of encapsulated cells; (iv) ensure technical scalability of scaffolding design on-demand.<sup>1–3</sup>

Among all of the materials used for the development of TE scaffolds, polymer hydrogels are among the most promising candidates due to their water-rich composition similar to those of biological tissues, allowing the encapsulation of cells and other biological entities, and the possibility to be injected in a liquid state in the site of action and form a gel *in situ*.<sup>4–8</sup> Moreover, by changing the natural or synthetic polymer used and/or the type of cross-linking, the properties of the obtained hydrogels can be easily tuned.<sup>9,10</sup> However, the isotropic nature of the hydrogels

Received: September 30, 2020

Accepted: December 23, 2020

Published: January 6, 2021



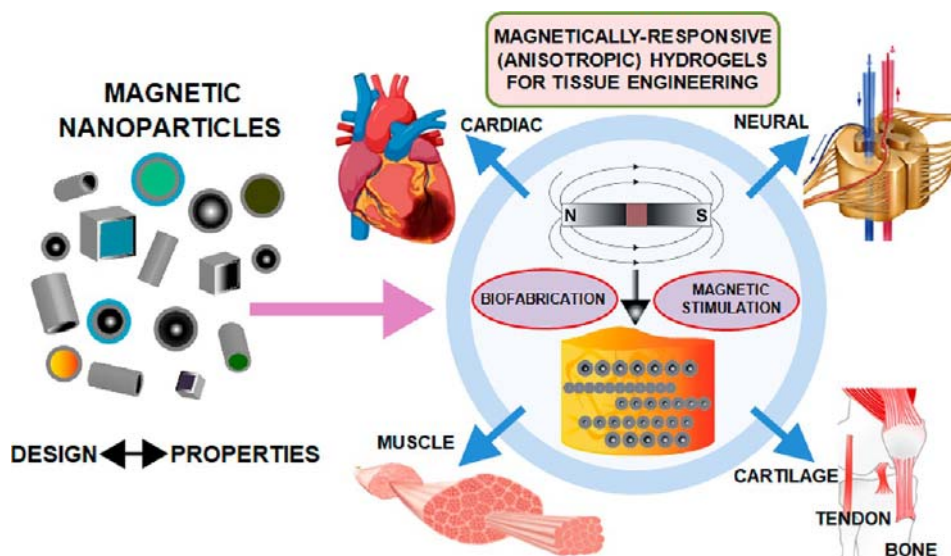


Figure 1. Schematic illustration: use of magnetic hydrogels to engineer different tissues of the human body. Adapted with permission from refs 32 (Copyright 2020 Springer Nature), 33 (Copyright 2014 Elsevier), 34 (Copyright 2017 Wiley-VCH), and 35 (Copyright 2015 Elsevier).

limits their potential to mimic the architectural features of the different tissues of the human body, which are characterized by highly anisotropic complex structures.<sup>11–15</sup> In order to engineer the sophisticated arrangements of native tissues, the incorporation of nano- and microstructured materials into a hydrogel 3D network has been widely explored, trying to mimic the characteristic nonhomogeneous structure and physicochemical properties observed in natural tissues.<sup>16–20</sup> Among the different nanomaterials used in the biomedical field, magnetic nanoparticles (MNPs) are one of the most interesting due to the possibility of being remotely actuated by externally applied magnetic fields. Their incorporation within the hydrogels, both alone or as part of more complex structures, has been extensively evaluated.<sup>21–23</sup> The intrinsic properties of MNPs can be exploited to manipulate their distribution within the 3D space of hydrogels' networks through the application of external magnetic fields, allowing a controlled design of anisotropic magnetically responsive scaffolding materials. Moreover, the magneto/mechanical stimuli that can be provided on-demand by externally applied magnetic fields combined with the anisotropic structures generated by the defined distribution of the magnetic materials can be harnessed to control the growth, migration, proliferation, and differentiation of cells encapsulated within magnetic hydrogels toward targeted lineages, allowing the production of cell-laden constructs with specific ordered features re-creating the architectures of native tissues (Figure 1).<sup>24–27</sup>

The use of magnetic hydrogels in TE has been increasingly proposed in the past few years.<sup>28–31</sup> However, in most of the works carried out in this field, the thorough design of suitable MNPs and the configurations used to generate the magnetic fields for nanoparticles' actuation have not been analyzed in detail. In this sense, a comprehensive review that covers the different approaches to design magnetic nanoparticles with tunable magnetic response, the experimental setups explored for the creation of magnetic fields used for particle manipulation and cell stimulation within the hydrogels, and the specific design of composite hydrogels for the regeneration of different tissues is important and timely.

In this work, we first discuss available strategies to have an increased control over the magnetic properties of MNPs in order to obtain nanoparticles with the desired features for their application in the biomedical field. The different synthesis methods, the main procedures to modify their magnetic properties, and the general requirements for their biomedical applications are exposed. Subsequently, the different approaches to produce magnetically responsive hydrogels are discussed, reviewing the methods that have been used to incorporate magnetic materials within the polymer matrices. The use of magnetism to create anisotropic structures and/or to remotely actuate over the seeded/encapsulated cells, as well as the different setup configurations adopted for the generation and application of external magnetic fields are also critically reviewed. Finally, the specific strategies on the development of magnetic responsive hydrogels with the required architectural properties to properly mimic different anisotropic tissues such as tendons, bones, or cartilages are discussed. In this way, we expect to provide guidance for the rational selection of magnetic materials design criteria, as well as for their manipulation by external magnetic fields in order to control hydrogel physical properties and their remote actuation capability. Ultimately, we intend to expose the potential of the application of magnetism and magnetic responsive hydrogels to improve the regenerative potential of different TE strategies.

## MAGNETIC NANOPARTICLES

The magnetic properties of MNPs are determined by their response when an alternating or nonalternating magnetic field is applied.<sup>36</sup> By controlling the physical and chemical features of the MNPs (Figure 2), it is possible to predict their response under the effect of magnetic fields.<sup>37</sup> Thus, the magnetic moment induced on these kinds of nanomaterials can be used to control their direction and/or accumulation inside other more complex structures, while preventing their aggregation, precipitation, and/or unspecific localization, as well as the occurrence of undesired interactions or potential harmful side effects with the surrounding environment.<sup>38</sup> For instance, the formation of magnetic aggregates can greatly affect the biological fate of the MNPs, preventing their internalization within cells, hindering

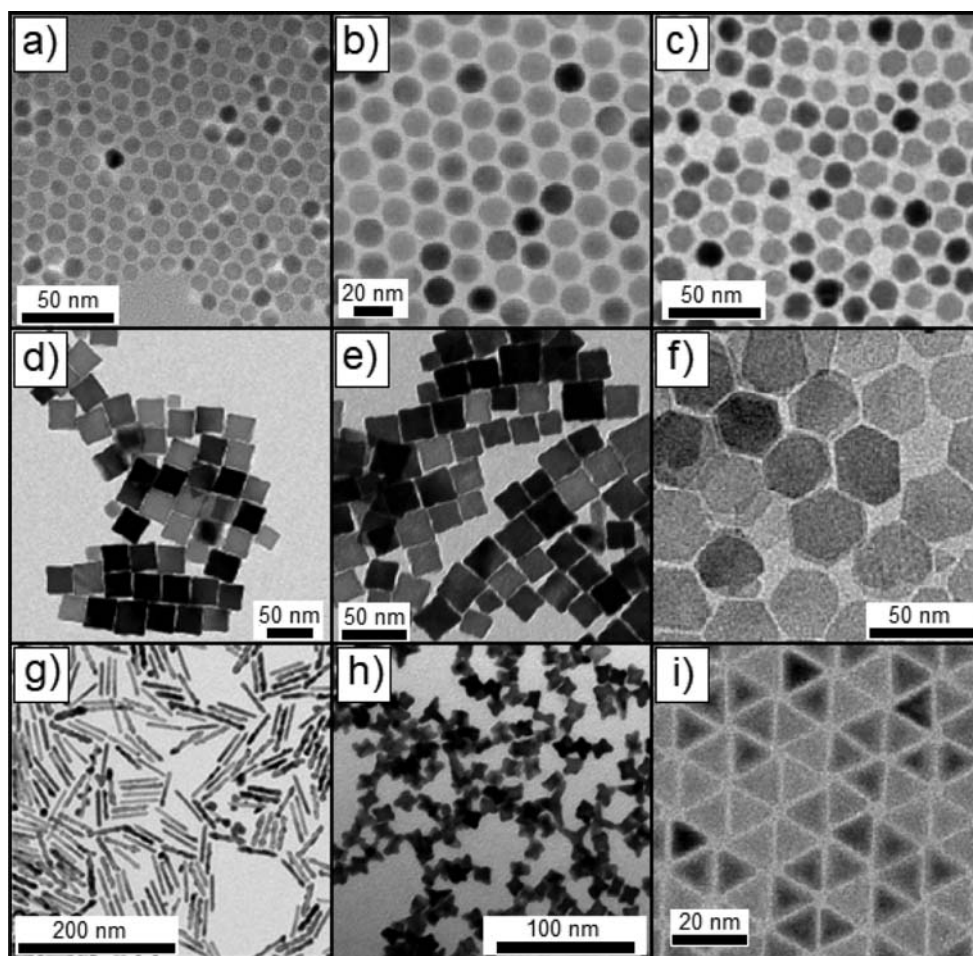


**Figure 2.** Transmission electron microscopy images of different MNPs: (a) *ca.* 10 nm spherical-shaped manganese-doped MNPs (Reproduced with permission from ref 87. Copyright 2015 American Chemical Society); (b) *ca.* 15 nm spherical-shaped zinc-doped MNPs (Reproduced with permission from ref 89. Copyright 2009 Wiley-VCH); (c) *ca.* 14 nm core-shell MNPs ( $\text{CoFe}_2\text{O}_4\text{-MnFe}_2\text{O}_4$ ) (Reproduced with permission from ref 87. Copyright 2015 American Chemical Society); (d) *ca.* 28 nm cubic-shaped iron oxide MNPs (Reproduced with permission from ref 90. Copyright 2014 Royal Society of Chemistry); (e) *ca.* 23 nm cubic-shaped cobalt-doped MNPs (Reproduced with permission from ref 84. Copyright 2016 American Chemical Society); (f) *ca.* 20 nm hexagonal plates of iron oxide (Reproduced with permission from ref 72. Copyright 2015 American Chemical Society); (g) *ca.* 75 nm length nanorods of cobalt coated with Sn-Pt-Au (Reproduced with permission from ref 73. Copyright 2015 American Chemical Society); (h) *ca.* 13 nm star-shaped iron-platinum MNPs (Reproduced with permission from ref 91. Copyright 2010 Royal Society of Chemistry); and (i) *ca.* 15 nm tetrahedral-shaped iron oxide MNPs (Reproduced with permission from ref 72. Copyright 2015 American Chemical Society).

their subsequent excretion, and thus affecting their cytotoxicity degree.<sup>39</sup> The ability to control the properties of MNPs is essential for their successful performance in many technological applications, which can range from electronics<sup>40,41</sup> and engineering<sup>42,43</sup> to biomedicine, where the use of MNPs has been tested in magnetic drug delivery,<sup>44,45</sup> hyperthermia treatments,<sup>46,47</sup> magnetic resonance imaging (MRI),<sup>48,49</sup> or TE,<sup>22,50</sup> for example.

In this section, the main synthetic methods to prepare MNPs are reviewed, as well as the most common strategies developed to modulate their response when an external magnetic field is applied. Moreover, the characteristics required on magnetic systems for their application in the biomedical field and, more specifically, in TE are also commented on.

**Initial Considerations: Magnetic Properties and Structure of MNPs. Synthetic Methods.** The special characteristics of MNPs justify their extended use in a wide range of applications. To provide a better understanding on the possible modification of the properties of MNPs, it is necessary

to introduce the following magnitudes, which define a magnetic material:<sup>51,52</sup>

- Saturation magnetization ( $M_S$ ): it is the maximum value of magnetization that the MNPs can reach under the application of a magnetic field.
- Remanent magnetization ( $M_R$ ): it represents the residual magnetization of MNPs after removing the applied magnetic field.
- Coercive field ( $H_C$ ): it is the magnetic field that must be applied to reverse the material's net magnetization back to zero.
- Magnetic anisotropy constant ( $K_a$ ): it is defined by the physical properties of the MNPs, especially by the symmetry of the crystal lattice. This magnitude determines the barrier energy to reverse the direction of the magnetic dipoles.

These parameters are obtained from the magnetization *vs* applied field curves of ferro- and ferrimagnetic materials, typically measured using a superconducting quantum interfer-



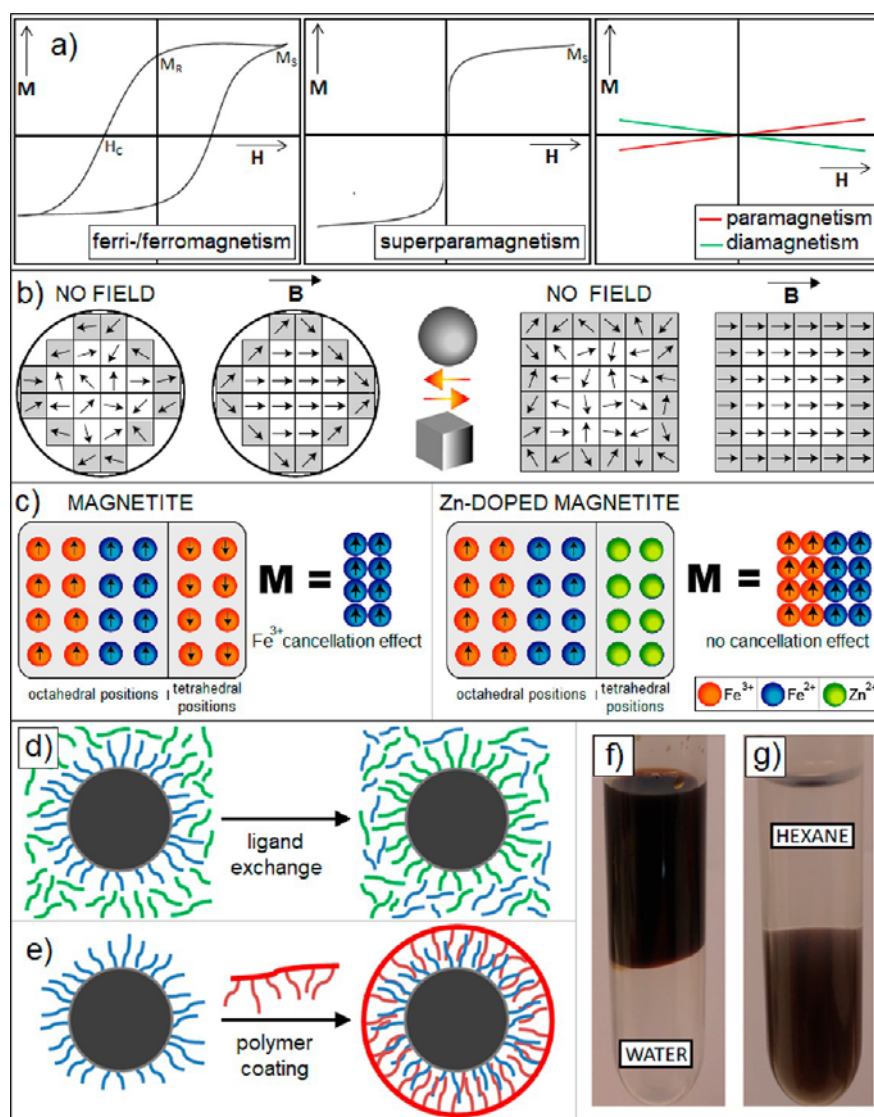


**Figure 3.** (a) Typical magnetization  $vs$  applied magnetic field ( $M vs H$ ) curves of ferro-/ferrimagnetic, superparamagnetic, diamagnetic, and paramagnetic materials ( $M_S$  = saturation magnetization;  $M_R$  = remanent magnetization;  $H_C$  = coercive field). (b) Schematic illustration of atomic magnetic moments orientation in spherical-shaped MNPs and cubic-shaped MNPs when an external magnetic field is applied. Border effects promote higher magnetization values on cubic-shaped MNPs. (c) Schematic illustration of the effect of zinc doping on magnetite MNPs. The substitution of  $Fe^{3+}$  by  $Zn^{2+}$  ions in tetrahedral positions cancels the antiferromagnetic coupling between octahedral and tetrahedral  $Fe^{3+}$  ions observed in magnetite, allowing higher magnetization ( $M$ ) values. Schematic representation of (d) ligand exchange (MNPs are incubated with new ligand in excess (in green), displacing the original ligand (in blue)) and (e) polymer coating (the MNPs are surrounded by a polymer layer (in red)). Original oleic acid-capped MNPs stable in a hexane (top)–water (bottom) mixture (f) before and (g) after a polymer-coating process using poly(maleic-*alt*-anhydride)-grafted-dodecylamine. Panels f and g Adapted with permission from ref 81. Copyright 2020 American Chemical Society.

ence device (SQUID) or a vibrating sample magnetometer (VSM). All of these magnitudes have a great dependence with the physicochemical properties of the magnetic materials, being possible to tune their values through an exhaustive control over the fabrication process of MNPs. On the other hand, nonmagnetic materials are characterized by an extremely weak response to the application of external magnetic stimuli and can be classified as diamagnetic (repelled by magnetic fields) or paramagnetic materials (attracted by magnetic fields) (Figure 3a).<sup>53</sup>

Among the different MNPs characteristics, the size is one of the most influential factors that define the behavior of MNPs composed of ferro-/ferrimagnetic materials, existing some critical dimensions below which these types of nanoparticles

enter the so-called superparamagnetic regime.<sup>54</sup> In this regime, the thermal energy of MNPs can exceed their magnetic stabilization energy, resulting in a demagnetization of the particles when the applied magnetic field is removed; that is, the magnetic hysteresis loops of the magnetization  $vs$  applied magnetic field plots show negligible areas ( $M_R$  and  $H_C$  equal to zero) (Figure 3a).<sup>55</sup> For practical purposes, the absence of permanent magnetic moment is translated into a high remote control over the MNPs distribution and a very low tendency to form particle clusters/aggregates under the application of an external magnetic field, which is of great importance in many of their potential bio-applications.<sup>56,57</sup> Among the different magnetic nanostructures that have shown promising magnetic properties for biomedical purposes, those based on iron oxide

MNPs are the most interesting because of their low cost, easy production, and reduced toxicity,<sup>58</sup> being hematite ( $\alpha$ -Fe<sub>2</sub>O<sub>3</sub>), maghemite ( $\gamma$ -Fe<sub>2</sub>O<sub>3</sub>), and magnetite (Fe<sub>3</sub>O<sub>4</sub>), the three most common phases of iron oxide.<sup>59</sup>

To achieve a full control over the properties of MNPs, the selection of the adequate synthetic method has a great importance.<sup>60</sup> In the past few years, the strategies to obtain MNPs with the desired characteristics in terms of size, shape, and composition have been considerably improved.<sup>61</sup> The synthetic routes to obtain MNPs are usually divided in physical and chemical methods. Physical methods, such as thermal evaporation, pulsed laser deposition, or grinding, result in bigger amounts of material but with poor properties (purity, homogeneity, and so on).<sup>62</sup> These kinds of synthetic techniques also require the use of expensive laboratory equipment. On the other hand, the amount of product obtained by chemical methods is smaller, but the obtained particles possess better quality and higher homogeneity. The most used chemical methods for the preparation of MNPs are as follows.

- (1) Sol-gel: this kind of synthetic methodology is based on the hydroxylation of molecular magnetic precursors in solution and, then, the MNPs are produced through their condensation and inorganic polymerization. Extra heat steps are usually required to obtain the final crystalline state.<sup>63</sup>
- (2) Solvothermal synthesis: in this kind of process the reactions take place under high-pressure (typically >1 bar) and -temperature conditions (above the boiling point of the solvent). When the solvent used is water, the synthesis is known to be hydrothermal, providing MNPs stability in aqueous media with a relatively high control over their characteristics. However, hydrothermal strategies still fail to synthesize quality nanocrystals with small dimensions with hydrophilic behavior.<sup>64</sup>
- (3) Co-precipitation: it is based on the co-precipitation of ferrous and ferric salts by the addition of a base, allowing a low control over the characteristics of the obtained MNPs. The produced MNPs are water-soluble, making it a commonly used methodology to prepare MNPs for biomedical purposes, but they exhibit an uncontrolled oxidation and present a broad size distribution, being sometimes a required secondary size selection.<sup>65</sup>
- (4) Thermal decomposition: this method consists of the reduction of metallic precursors under controlled conditions and at high temperatures, resulting in highly monodisperse MNPs with full control over their main characteristics. By controlling the dimensions and the crystalline structure of the obtained MNPs, their magnetic properties are also easily tunable. Nevertheless, in this case the obtained MNPs are not soluble in aqueous environments, being a necessary extra phase transfer step to make them water-soluble and allow their use for bio-applications.<sup>66</sup>

Therefore, all of the detailed chemical synthetic methods to prepare MNPs have advantages and drawbacks that have been summarized in Table 1.<sup>67,68</sup> However, to design highly monodisperse MNPs with a well-controlled magnetic response, a high control over their size, shape, and composition is required. In this sense, although co-precipitation is a commonly used synthetic route due to its simplicity and the obtaining of water-soluble particles, thermal decomposition is probable the most

**Table 1. Main Advantages, Disadvantages, and Tunable Synthetic Parameters of the Most Common Chemical Methods Used to Produce MNPs**

	advantages	disadvantages	synthesis params	size range MNPs
sol-gel	simple and low cost; relatively high control over size, shape, and crystallinity	low wear-resistance; easy oxidation; multistep method; MNPs containing sol-gel matrix components	pH, temperature, reagents concentration, and condensation rate	20–200 nm
solvothermal	relatively high control over shape and size; good crystallinity; possibility of obtaining water-soluble MNPs	high pressure and high temperature required; long reaction times that can cause oxidation; autoclave safety issues	pressure, temperature, reaction time, and type and concentration of reagents	larger than 10–15 nm
co-precipitation	water-soluble MNPs; simple, cheap, fast, and high-yield method; low reaction temperature	very low control over size and shape; uncontrolled oxidation; low-purity MNPs; multistep method	pH, temperature, ionic strength, ratio, and concentration of precursor salts	average size larger than 8–10 nm (broad size distribution)
thermal decomposition	excellent control over MNPs shape and size; high crystallinity; design of MNPs with tunable magnetic properties	low mass of product obtained; organic solvents involved, MNPs not soluble in water; high temperature required; inert atmospheres required	temperature, heating ramp, ratio and concentration of reagents, type of inert atmosphere, and solvents	minimum below 3 nm

Table 2. Main Physicochemical Characteristics and Magnetic Properties of Different Relevant MNPs

composition	size (nm)	shape	C@S	SC	$M_S^a$ (emu·g <sup>-1</sup> )	$H_C^a$ (T)	$M_R^a$ (emu·g <sup>-1</sup> )	ref
Fe <sub>3</sub> O <sub>4</sub>	20	hexagonal plates	no	OA	45 (RT)	0 (RT)		72
Fe <sub>3</sub> O <sub>4</sub>	16	octahedrons	no	OA	57 (RT)	0 (RT)		72
Fe <sub>3</sub> O <sub>4</sub>	15	tetrahedrons	no	OA	53 (RT)	0 (RT)		72
Co@PtSnAu	75 × 6	rods	yes	HAD	158 (4 K)	0.71 (4 K)		73
Zn <sub>0.4</sub> Fe <sub>2.6</sub> O <sub>4</sub>	18	cubes	no	OA	165 (RT) <sup>b</sup>	0 (RT)		77
Zn <sub>0.4</sub> Fe <sub>2.6</sub> O <sub>4</sub>	22	spheres	no	OA	145 (RT) <sup>b</sup>	0 (RT)		77
Zn <sub>0.4</sub> Fe <sub>2.6</sub> O <sub>4</sub>	60	cubes	no	OA	150 (RT) <sup>b</sup>	0.01 (RT)	30 (RT)	77
Zn <sub>0.4</sub> Fe <sub>2.6</sub> O <sub>4</sub> @ CoFeO <sub>4</sub>	60	cubes	yes	OA	190 (RT) <sup>b</sup>	0.14 (RT)	138 (RT)	77
Fe <sub>8</sub> Ni <sub>92</sub>	112	spheres	no	PEG	52 (RT)	0.01 (RT)		80
Fe <sub>32</sub> Ni <sub>68</sub>	64	spheres	no	PEG	58 (RT)	0.005 (RT)		80
CoFe <sub>2</sub> O <sub>4</sub>	15	cubes	no	DA	47 (RT)	0.07 (RT)		84
CoFe <sub>2</sub> O <sub>4</sub>	27	cubes	no	DA	63 (RT)	0.04 (RT)		84
CoFe <sub>2</sub> O <sub>4</sub>	20	cubes	no	DA	42 (RT)	0.05 (RT)		84
Co <sub>0.1</sub> Fe <sub>2.9</sub> O <sub>4</sub>	20	cubes	no	DA	74 (RT)	0.01 (RT)		84
Co <sub>0.5</sub> Fe <sub>2.5</sub> O <sub>4</sub>	20	cubes	no	DA	63 (RT)	0.11 (RT)		84
Mn <sub>0.3</sub> Fe <sub>2.7</sub> O <sub>4</sub>	14	spheres	no	OA	91 (RT)	0.03 (5 K)		87
Co <sub>0.5</sub> Fe <sub>2.5</sub> O <sub>4</sub>	15	spheres	no	OA	80 (RT)	1.84 (5 K)		87
Co <sub>0.5</sub> Fe <sub>2.5</sub> O <sub>4</sub> @ Mn <sub>0.3</sub> Fe <sub>2.7</sub> O <sub>4</sub>	13	spheres	yes	PMA	87 (RT)	0.51 (5 K)		87
Mn <sub>0.3</sub> Fe <sub>2.7</sub> O <sub>4</sub> @ Co <sub>0.5</sub> Fe <sub>2.5</sub> O <sub>4</sub>	14	spheres	yes	PMA	82 (RT)	2.20 (5 K)		87
MnFe <sub>2</sub> O <sub>4</sub>	15	spheres	no	OA	125 (RT)	0 (RT)		89
Zn <sub>0.2</sub> Mn <sub>0.8</sub> Fe <sub>2</sub> O <sub>4</sub>	15	spheres	no	OA	154 (RT)	0 (RT)		89
Zn <sub>0.2</sub> Fe <sub>2.8</sub> O <sub>4</sub>	15	spheres	no	OA	140 (RT)	0 (RT)		89
Zn <sub>0.4</sub> Fe <sub>2.6</sub> O <sub>4</sub>	15	spheres	no	OA	161 (RT)	0 (RT)		89
Fe <sub>3</sub> O <sub>4</sub>	27	cubes	no	OA	65 (5 K)	0.03 (5 K)	16 (5 K)	122
Fe <sub>3</sub> O <sub>4</sub>	48	cubes	no	OA	97 (5 K)	0.05 (5 K)	25 (5 K)	122
Fe <sub>3</sub> O <sub>4</sub>	94	cubes	no	OA	99 (5 K)	0.06 (5 K)	31 (5 K)	122
Mn <sub>0.4</sub> Fe <sub>2.6</sub> O <sub>4</sub>	12	spheres	no	PEG	46 (RT)	0 (RT)		123
Co <sub>0.4</sub> Fe <sub>2.6</sub> O <sub>4</sub>	8	spheres	no	PEG	38 (RT)	0 (RT)		123
Ni <sub>0.4</sub> Fe <sub>2.6</sub> O <sub>4</sub>	14	spheres	no	PEG	37 (RT)	0 (RT)		123
CoFe <sub>2</sub> O <sub>4</sub>	10	spheres	no	PEG	60 (RT)	0 (RT)		124
Fe <sub>2</sub> O <sub>3</sub>	12	spheres	no		65 (RT)	0 (RT)	1 (RT)	125

<sup>a</sup>C@S = core-shell structure; SC = surface coating;  $M_S$  = saturation magnetization;  $H_C$  = coercive field;  $M_R$  = remanent magnetization; OA = oleic acid; PEG = poly(ethylene glycol); DA = decanoic acid; HDA = hexadecylamine; PMA = poly(maleic-*alt*-anhydride)-grafted-dodecylamine. Measurements temperature in brackets; RT = room temperature. <sup>b</sup>Units: emu·g<sub>metal</sub><sup>-1</sup>.

suitable methodology to design MNPs with well-controlled magnetic response.

**Magnetic Properties Modification: Morphology, Composition, and Core-Shell Structures.** As mentioned above, iron oxide MNPs with superparamagnetic behavior (SPIONs) are the most commonly used in a wide range of applications, due to the low toxicity of iron oxide and their low tendency to form aggregates under the application of external magnetic fields. For this reason, current research is focused on the design and preparation of iron oxide-based MNPs with a high magnetic power without significant increases in their dimensions, thus maintaining their superparamagnetic behavior.<sup>69</sup> The main strategies used to achieve this goal are the modification of the MNPs' shape, the growth of magnetic shells surrounding the particles (core-shell MNPs), or the modification of the internal composition of the MNPs by the partial substitution (doping) of iron by other metallic elements on their crystalline structure (Figure 2 and Table 2).

**Particle Morphology.** The particles with dimensions in the nanometric scale are characterized by high surface-to-volume ratios, and consequently the contributions of the surface atoms to their physical properties become more important than in larger particles. In this sense, the morphology of MNPs determines the percentages of atoms located in their core and their surface, as well as the magnetic symmetry coordination

between them, having a significant impact on their electrical, optical, and magnetic properties.<sup>70</sup> In this way, cubic-shaped MNPs are particularly interesting since they maintain the symmetry coordination of their core crystalline structure on their internal surface. Thus, when MNPs with cubic shape are subjected to an external magnetic field, all of the atomic magnetic moments are oriented in the field direction. However, in MNPs with other morphologies, such as spherical-shaped MNPs, the magnetic moments of the surface atoms are slightly deviated from the field direction due to border effects (Figure 3b). For this reason, these cubic-shaped MNPs can reach the highest levels of magnetization under the application of external magnetic fields.<sup>71</sup>

Nevertheless, the synthesis of anisotropic iron oxide-based MNPs with the desired characteristics in terms of monodispersity is still a challenge. A full control over the size of spherical MNPs has been achieved through different synthetic routes, but the existing methodologies developed to produce MNPs with elongated, branched, or flat shapes present a poor reproducibility and yield yet.<sup>72</sup>

Several previous works have analyzed the effect of the shape on the magnetic properties of MNPs. Therefore, magnetic structures with different morphologies such as nanorods,<sup>73</sup> hexagonal nanoplates,<sup>74</sup> or star-shaped<sup>75</sup> MNPs have been synthesized, but most of the related works focused on the



analysis of cubic-shaped particles. For instance, Guardia *et al.*<sup>76</sup> observed that the saturation magnetization of iron oxide MNPs decreases progressively when their shape is modified from cubes to cylinders and to spheres. In other relevant work, it was determined that zinc-doped iron oxide MNPs with cubic shape showed higher saturation magnetization than their spherical counterparts, quantifying that the percentages of disordered surface spins were 4% and 10% for cubical and spherical MNPs, respectively.<sup>77</sup>

**Particle Composition.** A different strategy to modulate the magnetic properties of MNPs consists of the modification of their internal composition. Several magnetic materials such as iron carbides,<sup>78</sup> iron–platinum,<sup>79</sup> or iron–nickel<sup>80</sup> have been prepared in the form of nanoparticles. However, as mentioned above, iron oxide-based MNPs are the most commonly used due to their easy/cheap synthesis and low toxicity degree, so here we will focus in the modification of the composition of these kinds of MNPs. In this sense, the partial substitution of iron by other metallic elements such as manganese, cobalt, nickel, or zinc represents a good approach to change the magnetic properties of iron oxide MNPs without affecting their size.<sup>81</sup> In the inverse spinel structure of magnetite, the Fe<sup>3+</sup> ions located on tetrahedral and octahedral sites show an antiferromagnetic coupling, being the magnetization of these MNPs caused only by the Fe<sup>2+</sup> ions that occupy the other half octahedral sites.<sup>82</sup> Thus, the doping of MNPs during the synthetic processes gives rise to changes on the magnetic moment distribution within the nanoparticles and, consequently, to variations on their magnetic properties.

For instance, when the composition of the MNPs is modified with zinc, the doping cations are arranged in tetrahedral sites replacing Fe<sup>3+</sup> ions and breaking the antiferromagnetic coupling with the Fe<sup>3+</sup> ions in octahedral positions (zinc is not magnetic). Thus, with these kinds of doping it is possible to reach high increases on the MNPs' magnetization values (Figure 3c).<sup>71</sup> Other metallic elements, such as cobalt or nickel, are arranged in closely packed octahedral sites and increase the anisotropy of the particles, thus raising their coercive fields/remanent magnetization.<sup>83</sup>

The doping strategy to modify the response of iron oxide-based MNPs under the application of an external magnetic field has been widely analyzed in several previous works. Different authors determined that the doping of iron oxide MNPs with cobalt promoted large increases on their coercive fields and remanences, especially at high degrees of substitution, while the effect over their saturation magnetizations was reduced.<sup>71,84</sup> Similar effects were observed in the case of nickel doping strategies.<sup>85</sup> In other studies, important increases were measured on the saturation magnetizations of iron oxide MNPs when iron was partially replaced by zinc, not changing significantly the values of remanences and coercivities in these cases.<sup>77,81</sup>

**Core–Shell Structures.** Another thoroughly explored strategy to modify the anisotropy and the subsequent magnetic behavior of MNPs consist of the growth of a magnetic shell surrounding the particles (core–shell MNPs). The coupling between both parts of the dual structure and the exchange energy between them originate important variations on the anisotropy constant value. This strategy allows increasing the superparamagnetic critical size of the particles, being possible to obtain MNPs which keep their superparamagnetic behavior having dimensions above the critical ones for homogeneous-composed structures.<sup>86</sup>

Typically, core–shell MNPs have one part consisting of a soft magnetic material (low anisotropy constant, as manganese oxide) and another part consisting of a hard magnetic material (high anisotropy constant, as cobalt oxide). Depending on the size and the composition of both parts, the anisotropy constant of the core–shell MNPs can present a value in an optimal range that allows one to increase the MNPs' size within the superparamagnetic regime and, at the same time, the magnetic power of the particles for specific applications.<sup>87</sup>

In this way, Lee *et al.*<sup>88</sup> synthesized core–shell MNPs with different compositions in both parts of their structure, observing that the particles with iron oxide core doped with cobalt and iron oxide shell doped with manganese provide a high magnetic power for magnetic hyperthermia applications. In other work, it was demonstrated that core–shell MNPs with hard–soft structure (iron oxide doped with cobalt in the core and iron oxide doped with manganese in the shell) provide higher magnetic power than those with the opposite composition (soft–hard).<sup>87</sup>

**Biocompatibility of MNPs.** The incorporation of MNPs within scaffolding materials enables a wide range of potential applications in the field of TE, such as, for instance, the control of scaffolds' mechanical properties under the exposure to external magnetic fields or the loading/controlled release of different biological agents, such as growth factors, to control cell biological behavior.<sup>23</sup> In this way, MNPs' biological fate and their interactions with surrounding cells and tissues should be thoroughly evaluated, considering the hypothesis that they can spread throughout the human body during the scaffolds biodegradation and clearance. This analysis nevertheless has been largely hampered by several factors such as (i) the numerous types of MNPs with different sizes, morphologies, compositions, and surface coatings, *etc.*;<sup>92</sup> (ii) the vast range of engineered scaffolds with changing chemical composition, structure, and physicochemical properties, and, most importantly, cell types and culture conditions of each particular TE strategy, factors which must be considered when evaluating the biological interactions established with MNPs;<sup>93</sup> (iii) the lack of widespread standardized protocols, conditions, and techniques to analyze MNPs physicochemical properties, concentrations, and their cell interaction mechanisms, biocompatibility and induced cell/tissue responses, particularly in the complex biological intracellular and tissue microenvironment;<sup>94,95</sup> and, as consequence of the latter, (iv) the need for developing reliable *in vitro* models to adequately emulate the complexity of the *in vivo* tissue environment.<sup>96</sup>

When incorporated in polymeric scaffolds, MNPs are embedded within the biomaterials designed to be implanted at a specific tissue or organ site. However, the gradual degradation of the polymer matrix will locally release the MNPs and therefore, their subsequent entrance in the circulation system and potential enhanced degradation or bioaccumulation in other organs is a possibility that must be considered. In general, MNPs circulating in the bloodstream are typically filtered and, in some cases, at least partially degraded by liver and spleen macrophages,<sup>97</sup> being then excreted through the gastrointestinal tract. However, when they are present in high dosages, the excess of MNPs tend to get accumulated in other macrophage-rich tissues such as lung and adipose tissue. In the case of kidneys, these organs act as filters that only allow the passing of MNPs with hydrodynamic size smaller than 10–15 nm to leave the bloodstream and get excreted from the body.<sup>93</sup>

Iron oxide-based MNPs were believed for a long time to be completely biologically safe, given the high tolerance of cells to ferric iron ions as an essential element for cell growth, as well as the existence of a proper pathway for metabolization and clearance of this metal ion in the human body.<sup>98</sup> However, with the increased interest in MNPs boosted by their envisioned outstanding potential in different biomedical applications, more in-depth studies on the cytotoxicity and biological fates of these nanoparticles have progressively emerged in the past two decades.<sup>99</sup> These studies have shown that MNPs' cytotoxicity is largely dependent on the degree to which they interact with cells.<sup>93</sup> Similar to most nanosystems, particle size, shape, chemical composition, and surface coating are key factors in defining not only cell/tissue cytotoxicity but also MNPs colloidal stability in physiological environments. These parameters affect the potential agglomeration of the particles and, as a consequence, their interaction mechanisms with cells,<sup>100</sup> intra- and extracellular cell biological activity, biodegradability, and excretion ability.<sup>101</sup> Among the different possible cell–MNP interaction mechanisms, their potential internalization by endocytosis (phagocytosis, pinocytosis, or clathrin-/caveolae-mediated endocytosis) is one of the main factors with influence on their biological fate.<sup>100</sup> As mentioned, these processes are highly dependent on the type of cells and also on the physicochemical characteristics of MNPs. Among them, the particles' surface charge is an essential parameter, being well-known that positively charged MNPs favor endocytosis due to their easier attachment to negative cell membranes. On the other hand, the exocytosis of MNPs is a less studied mechanism than their internalization pathways, but the type of cells, biological environments, and particles' characteristics are again key factors that affect the intercellular processes that lead to lysosomal- or Golgi apparatus-mediated particles exocytosis. For instance, it has been reported that the exocytosis rate is slower in MNPs with larger dimensions, being also affected by the surface functionalization of the particles.<sup>101</sup>

In nanocomposite scaffolds, the proposed functions for incorporated MNPs are not intrinsically related with their cell internalization. Nevertheless, this possibility cannot be excluded, particularly in the case of cell-laden hydrogels where cell–MNPs contacts are more likely to occur since the initial steps of cell encapsulation, and should therefore be considered in the design of magnetic scaffold biomaterials.<sup>102</sup> The release of metallic ions during cellular internalization processes, induced by the particle degradation in the acidic and harsh endosomal/lysosomal environments, is one of the key factors that must be carefully evaluated. The release of Fe ions from MNPs might not necessarily lead to negative biological effects. For example, when MSCs were exposed to carboxydextran-coated MNPs, it was observed that whole particles had a potent peroxidase-like activity, whereas the released iron ions promoted an enhanced MSC proliferation.<sup>103</sup> Ionization of MNPs into iron atoms inside myoblast cell line H9C2 cocultured with MSCs was also found to trigger a gap functional signaling cascade to develop CX43 expression and subsequent cell crosstalk in order to promote the controlled cardiac phenotype development of MSC cells.<sup>104</sup> However, these free metallic ions can enter into the label iron pool in the cell cytoplasm and may affect their iron metabolism,<sup>105</sup> as well as induce a strong increase in reactive oxygen species, ROS, by means of the well-known Fenton reaction,<sup>106</sup> which can lead to secretion of undesirable cytokines and chemokines and/or alterations in ferritin levels.<sup>107</sup> As well, highly toxic ions could be released from MNPs modified with

doping elements such as cobalt or nickel if the surface coatings do not provide a sufficiently protective barrier.<sup>108,109</sup> All of these phenomena indicate that MNPs must be carefully designed in order to avoid a variety of uncontrolled detrimental biological effects such as DNA damage, changes in cell morphology, cell cycle progression and signaling processes.<sup>110</sup>

Although significant progresses have been made in decrypting the biological fate of MNPs and its relationship with the nanoparticles' design parameters, the amount of conflicting data about the biocompatibility of MNPs with relatively similar characteristics suggest that the full understanding of the interactions between magnetic nanostructures and living organisms remains incomplete.<sup>111</sup> This is particularly true in the case of magnetic nanocomposite scaffolds, for which quite limited data on their biocompatibility after *in vivo* implantation exists. Future research should include these studies in their experimental designs to further demonstrate the full potential of magnetic hydrogels as scaffolding biomaterials in TE strategies.

**Design Considerations of MNPs for TE with Magnetic Hydrogels.** The strategies reviewed in the previous sections are useful to design MNPs with tunable internal structure, which can allow one to obtain the desired particle response when an external magnetic field is applied. However, for their incorporation within hydrogels to be used as biomaterials for TE applications, MNPs have to meet several additional requirements:<sup>112,113</sup>

- (1) MNPs must be colloidal stable in aqueous-based hydrogel precursor solutions. Moreover, they also must be stable in physiological-mimicking media (aqueous media with high ionic strength and high concentrations of different biomolecules) and even in serum/blood, to prevent the aggregation when released from the scaffolds while they undergo degradation.
- (2) MNPs have to show a nontoxic behavior, preferably with surface coatings that avoid any leakage of potential toxic ions (if used) within their structure. The MNPs must be biocompatible not only with cells encapsulated within the magnetic hydrogels but also with general human tissues if they are released from the constructs at the implanted site and enter in circulation.
- (3) Degradation of MNPs must be controlled to ensure functionality. As discussed in the previous section on MNPs' biocompatibility, although the particles can degrade without inducing significant detrimental biological effects, this phenomenon alters their magnetic properties and remote response. It is an especially critical requirement in the design of magnetic composites that require long-term stimulation *in vitro* and/or must be magnetically stimulated *in vivo* after their implantation.
- (4) MNPs should be specifically functionalized to form part of the cross-linked polymeric network. In addition to promoting their stability, the functional groups bonded to MNPs' surfaces can act as cross-linking points of the hydrogel network, promoting the formation of hydrogels with covalently bonded MNPs that have lower risk of magnetic leakage and improved mechanical properties.
- (5) MNPs must present high magnetic responsiveness. The use of MNPs highly sensitive to magnetic fields allows one to decrease the contents of the magnetic material and the intensity of the magnetic irradiations required for their remote control, minimizing the potential toxicity/safety risks associated with these factors.



To provide several of these features it is necessary for the surface modification of the MNPs. As mentioned previously, thermal decomposition is the most adequate method to obtain high-quality MNPs, but the resulting particles are only stable in organic media. Therefore, an additional step to make them stable in aqueous solutions is needed. In any case, the surfactants used to directly obtain water-soluble MNPs by synthetic techniques such as co-precipitation do not provide high stability, typically requiring an additional surface functionalization. Among the most common strategies to provide MNPs with high stability in aqueous solution and preclude their degradation and/or agglomeration are ligand exchange (Figure 3d), polymer coating (Figure 3e), encapsulation within organic particles, and formation of silica shells wrapping the particles. Polymer coating<sup>114</sup> and ligand exchange<sup>115</sup> are previously well-reviewed methods that consist of the formation of hydrophilic polymeric micelles surrounding the MNPs and in the substitution of the original ligands of the particles by others (e.g., dimercaptosuccinic acid) with higher affinity for the inorganic surfaces, respectively. In the encapsulation<sup>116</sup> and silica shell<sup>117</sup> strategies, MNPs can be incorporated into emulsions and the surrounding particles are subsequently formed by precipitation or evaporation, or the coatings can be grown layer by layer retaining the MNPs within them. Other very interesting little-explored functionalization strategies are the formation of coatings using phase-transitioned lysozymes (PTLs) and polyphenol-based complexes. In PTL method pure protein shells are quickly grown through the immersion of the MNPs in enzymatic buffers, resulting in coatings with high resistance against mechanical/chemical degradation that allow subsequent modification steps of particles' surfaces.<sup>118</sup> On the other hand, polyphenol method can be applied by coating polymeric emulsion templates loaded with MNPs using a specific polyphenol complex, and the subsequent removal of the emulsion produces polyphenol-based capsules loaded with MNPs.<sup>119</sup> The characteristics and the nature of these organic layers grown surrounding MNPs using the aforementioned strategies are even more important than the internal structure of the particles to control their behavior when an external magnetic field is applied (Figure 3f,g). Unfortunately, as discussed in detail in the previous section, attaining full control over the MNPs once they are incorporated into biological systems is still a challenge.

In addition to the importance of obtaining highly monodisperse MNPs with functionalized surfaces that make them stable and prevent their aggregation within hydrogel networks and if they are released from the scaffolds, the ideal MNPs for TE applications have to bear specific magnetic properties. In this sense, the designed MNPs must allow their manipulation through external magnetic fields for the fabrication of nanocomposite hydrogels with ordered structure. Moreover, magnetic nanostructures must behave as effective remote actuators for the magnetomechanical stimulation of the cells encapsulated within the scaffolds. For these purposes, superparamagnetic MNPs with high sensitivity to the application of external magnetic stimuli are especially appealing, allowing that hydrogels modified with low amounts of MNPs can be remotely stimulated by applying low-intensity magnetic fields. As mentioned, the concentration of MNPs and the intensity of the applied magnetic fields are two critical toxicity/safety factors that need to be minimized to bring magnetic hydrogels from bench to bedside. The sensitivity of MNPs to be controlled by an external magnetic field is quantified by the magnetophoretic mobility, a magnitude that increases in MNPs with large

magnetizations.<sup>120</sup> Among the different forms of iron oxides, MNPs with magnetite structure are those with higher magnetization values and, consequently, with higher magnetophoretic mobility, thus being the most indicated for TE applications.<sup>121</sup> MNPs with high magnetization for TE applications can also be obtained through the different aforementioned strategies, such as the incorporation of metallic dopants in their structure or the design of cubic-shaped MNPs.

Although MNPs with superparamagnetic behavior are the most commonly used in biomedical applications to preclude their aggregation as well as to avoid the generation of heat by magnetic hyperthermia when magnetic fields are applied, ferromagnetic MNPs can also be used in the field. It was reported that weakly ferromagnetic MNPs can self-organize in one-dimensional magnetic chains, it being an interesting non-explored strategy to fabricate magnetic nanocomposite hydrogels with anisotropic nano-/micro-topographies for TE.<sup>122</sup> Moreover, ferromagnetic MNPs (with no negligible remanences) can also be used to achieve higher magnetomechanical stimulation over cells encapsulated/seeded in the hydrogels under the application of alternating magnetic fields (AMFs). To design MNPs with weak ferromagnetic responses, increasing their size or doping levels with elements as cobalt or nickel might be suitable approaches.<sup>71</sup> Nevertheless, in the case of doping, the toxicity of cobalt and nickel ions must be considered, being necessary for the growth of nonpermeable coatings surrounding the MNPs to prevent potential metal ion leakage. Even so, the concentration of both cobalt-/nickel-doped magnetic material that can be used in biomedical applications must be rather low in order to prevent their potential associated cytotoxic effects.<sup>108</sup>

## MODULATION OF BIOMATERIAL'S FEATURES WITH MNPs FOR TISSUE ENGINEERING: ANISOTROPIC HYDROGELS AND REMOTE ACTUATION

Most tissues in the human body are characterized by a highly anisotropic hierarchically ordered structure.<sup>126</sup> This anisotropy stems from the extracellular matrix (ECM) organization, which defines the mechanical properties of these tissues and provides cells with the suitable biochemical and biophysical cues for their adhesion, proliferation, migration, and renovation.<sup>127</sup> The main challenge of TE and regenerative medicine is to design constructs that mimic the ECM properties and the cellular organization of native tissues, in order to induce the recovery of their specific features during the healing step.

Hydrogels are among the most promising materials to prepare scaffolds for tissue regeneration thanks to their water-rich structure, similar to that observed in biological tissues, mechanical performance, and high biocompatibility.<sup>7,8,128</sup> Several polymers of natural or synthetic nature can be used to produce hydrogels by polymer chain cross-linking using different triggers such as light, pH, temperature, or ionic strength.<sup>129</sup> By controlling the selected polymer and the cross-linking process, it is possible to prepare hydrogels with properties similar to those of different native tissues. However, the main drawback of hydrogels is their inherently isotropic and disorganized internal structure, characterized by randomly oriented 3D networks, which limits their applicability in engineering oriented biological tissues.<sup>130</sup> This characteristic has raised in recent years significant interest in the development of strategies allowing the modification of the hydrogel microstructure to provide them with the anisotropic organization required for their improved use in TE applications.<sup>16,34,131</sup> Numerous fabrication strategies have been devised

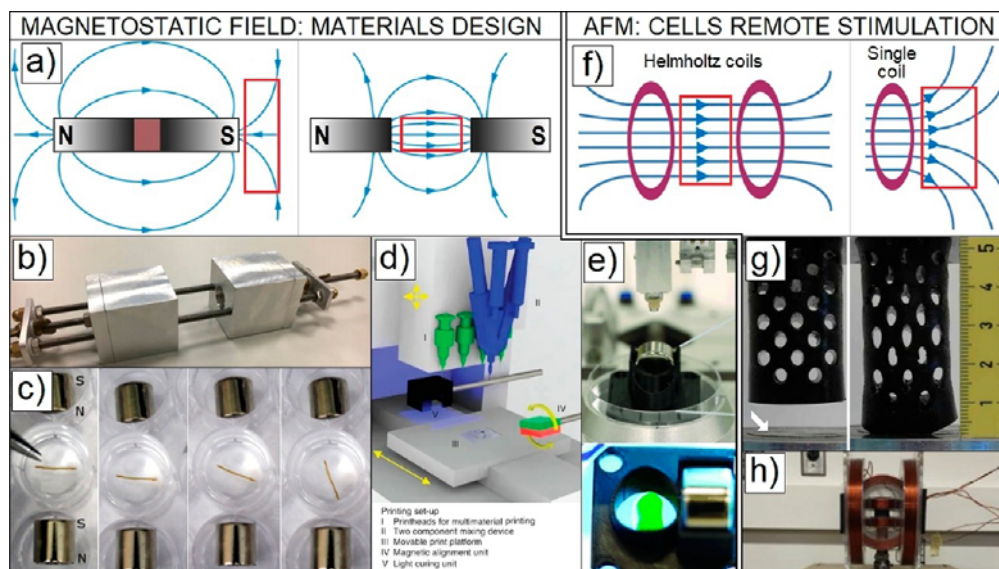


**Figure 4.** Magnetostatic fields to create anisotropic biomaterials: (a) Scheme of the magnetic field lines in a single magnet and in a two parallel magnets arrangement (in the first case, the lines are directed to the other pole of the magnet, while in the second one the lines go to the other magnet, creating a highly uniform field between them); (b, c) images of experimental configurations consisting of two permanent parallel magnets (Reproduced with permission from refs 29 and 144. Copyright 2019 American Chemical Society); (d) scheme of a 3D printer equipped with a rotary magnet (Adapted with permission from ref 147. Copyright 2015 The Authors under a Creative Commons CC BY License (<https://creativecommons.org/licenses/by/4.0/>), published by Springer Nature); (e) images of a magnetically assisted 3D printing system with a single magnet (Reproduced with permission from ref 148. Copyright 2018 Wiley-VCH). AMF for cells stimulation: (f) Scheme of the magnetic field created by a pair of Helmholtz coils and by a single coil, being the field more uniform in this first configuration; (g) single coil (white arrow) used to induce elongations and contraction of a magnetically responsive hydrogel (Reproduced with permission from ref 150. Copyright 2009 Wiley-VCH); (h) image of a experimental magnetic setup consisting on three pairs of Helmholtz coils (Reproduced with permission from ref 153. Copyright 2019 Elsevier).

in this field, the common ultimate goal being the preparation of biomaterials able to retain the desired anisotropic microstructure, establishing in this way a biomimetic tissue template to recover the native tissue architecture.

Besides the use of magnetic materials and their manipulation by external magnetic fields, which will be discussed in detail below, there are many other different strategies to generate anisotropic hydrogels. In this sense, directional freeze casting,<sup>132</sup> preparation of hybrid constructs with easily degradable/porous component,<sup>133</sup> shear-force<sup>134</sup> and electric-force<sup>135</sup> orientation of nanofillers, unidirectional compression<sup>136</sup> and ion diffusion<sup>137</sup> of hydrogel precursor solutions, or the controlled bottom-up assembly of microgel units<sup>138</sup> are strategies that have been proposed to create hydrogels with anisotropic architectures. Despite the promising results obtained with these systems, in most cases the proposed strategies do not allow the desired control over the hydrogels' architecture to engineer highly ordered tissues. Moreover, these approaches often require invasive postprocessing techniques to manipulate the hydrogel's architecture and have limited potential for their further external actuation.

In this sense, hydrogels with magnetically responsive properties are emerging as biomaterials with added functionalities allowing non-invasive remote control over their internal architecture and actuation. The application of external magnetic fields, typically combined with the previous incorporation of magnetic materials within hydrogels' structures, is a widely explored approach to create biomaterials with controllable anisotropic architectures.<sup>131,139</sup> Moreover, these designed scaffolds have other functions beyond acting as static structural support for TE applications. Mechanical stimuli are recognized to play key roles on the regulation of cell behavior. Remote

magnetic stimulation through magnetic responsive materials is emerging as one of the most interesting approaches to provide cells the adequate mechanical cues.<sup>140,141</sup> In this section, we cover the use of magnetism to design 5D hydrogel-based composites, which combine the typical 3D structure of hydrogels with the simultaneous remote control over their architecture and the possibility to stimulate encapsulated/seeded cells. The typical system configurations applied to generate and manipulate the magnetic fields in these strategies are also discussed.

**Magnetic Fields: Experimental Configurations for Fabrication and Cell Stimulation.** Fine control over the applied magnetic fields is a critical factor to achieve the desired design of magnetic scaffolds for their subsequent application in the field of TE. Depending on the experimental setup, the generated magnetic field can be static (at any given point its amplitude and direction are constant) or alternating (amplitude and direction continuously change, typically in periodic cycles). In the field of TE, magnetostatic fields are typically applied to generate anisotropy in the scaffolds, while AFMs are the most commonly used for the stimulation/remote actuation over materials and cells. However, in many published studies on magnetic strategies for TE, the description of magnetic configurations to produce the magnetic fields is not included. Aiming to encourage a more critical discussion on the topic in future studies, in this section the most often used setups for the generation of magnetic fields are reviewed in detail.

In order to produce magnetostatic fields, the most common experimental setup consists of two parallel permanent magnets, which allow one to control the amplitude of the generated field depending on the magnet intensities (by changing their size, composition, and purity, *etc.*) and the distances between

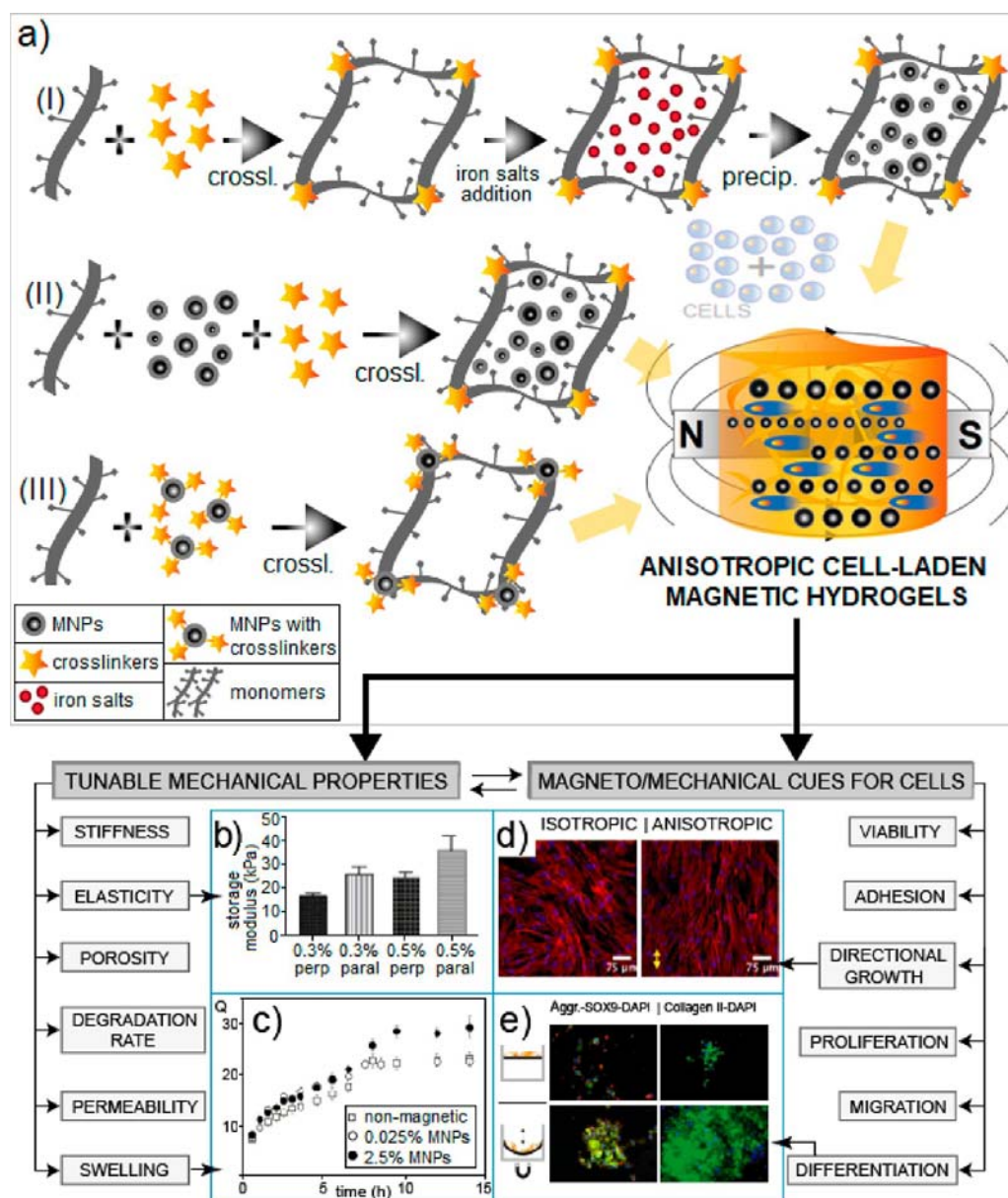


Figure 5. (a) Schematic representation of different strategies that can be used to prepare MNPs-loaded hydrogels: (I) *in situ* precipitation method (MNPs are synthesized by salt coprecipitation in the previously cross-linked hydrogels); (II) blending method (presynthesized MNPs are incorporated into a hydrogel precursor solution, resulting in a magnetic-loaded hybrid hydrogel after the cross-linking step); and (III) grafting-onto method (the surfaces of the presynthesized MNPs are modified with agents/molecules which act as cross-linkers for the formation of hydrogel networks). Combinations of these materials with cells under the application of external magnetic fields can be explored to design composites with tunable mechanical properties and magneto/mechanical remote actuation capability to control cell behavior. (b) Effect of incorporation of different amounts of perpendicularly and parallelly aligned magnetically responsive cellulose nanocrystals on the storage modulus of gelatin hydrogels (Adapted with permission from ref 29. Copyright 2019 American Chemical Society). (c) Swelling ratio ( $Q$ ) in phosphate buffered saline of  $\kappa$ -carrageenan hydrogels with and without MNPs inside at different concentrations (Adapted with permission from ref 184. Copyright 2012 Elsevier). (d) Influence of isotropic and anisotropic gelatin hydrogels on the alignment of seeded human adipose-derived stem cells (hASCs) (Adapted with permission from ref 29. Copyright 2019 American Chemical Society). (e) Up-regulation of chondrogenic markers aggrecan (in red), SOX9 (in green), and collagen II (in green) in magnetic hydrogels after the encapsulation of human mesenchymal stem cells, which are cultured under the application of magnetic stimulation (cell nuclei in blue, stained with DAPI) (Adapted with permission from ref 185. Copyright 2013 The Authors under a Creative Commons CC BY 3.0 License (<https://creativecommons.org/licenses/by/3.0/>), published by PLOS).

them.<sup>142</sup> More complex configurations based on a large number of permanent magnets with specific space distribution can also be established, their use being more extended in other applications such as magnetic drug delivery.<sup>143</sup> A single magnet could also be used to generate a magnetostatic field, but the field lines close on the other pole of the same magnet, making it

difficult to achieve uniform fields far from the magnet (Figure 4a). For instance, two parallel neodymium N52 magnets have been used to generate a magnetostatic field with an intensity of 108 mT to align magnetically responsive particles within hydrogel matrices (Figure 4b).<sup>29</sup> Similarly, in other work two 45 MegaGauss-Oersted neodymium magnets were positioned



35 mm apart to create a magnetic field of 30 mT in the center line of the magnets (Figure 4c).<sup>144</sup> As well, Tognato *et al.*<sup>145</sup> designed an experimental setup of two neodymium magnets separated 5 cm on a Teflon support, creating a 20 mT magnetic field that allowed the self-assembly of iron oxide MNPs along the field lines within hydrogels precursor solutions before their gelation.

Furthermore, magnetostatic fields can be combined with oscillation. There are commercially available devices that allow the application of magnetostatic fields at the same time as the magnets are subjected to periodic oscillations. For instance, using a commercial device (Magnefect, nanoTherics), cells seeded on magnetic scaffolds were stimulated under the application of 350 mT field combined with oscillation cycles of the magnets of 2 Hz and 0.2 mm of displacement.<sup>146</sup> In fact, these types of fields are not completely stationary; the low oscillation of the magnets causes small continuous variations in both the direction and field intensity applied to the samples. However, these variations are negligible and stimuli can be considered quasi-magnetostatic fields.

Three-dimensional (bio)printing techniques have emerged in recent years as one of the most interesting approaches to fabricate the scaffolds and cellularized constructs. By this methodology, it is possible to produce composites with a high degree of complexity and precision, where the final details can be designed at a micrometer scale level. In the case of magnetic scaffolds, the strategy of magnetically assisted 3D printing has been also proposed. Basically, it consists of the application of an external magnetic field at the same time that the printing process is taking place, in order to achieve the desired distribution of the magnetic elements incorporated into the (bio)inks. In this sense, all of the aforementioned magnetic configurations can be incorporated in the 3D printers to create the desired magnetically assisted printing system. In one of the pioneering works in this field, Kokkinis *et al.*<sup>147</sup> customized a commercial 3D printer with a rotary neodymium magnet. Using this configuration, the authors applied a 40 mT magnetic field rotating at 8.3 Hz to the magnetic inks during the 3D printing processes, achieving the drag forces required to promote a biaxial alignment of the magnetic elements within the plane of the rotating field (Figure 4d). More recently, an adaptor for a 2 mT cylindrical single magnet was designed and placed close to the printing surface, enabling the real-time remodeling of the magnetic (bio)ink while bioprinting (Figure 4e).<sup>148</sup>

On the other hand, the easiest form to produce AMF is using electromagnetic coils. When a current carrying conductor is arranged in the form of several loops (coil), a magnetic field that flows through the center of the coil along its longitudinal axis is created. If the applied current shows an alternating behavior, then the magnetic field will also be time-varying. In this case, the intensity and the frequency of the applied current, as well as the dimensions and number of turns of the coil, will define the characteristics of the generated magnetic field.<sup>142</sup> However, the main disadvantage of this configuration is the difficulty to achieve uniform magnetic fields (very long coils are required). In this sense, the use of Helmholtz coils has been more extensively adopted, since they allow obtaining quasi-uniform AMF in larger spaces between the two coils that configure the system (Figure 4f).<sup>149</sup> For instance, Fuhrer *et al.*<sup>150</sup> used a single coil to create variable magnetic fields and magnetomechanically stimulate hydrogels modified with cobalt MNPs for muscle TE purposes. By varying the current on the coil between 0 and 1.58 A, the highest magnetic field strength generated on the pole of the

electromagnet was 530 mT, enough to induce elongation and contraction movements on the designed scaffolds (Figure 4g). Helmholtz coils have been used for the magnetic stimulation of cardiac cells seeded on alginate-based hydrogels.<sup>151</sup> By passing an electrical current of 1.37 A through the coils separated 45 mm apart, the authors generated an AMF with 1.5 mT of intensity and 40 Hz of frequency. In a more recent work, the AMF produced by a pair of Helmholtz coils was used to promote the osteogenic differentiation of stem cell cultures on hydroxyapatite/collagen scaffolds.<sup>152</sup> The coils (30 cm radius) were placed at a distance of 15 cm, allowing the generation of uniform magnetic fields with adjustable intensities and frequencies (up to 4.7 mT and 100 Hz, respectively). Complex systems consisting of more than one pair of Helmholtz coils have been also considered for TE applications, in order to alter the 2D plane of the applied field during the magnetic stimulation (Figure 4h).<sup>153</sup> Taken together, the wide design space allowed by the use of Helmholtz coils or similar AMF setups in biomaterials fabrication, particularly if combined with advanced biofabrication strategies such as 3D bioprinting systems, suggest that there are promising approaches open to be explored in the field.

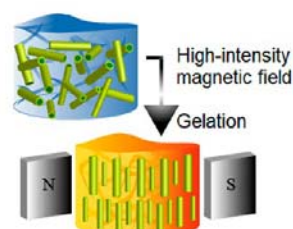
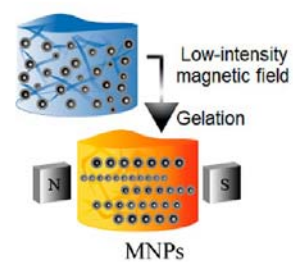
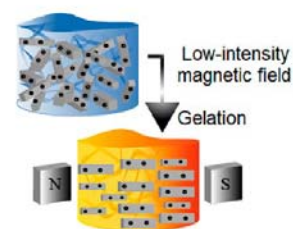
#### Magnetically Assisted Design of Anisotropic Biomaterials and Remote Actuation to Guide Cell Behavior.

Magnetism has been widely used to induce the desired anisotropy degree in hydrogels that mimic native tissues of the human body. The weak magnetic response of different nonmagnetic materials, such as polymers or proteins, has been exploited to create anisotropic structural patterns in hydrogels through the application of high-intensity magnetic fields. However, the incorporation of magnetic materials and the control over their response under low-intensity external magnetic stimuli has been the preferred strategy for the design anisotropic hydrogels.<sup>22,23</sup> The possibility of remotely controlling the behavior of MNPs through the application of external magnetic fields makes these particles excellent candidates to modify the characteristics of magnetically responsive nanocomposite hydrogels.<sup>154</sup>

To achieve the desired distribution of the magnetic elements within the biomaterials, the applied magnetic fields are typically magnetostatic (the field intensity and direction do not change with time). Under the effect of these fields, magnetic materials are subjected to uniform forces, allowing one to reach the desired anisotropy by controlling the intensity, the direction, and the duration of the magnetic stimulus (Figure 5). The anisotropic physical properties of composite scaffolds are key biophysical cues able to activate intracellular biochemical signals that control the functional processes of encapsulated/seeded cells, such as their growth, migration, and, in the case of stem cells, their differentiation into specific lineages.<sup>25</sup> Moreover, the incorporation of the fillers has also important effects over other physical properties of the resulting composites. Since MNPs act as reinforcement elements, their presence modifies the stiffness, toughness, and elasticity of the scaffolds, among other physical properties that can be harnessed for particular TE strategies. The influences of biomaterials stiffness,<sup>155</sup> degradation rate,<sup>156</sup> swelling ability,<sup>157</sup> or nonlinear elasticity<sup>158</sup> over cell behavior are well-documented (Figure 5b–e).

On the other hand, the application of magnetic fields has on its own an important influence on biological systems, independently of the presence of magnetic materials.<sup>159,160</sup> Magnetic stimulation can activate numerous sensitive receptors on the cell's surface and further activate related signaling pathways. It was recently demonstrated that even extremely

**Table 3. Main Advantages and Disadvantages of Using the Different Types of Fillers Explored to Prepare Magnetically Responsive Hydrogels**

type of filler	advantages	disadvantages
 <p>DIAMAGNETIC MATERIALS</p>	<p>Natural materials with low toxicity potential that present a weak magnetic response can be used.</p> <p>Constructs with highly-anisotropic structures can be designed using diamagnetic fillers with high aspect ratio.</p> <p>Simple preparation process.</p>	<p>Potential damaging high-intensity magnetic fields are required to manipulate the fillers (&gt; 400 mT for cellulose nanocrystals, &gt; 5 T for collagen).</p> <p>Non suitable for the remote magnetic stimulation of cells encapsulated within the constructs.</p>
 <p>MNPs</p>	<p>Low-intensity magnetic fields are required to manipulate these materials (&lt; 10 mT).</p> <p>Suitable for the remote magnetic stimulation of cells encapsulated in the constructs.</p> <p>Simple preparation process.</p>	<p>Low control over individual MNPs interdistance and over their aggregation degree.</p> <p>High amounts of MNPs are typically required to design anisotropic hydrogels with remote actuation capability.</p>
 <p>MAGNETIC ANISOTROPIC NANO/MICROSTRUCTURES</p>	<p>Low-intensity magnetic fields are required to manipulate these materials (&lt; 10 mT).</p> <p>Composites with very high anisotropic degrees can be prepared.</p> <p>Low amounts of magnetic material are sufficient to design the composites.</p> <p>Suitable for the remote magnetic stimulation of cells encapsulated in the constructs.</p>	<p>Complex preparation process with multiple steps: nano/microstructures synthesis, magnetic modification, incorporation within hydrogels, etc.</p> <p>Potential low colloidal stability of magnetically-modified microstructures due to their large size and magnetic attraction.</p>

weak magnetic fields have an important effect over stem cells' proliferation and differentiation *in vivo*.<sup>161</sup> The authors found that the application of 100–400  $\mu\text{T}$  magnetic fields during the first 3 days postinjury induces faster regeneration of amputated planarias (free-living flatworms capable of regenerating all tissues owing to a large adult stem cell population). This behavior was attributed to the interaction of biological systems and magnetic fields through s radical pair's recombination, producing changes in the reactive oxygen species accumulation and proteins expression.

As well, the incorporation of MNPs within the hydrogels creates nanoscale magnetic fields that generate micromagnetic driving forces in the interfaces between cells and scaffold, allowing remote cell stimulation. Thus, the presence of MNPs promotes the activation of numerous sensitive receptors on cells' surfaces, thereby interfering with cell activity and allowing control of their behavior.<sup>162</sup> The combination of cell-laden hydrogels with magnetic materials within their structure and the application of external magnetic fields produces high variations on the mechanical loading of the composites.<sup>163,164</sup> Tay *et al.*<sup>165</sup> quantified the forces associated with the magnetic stimulation of magnetic microparticles encapsulated within hyaluronic acid hydrogels. Depending on the distance between a 2 T permanent magnet and the polymeric samples, these authors calculated that the force exerted on the particles, and consequently on the

encapsulated neural cells, varied between 0.15 (at 6.5 cm) and 1.00  $\mu\text{N}$  (at 3.5 cm).

The typical magnetic fields applied for remote cell stimulation are alternating, although magnetostatic fields have been also used for this purpose.<sup>166,167</sup> The continuous variation of both the field intensity and direction causes the forces over the cells and the magnetic materials also to vary in the same way. Thus, by controlling the intensity, the frequency, and the duration of the magnetic field, magnetomechanical stimulation of cells has emerged as a potential tool to direct cell behavior. Specific examples of magnetomechanical cell stimulation are explained in detail in the following sections.

Overall, the application of external magnetic fields can be used both to fabricate anisotropic hydrogels and to remotely stimulate the encapsulated cells. The combination of magnetic stimuli with the incorporation of magnetic materials within the hydrogels allows higher mimicking degrees of the anisotropic physical/mechanical properties of native tissues (Figure 5b,c), while enabling remote mechanical stimulation of the encapsulated/seeded cells at relevant cell scale levels. By controlling the magnetic forces exerted on the composites, it is possible to modify the mechanical loading of the magnetic hydrogels to promote cells differentiation toward different lineages, as well as their positioning, growth, and proliferation (Figure 5d,e). This combined control over biomaterial's architecture and actuation over the biological component is a key advantage of magnetic

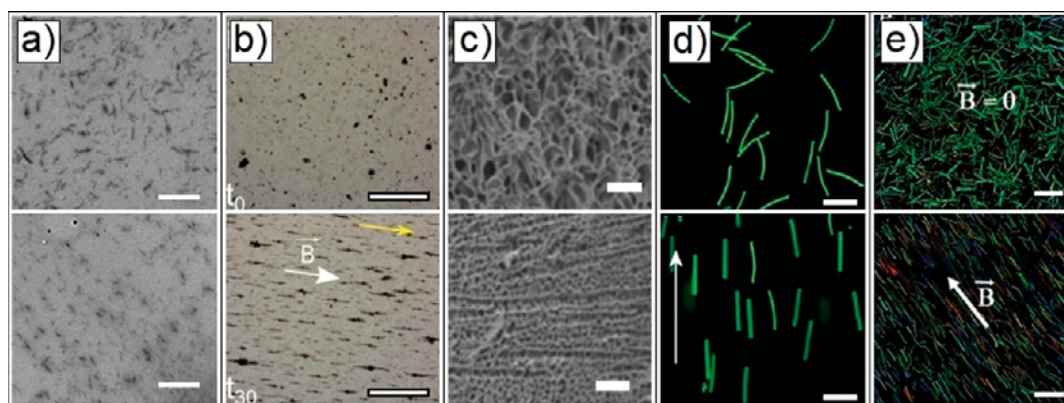


**Figure 6.** Microscopy images of anisotropic hydrogels prepared by incorporating magnetically responsive materials and the subsequent application of external magnetic fields. Top images show the samples in static conditions and down images show the samples under the effect of a magnetic field. (a) Cryosectioned TEM images of poly(oligoethylene glycol methacrylated)-based hydrogels with incorporated diamagnetic cellulose nanocrystals in static conditions and exposed to 1.2 T magnetic field during gelation (Scale bars = 1  $\mu\text{m}$ . Reproduced with permission from ref 177. Copyright 2017 American Chemical Society). (b) Time-lapsed pictures of the growing filaments of maghemite MNPs in GelMA solutions when subjected to a magnetostatic field. Initially, the MNPs are randomly dispersed, assembled along the magnetic field lines when it is applied (Scale bars = 500  $\mu\text{m}$ . Adapted with permission from ref 145. Copyright 2018 Wiley-VCH). (c) SEM images of freeze-dried gelatin hydrogels containing 0.5% (w/w) cellulose nanocrystals modified with MNPs in static conditions and under 108 mT magnetic fields (Scale bars = 10  $\mu\text{m}$ . Reproduced with permission from ref 29. Copyright 2019 American Chemical Society). (d) Optical microscopy images of poly(ethylene oxide-*stat*-propylene oxide) rod-shaped microgels modified with MNPs in static conditions and under a 100 mT magnetic field (Scale bars = 50  $\mu\text{m}$ . Reproduced with permission from ref 196. Copyright 2017 American Chemical Society). (e) Depth color-coded images of electrospun PLGA magnetic short fibers inside fibrin hydrogels in static conditions and in the presence of 100 mT magnetic field (Scale bars = 100  $\mu\text{m}$ . Reproduced with permission from ref 204. Copyright 2017 Wiley-VCH).

hydrogels over nonmagnetic systems that can be explored to closer mimic the microenvironments of complex native tissues in multiple axes.

**Strategies to Prepare Anisotropic Magnetically Responsive Hydrogels.** To manipulate the physical properties and enable remote actuation of hydrogels, the incorporation of monodisperse and biocompatible nano- and/or microelements and their further controlled organization are usually required.<sup>16,50</sup> As mentioned previously, in order to control the behavior of these elements within the hydrogel's structure, the use of magnetism has been one of the most explored mechanisms.<sup>21</sup> Typically, the preferred strategies rely on the control of the organization of MNPs, free or as a part of larger anisotropic hierarchical nano-/microparticles, within polymer matrices to create anisotropic and magnetically responsive hydrogels. However, although diamagnetic materials are usually considered nonmagnetic, they can respond to high-intensity magnetic fields and, therefore, their magnetic manipulation has also been explored for the design of anisotropic hydrogels. Advantages and disadvantages of both strategies are discussed here (Table 3).

**Diamagnetic Materials-Loaded Hydrogels.** Under the presence of an external magnetic field, the electrons surrounding the atomic nuclei of the materials respond, generating currents that try to counteract the effects caused by the applied field. Any material shows this weak opposition to an applied magnetic field, which is known as diamagnetism.<sup>168</sup> In this way, for example, when diamagnetic rod-shaped particles are exposed to an external magnetic field, they align perpendicularly to it, since only their smallest dimension opposes the field, thus minimizing the repulsion force.

The diamagnetic properties of various materials have been explored to generate anisotropic structures after their incorporation in hydrogel matrices. However, the weak response of diamagnetic materials requires high-intensity magnetic fields to allow their desired orientation.<sup>169–171</sup> Although the advances on

superconducting technology in the past few years have allowed the production of strong magnets needed to generate these high-strength magnetic fields, in some cases, the required intensities are too high and compromise the safety in view of the potential transfer of the experiments to clinical practice. The diamagnetic response of different hydrogel precursor compounds has been analyzed to obtain anisotropic constructs. For instance, collagen<sup>172</sup> and fibrin gels<sup>173</sup> with highly anisotropic architectures were prepared through the application of external magnetic fields up to 7 and 9.4 T, respectively, taking advantage of their diamagnetic properties. In other relevant work, a rotating magnetic setup (7 T) was used to obtain hydrogels with consecutive collagen layers showing orthogonal anisotropy (mimicking the architecture of the cornea).<sup>174</sup> Human corneal cells (keratocytes) seeded onto the designed constructs were aligned both on the surface and within the bulk of the orthogonal collagen hydrogels, mimicking the biological structure of native corneal.

The diamagnetic response of carbon nanotubes<sup>175</sup> and graphene oxide particles<sup>176</sup> was also exploited to create anisotropic polymer gels, observing in both cases that magnetic fields up to 10 T are required to obtain the desired alignment. De France *et al.*<sup>177</sup> designed an injectable anisotropic PEG-based hydrogel modified with magnetically responsive cellulose nanocrystals. The authors demonstrated that a 1.2 T magnetic field was enough to induce the alignment of the nanocrystals during gelation, generating anisotropic scaffolds with directional-dependent mechanical properties and able to promote the alignment and differentiation of encapsulated skeletal muscle myoblasts (Figure 6a). In a similar approach, a 400 mT magnetic field allowed the orientation of cellulose nanocrystals within gelatin hydrogels, in this case trying to mimic tendon architecture.<sup>178</sup> The low magnetic field required for the alignment of the nanocrystals was attributed to the adsorption of polymer chains onto their surface that increases their effective volume and, consequently, cooperatively contribute with other



particle–particle physical interactions for their susceptibility to magnetic alignment.

These studies are representative examples of how the diamagnetic response of different nanomaterials is certainly a promising approach to create hydrogels with well-defined anisotropic structures. However, as mentioned, this strategy requires the use of potentially damaging high-intensity magnetic irradiations. Moreover, the composites synthesized on the basis of this method do not allow their further remote actuation using non-invasive techniques.

**MNPs-Loaded Hydrogels.** The most efficient approach to induce internal order within hydrogel matrices by the application of external magnetic fields is through the incorporation of MNPs.<sup>179</sup> The strategies described in **Magnetic Nanoparticles** can be used for the design of highly monodisperse MNPs with the desired magnetic properties, allowing great control over their response within the hydrogels when magnetic fields are applied. Thus, MNPs should be superparamagnetic in order to control their behavior and prevent aggregation phenomena. Furthermore, MNPs with high magnetization values can be guided using low-amplitude magnetic fields, avoiding the risks and the expensive setups associated with intense magnetic irradiations. However, in most cases the preparation of MNPs with a high control over their physicochemical and magnetic properties has not been among the main priorities in the design of magnetically responsive scaffolds for TE.

Hydrogels with a magnetic component embedded in the matrix are commonly named as magnetic hydrogels or ferrogels. Several procedures have been reported for the preparation of magnetic hydrogels, including *in situ* precipitation, dip-coating, blending, and grafting-onto as the most common methodologies.<sup>23</sup> In the *in situ* precipitation method, iron salts are incorporated into a hydrogel matrix and, then, the coprecipitation of these salts yields MNPs within the hydrogel network.<sup>180</sup> As mentioned in previous sections, the last synthetic method does not allow great control over the MNPs' physical and magnetic properties and their subsequent order (Figure 5a). In the dip-coating, blending, and grafting-onto methods, the MNPs and the hydrogels are prepared separately, which allows the design of high-quality MNPs as well as of well-controlled nano-/micro-topographies. The dip-coating procedure consists of the preparation of a porous scaffold and its subsequent immersion in a ferrofluid for a specific time, allowing the magnetic fluid to impregnate the surface and penetrate into the polymeric composite.<sup>181</sup> The main disadvantage of this method is the difficulty of achieving full control over the distribution of the MNPs on the final magnetic scaffolds. In both the *in situ* precipitation and dip-coating methods, simultaneous cell encapsulation during hydrogel preparation is not possible. The blending method consists of the simple mixture of MNPs and the hydrogel precursor solution and the subsequent polymer cross-linking, producing hybrid magnetic loaded hydrogel networks.<sup>182</sup> However, this procedure usually tends to produce undesirable MNPs aggregates within the hydrogel matrix (Figure 5a). In the grafting-onto method or covalent bonding, the MNPs surfaces are modified with suitable functional groups that act as cross-linkers in the presence of the hydrogel precursor, allowing the formation of hydrogels with the MNPs covalently bonded to the polymeric networks (Figure 5a).<sup>183</sup> The use of nanofillers as multifunctional cross-linkers often results in nanocomposites with considerably higher mechanical

properties than those achieved by the simple noncovalent incorporation of nanofillers within the polymer matrix.

Following a blending methodology, methacrylated gelatin (GelMA) anisotropic hydrogels modified with co-precipitated maghemite MNPs were designed for skeletal muscle TE.<sup>145</sup> Presynthesized MNPs were incorporated in the hydrogel precursor solutions and assembled in oriented filaments using 20 mT magnetostatic fields generated with a two parallel magnets configuration. Then, the solutions were cooled below the melting temperature to stabilize the assembled structures prior to the final UV-light cross-linking (Figure 6b). In another work, magnetically responsive hydrogels were prepared through an *in situ* precipitation strategy.<sup>186</sup> Hydrogels consisting of a  $\kappa$ -carrageenan and PVA mixture were prepared and immersed in a 0.1 M solution of iron(II) chloride for 2 h. After that, sodium hydroxide and hydrogen peroxide were added to produce ferrous hydroxide and oxidize it, respectively, rendering 50–100 nm iron oxide MNPs in the form of elliptical magnetic clusters. A rod-shaped magnet was used to apply a 150 mT magnetic field, observing that the distribution of MNPs provided composites with anisotropic response to external magnetic stimuli. On the other hand, the grafting-onto approach has also been explored to synthesize magnetic hydrogels with anisotropic architectures. For instance, spindle-like hematite NPs functionalized with methacrylate groups were used as exclusive cross-linkers in the preparation of magnetically responsive polyacrylamide hydrogels.<sup>187</sup> The elongated magnetic particles were oriented through the application of external magnetic fields during the polymerization process, creating composites with highly uniaxial anisotropic structure. Due to the antiferromagnetic nature of hematite, magnetic fields up to 587 mT were required to align the particles within the polymeric networks.

Although iron oxide-based MNPs are the most commonly incorporated within the hydrogels' networks to generate magnetically responsive scaffolds, other nanoparticles with different compositions have also been evaluated. For example, the use of magnetic stimuli to control the distribution of nickel nanorods incorporated in gelatin-based hydrogels following a blending method has been successfully explored.<sup>188</sup> In a similar way, agar composites modified with carbonyl iron particles were prepared and then aligned by the application of external magnetic fields.<sup>189</sup>

**Hierarchical Hydrogels Incorporating Magnetic Anisotropic Nano-/Microstructures.** In many cases, the control over the anisotropy degree and the remote actuation capability of magnetic hydrogels by the direct incorporation of free MNPs is not satisfactory for the intended application. A full control over the aggregation state and/or the interdistances between the individual MNPs under an external magnetic field is still a challenge, hindering the generation of global anisotropy in the hydrogel networks.

As alternatives, the use of anisotropic nano- and, particularly, micrometric particles is especially interesting. Since they can be aligned according to their main axis within the hydrogels, this strategy can recreate the hierarchical and highly anisotropic organization of the native tissues.<sup>190–192</sup> Unfortunately, although most common magnetic materials such as iron oxide nanoparticles have shown good biocompatibility, *a priori* it is not biologically viable to incorporate micrometric sized fully magnetic particles in hydrogels because the high amount of magnetic material required to provide anisotropic microstructures would jeopardize their biocompatibility. The critical toxic concentration of MNPs depends on their physicochemical

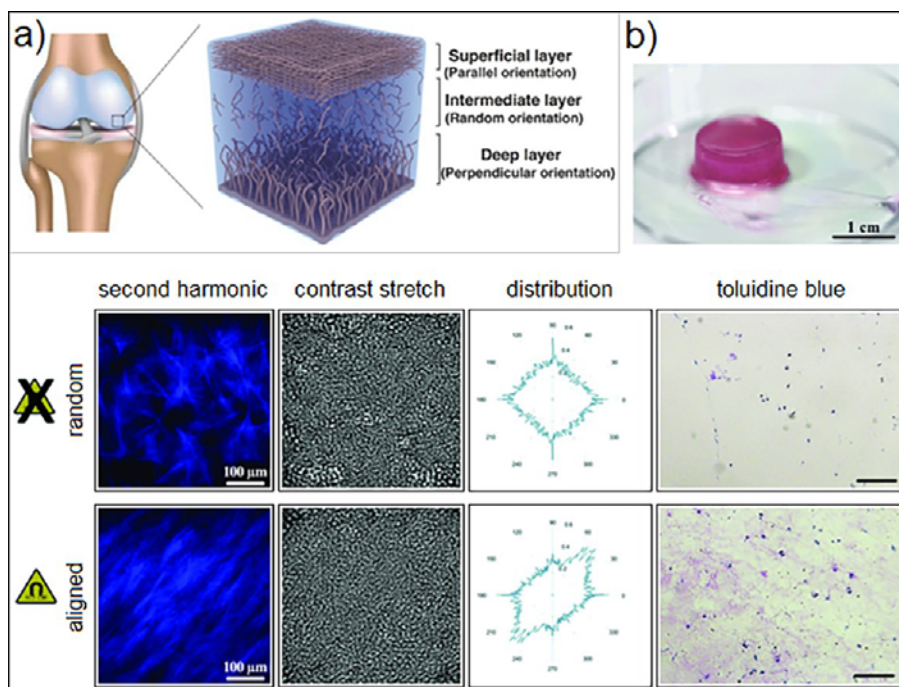


**Figure 7.** (a) Schematic illustration of the anisotropic architectural organization of cartilage tissues (Reproduced with permission from ref 34. Copyright 2017 Wiley-VCH). (b) Application of magnetic hydrogels in cartilage TE: development of bioprinted two layered collagen-based hydrogels. Second-harmonic and contrast stretch images showed that in the superficial layer the collagen fibers were aligned by applying an external magnetic field, while in the middle layer the fibers are randomly oriented, mimicking the anisotropy of cartilage tissue. Toluidine blue histological staining demonstrated the proteoglycans production in bioprinted samples with random and aligned collagen fibers (Scale bars = 100  $\mu\text{m}$ . Adapted with permission from ref 148. Copyright 2018 Wiley-VCH).

characteristics, but as reference, it is usually around a few tens to a few hundred of milligrams per liter.<sup>193–195</sup> Moreover, the desired superparamagnetic behavior of MNPs also limits their size to a few tens of nanometers.

To decrease the amount of required magnetic material and prevent the associated cytotoxic effects, nonmagnetic anisotropic elements can be prepared and further magnetically modified, either by binding MNPs to their surface<sup>29</sup> or by incorporating MNPs inside their volume.<sup>196</sup> Afterward, it is possible for the subsequent alignment of the anisotropic elements by the application of low-intensity external magnetic fields. As mentioned above, due to their low cost, low toxicity, easy production, and suitable magnetic properties, SPIONs are the most commonly used particles to provide magnetic response to these structures, allowing their remote guiding within the 3D space of hydrogels networks.

Several methods have been developed in the past decades for the production of these biocompatible anisotropic elements, the most common ones being photolithography,<sup>197</sup> electrospinning,<sup>198</sup> molding,<sup>26</sup> microfluidics,<sup>199</sup> or liquid shearing.<sup>200</sup> Fibers and rod-shaped micro- and nanoparticles are especially interesting, since their highly elongated shapes can induce relevant anisotropy degrees within the hydrogels by their alignment at reduced magnetic material contents. For instance, we synthesized iron oxide MNPs through the co-precipitation of  $\text{Fe}^{2+}$  and  $\text{Fe}^{3+}$  salts in the presence of rod-shaped cellulose nanocrystals, obtaining cellulose rods decorated with 6.5 nm sized SPIONs.<sup>29</sup> The derived magnetic structures were incorporated into injectable gelatin hydrogels, resulting in solutions with a global SPIONs concentration of 0.0005% (v/v). Next, a 108 mT magnetostatic field created by two parallel magnets during gelation was enough to align the hybrid particles

in order to generate anisotropic scaffolds that allowed the directional growth of hASCs (Figure 6c). Compared with the works of our group and others mentioned above,<sup>177,178</sup> the incorporation of MNPs to the structure of cellulose nanocrystals allowed a significant decrease on the applied magnetic field required for hybrid rod-shaped particles alignment (from 400 to 1200 mT to 108 mT). In another work, calcium sulfate rods were coated with SPIONs and incorporated into a PEG-based hydrogel precursor solution.<sup>201</sup> The authors showed that the alignment of the magnetic rods could be achieved through the application of external magnetic fields up to 100 mT, and these can be then dissolved in aqueous solution generating anisotropic pores within the hydrogel network. However, the size of the pores created was too small for cell in-growth.

MNPs can also be incorporated into the internal structure of rod-shaped microparticles during their preparation, avoiding subtle hydrodynamic size increases and/or colloidal stability issues faced when MNPs are bonded on the surface of nonmagnetic particles. Rose *et al.*<sup>196</sup> prepared rod-shaped microgels by a mold lithography approach using a star-PEG solution containing water-soluble SPIONs, giving rise to anisotropic and magnetic responsive polymer microgels. These magnetic structures were mixed with a polymer precursor solution before cross-linking under an applied magnetic field of 130 mT, rendering hydrogels with well-defined anisotropic structure provided by alignment of the rod-shaped magnetic microgels (Figure 6d). In a slightly different approach, the microgels modified with MNPs can be bottom-up-assembled in a controlled way under the application of magnetic fields, generating magnetically responsive hydrogels with the desired anisotropic architectures.<sup>202</sup> Following this strategy, MNPs were incorporated within PEG microgels prepared by a micromolding

technique and then their magnetic assembly was promoted.<sup>203</sup> By controlling the microgel's size, the MNPs concentration, and the characteristics of the applied magnetic fields created by parallel magnets, the authors obtained different assembled structures, such as single rows, arrays, or three-layer spheroids. Magnetically modified electrospun fibers are another example of fillers that have been used to design anisotropic hydrogels. Omidinia-Arkoli *et al.*<sup>204</sup> added SPIONs to a poly(lactide-co-glycolide) (PLGA) solution for the preparation of short microfibers by electrospinning/microcutting technique. The magnetic microfibers were then incorporated to a fibrin-based hydrogel matrix, and their alignment was achieved under the application of magnetic fields between 100 and 300 mT, depending on the fibers' length and SPIONs' concentration. The induced microfiber anisotropic organization modified the mechanical properties of the hydrogel and also provided remote control over the morphology and directional growth of the encapsulated cells (Figure 6e).

These representative examples showed that the use of magnetically modified fibers/rod-shaped microparticles is a promising strategy to create anisotropic hierarchical hydrogels with native tissues-like ordered microstructures which have the potential to impact the behavior of encapsulated cells.

## APPLICATIONS OF MAGNETIC HYDROGELS IN TISSUE ENGINEERING

The healing response of the human body following an injury event is naturally programmed to reestablish hemostasis and invariably leads to the formation of a reparative fibrotic scar tissue that replaces the original cells and the ECM. However, the newly formed scar tissue has lower structural organization, poorer biomechanical properties, and inferior functionality compared to the uninjured ones.<sup>205</sup> The ultimate goal of regenerative strategies is to bioengineer systems capable of either triggering this natural reparative process or even completely replacing damaged and low-functional tissues, while guiding new tissue formation and recovering their original functionality. The achievement of this ultimate goal implies the need to control multiple biophysical, biochemical, and biological cues of cells' microenvironment *in vitro* during the maturation steps and *in vivo* after transplantation of the tissue-engineered construct. Magnetic hydrogels are multifunctional scaffolding biomaterials that provide the means to (remotely) control many of these cues, in particular the biophysical, which are not available in other nonmagnetic responsive systems.

Many tissues in the body present an anisotropic organization of specific elementary structures with dimensional levels spanning from the nano- to macroscale (Figures 7–12), which confers them different mechanical, optical and electrical properties.<sup>126</sup> In native tissues, the biological signaling originated from cell morphology (the orientation and localization of subcellular organelles and cell polarity) defined in response to the structural and mechanical properties of tissues are known regulators of cell fate. In TE applications, controlling the 3D geometrical parameters of scaffolding biomaterials are effective strategies to regulate cell spreading, migration, and morphology that consequently impact their morphogenesis.<sup>206</sup>

As mentioned above, magnetic hydrogels with anisotropic architectures provide not only an ordered 3D template in which the complex architectural properties of native tissues can be replicated but also add control over cell behavior. It is well-known that the topography and hierarchical architecture of scaffolding biomaterials impact the response of the encapsu-

lated/seeded cells, controlling their proliferation, migration, and differentiation (cell contact guidance phenomenon), whose specific requirements are highly tissue dependent.<sup>207</sup>

For instance, tendon (tenocytes) and skeletal muscle cells are characterized by elongated morphologies, reminiscent of the uniaxially aligned topography and fibrous hierarchical organization of their ECM niche. Therefore, anisotropic scaffolding biomaterials with a high degree of structural alignments have been shown to prevent phenotype drift of tenocytes, induce the tenogenic differentiation of the stem cells,<sup>141,208</sup> and promote tissue regeneration *in vivo*. Similar architectural requirements are also needed for proper cardiac and neuronal tissue regeneration, whose cells are characterized by anisotropic morphologies and organizations, being short, narrow, and fairly rectangular in shape in the case of cardiomyocytes and presenting more complex shapes in the case of neural cells.<sup>209</sup> Anisotropic hydrogels are a promising approach to recreate not only the proper 3D topographical cues that characterize tissues with characteristic uniaxial alignment but also tissues that present gradients of ECM architectural organization such as cartilage or tissue interfaces such as tendon-to-bone<sup>210</sup> and osteochondral tissues.<sup>211</sup>

In addition to the geometrical (topographical and architectural) cues, the cells' response to external forces plays crucial roles in the development, organization, function, and fate of different tissues.<sup>212</sup> The mechanisms by which cells convert mechanical stimuli into biochemical signaling, known as mechanotransduction,<sup>213</sup> are complex, but among its different origins is the signaling resulting from the integrin-mediated interaction with the ECM and the forces conveyed by cell cytoskeleton organization.<sup>214</sup> The direct application of mechanical stimuli has been shown to considerably improve the *in vitro* maturation performance of tissue-engineered constructs developed for the regeneration of several mechanosensitive tissues such as tendon, skeletal muscle, cartilage, or bone.<sup>215,216</sup> Thus, besides the advantages related to fabrication aspects of the biomaterial, magnetic hydrogels where cells are seeded or encapsulated can be intrinsically leveraged as mechanostimulatory materials to actively interact with these biological systems. Since the remote magnetomechanical stimulation of the cells (compression, tension, and shear) can be wirelessly performed by exerting forces in the incorporated magnetic materials with external magnetic fields, this supposes an additional non-invasive tool that can be exploited to provide cells with the adequate biomechanical stimuli. The mechanical stimuli delivered through magnetic hydrogels are usually related to the magnetically actuated deformation and movement of the polymeric material where the nanoparticles are embedded. However, the nano-/microscale dimensions of the cell focal adhesion clusters (typically 0.2–10  $\mu\text{m}^2$ )<sup>217</sup> also suggest that the nanoparticles themselves can directly actuate on these important cell surface mechanotransducers if they come in close proximity within the hydrogel network.

Besides the aforementioned biomechanical forces, other biophysical cues of the cell microenvironment such as ECM or scaffold stiffness are now well-established factors implicated in the specification of cell fate.<sup>212</sup> For instance, it has been widely demonstrated that soft hydrogels tend to direct stem cell commitment toward soft tissue phenotypes (*e.g.*, neurogenic), whereas stiff hydrogels favor their differentiation into hard tissue phenotypes (*e.g.*, osteogenic). Moreover, while in 2D surfaces cells tend to develop stronger adhesion on stiffer surfaces; in 3D matrices the dynamic remodeling of these transmembrane



**Table 4. Characteristics and MNPs Concentrations in Magnetic Hydrogels and Magnetic Field Intensities Used in Different Tissue Engineering Applications**

composition	size (nm)	synthetic method <sup>a</sup>	concentration	magnetic field (mT)	TE type	ref
Fe	11	C. A.	10% (v/v)	2	cartilage	148
cobalt		C. A.	166 mg·mL <sup>-1</sup>	800	cartilage	185
Fe <sub>3</sub> O <sub>4</sub>	110	C. A.	0.1% (v/v)		cartilage	227
Fe <sub>3</sub> O <sub>4</sub>	100	C. A.	1–20% (w/w)	500	cartilage	228
Fe <sub>3</sub> O <sub>4</sub>	10	thermal decomposition	0–10% (w/w)	15	bone	243
Fe <sub>3</sub> O <sub>4</sub>	71.5	co-precipitation	2.5–5.0 mg·mL <sup>-1</sup>	240	bone	246
Fe <sub>3</sub> O <sub>4</sub>	10	co-precipitation	0.5–1.0 mg·mL <sup>-1</sup>	400	bone	249
γ-Fe <sub>2</sub> O <sub>3</sub>	10–15	co-precipitation	0–80% (w/w)		bone	250
iron oxide <sup>b</sup>	7	co-precipitation	5 × 10 <sup>-4</sup> % (v/v)	108	tendon	29
Fe <sub>3</sub> O <sub>4</sub>	250	C. A.	0.018:1 (% w/w)	350	tendon	146
Fe <sub>3</sub> O <sub>4</sub>	10	<i>in situ</i> precipitation		350	tendon	261
Fe <sub>3</sub> O <sub>4</sub>	250	C. A.	1.8–3.6% (w/v)	350	tendon	299
iron-based	7	co-precipitation	0.2–0.4 mg·mL <sup>-1</sup>	350	enthesis	28
cobalt	25	C. A.	150 mg·mL <sup>-1</sup>	530	skeletal muscle	150
Fe <sub>3</sub> O <sub>4</sub>	200	C. A.	37.5% (w/w)	335	skeletal muscle	273
iron oxide	50	C. A.	2.5 mg·mL <sup>-1</sup>	150	skeletal muscle	291
Fe <sub>3</sub> O <sub>4</sub>	780	co-precipitation	1.2% (w/v)	1.5	cardiac	151
iron oxide	80	co-precipitation			cardiac	290
iron oxide		co-precipitation	20–40 mg·mL <sup>-1</sup>		cardiac	292
iron oxide <sup>c</sup>	11–12		2–8% (w/w)		neural	144
	1000	C. A.	500 μM		neural	165
iron oxide <sup>d</sup>		C. A.	0.4–1.0 mg·mL <sup>-1</sup> ; 1.0–3.0% (v/v)	130	spinal cord	196
Fe <sub>3</sub> O <sub>4</sub> <sup>e</sup>	5.2		1% (w/w); 0.015% (v/v)	300	muscle/neural	204
Fe <sub>3</sub> O <sub>4</sub> ; γ-Fe <sub>2</sub> O <sub>3</sub>	100	C. A.	0.05% (w/v)	26	neural	296
iron oxide	100	<i>in situ</i> precipitation			blood vessel	300
Ni	151 × 18 (rods)	current-pulsed electrodeposition		500		188
carbonyl iron	2010	C. A.	0.5% (w/v)	30		189
γ-Fe <sub>2</sub> O <sub>3</sub>	23	nucleation	0.005% (w/v)			301

<sup>a</sup>C. A. = commercially available. <sup>b</sup>Rod-shaped cellulose nanocrystals decorated with 7 nm iron oxide MNPs. <sup>c</sup>Iron oxide MNPs incorporated into poly-L-lactic acid fibers. The MNPs concentration in these fibers was 2–8% (w/w). <sup>d</sup>Iron oxide MNPs incorporated into poly(ethylene oxide-*stat*-propylene oxide)-based rod-shaped microgels. The microgels concentration in the hydrogels was 1.0–3.0% (v/v), while the MNPs concentration in the microgels precursor solution was 0.4–1.0 mg·mL<sup>-1</sup>. <sup>e</sup>5 nm Fe<sub>3</sub>O<sub>4</sub> MNPs incorporated into PLGA fibers. The fibers concentration in the final composite was 0.015% (v/v), and the MNPs concentration in the fibers precursor solution was 1% (w/w).

clusters is favored by more pliable scaffolds.<sup>206</sup> Interestingly, the temporal stiffness of many biological microenvironments, such as myocardial ECM during development,<sup>218</sup> has a dynamic nature that is not easy to recreate in scaffold biomaterials. Therefore, besides the stiffening effect usually resulting from the incorporation of magnetic nanoparticles into the soft hydrogel matrices, actuation of magnetic hydrogels can also be explored for the reversible spatiotemporal modulation of hydrogels' elasticity, a strategy that was shown to be effective in the dynamic modulation of stem cell activity, including spreading and differentiation.<sup>219</sup>

Considering these aspects, magnetically responsive hydrogels can be leveraged for designing tailored scaffolding biomaterials with the desired anisotropic characteristics and/or for providing on-demand wireless mechanical stimulation in tissue-specific TE strategies (Table 4). As aforementioned, despite the existence of common general features, each tissue is characterized by its own properties related to its composition and architecture, as well as with its mechanical and biological functions.

In this section, the use of magnetic hybrid hydrogels in TE strategies to mimic different specific tissues, namely, cartilage, bone, tendon, skeletal muscle, cardiac muscle, and neural tissues, is reviewed. The main characteristics of each tissue will be briefly expanded before discussing the most relevant TE works that have been published regarding the design of magnetic hydrogels.

**Cartilage.** Native cartilage tissues are characterized by a complex ECM structure based on collagen fibers and proteoglycans populated by a single type of cells, the chondrocytes.<sup>220</sup> Among these, articular cartilage presents three parts with different collagen fiber arrangements: in the superficial zone, collagen fibers are packed tightly and aligned parallel to the external surface; in the middle layer, they are randomly oriented, whereas in the deepest area, before the interface with bone tissue, they are aligned perpendicularly to the cartilage surface. Moreover, the phenotype of chondrocytes is different in each zone, and the concentration of proteoglycans increases from the cartilage surface to the bone side, as well as the resistance to compressive forces (Figure 7a).<sup>26,221,222</sup>

In order to mimic the cartilage ECM, different hydrogels based on natural (e.g., hyaluronic acid, alginate, agarose, or chitosan) and synthetic (e.g., PEG or PVA) polymers and/or proteins (e.g., collagen, gelatin, or fibroin) have been evaluated as potential materials to prepare cartilage-mimetic scaffolds.<sup>223–225</sup> In addition, as mechanosensitive tissue, mechanical stimulation can be an effective strategy to enhance the mechanical, structural, and cellular properties of tissue-engineered constructs toward mimicking those of native cartilage.<sup>226</sup>

The use of magnetic materials to induce the magneto-mechanical stimulation of cells in cartilage TE has been quite an

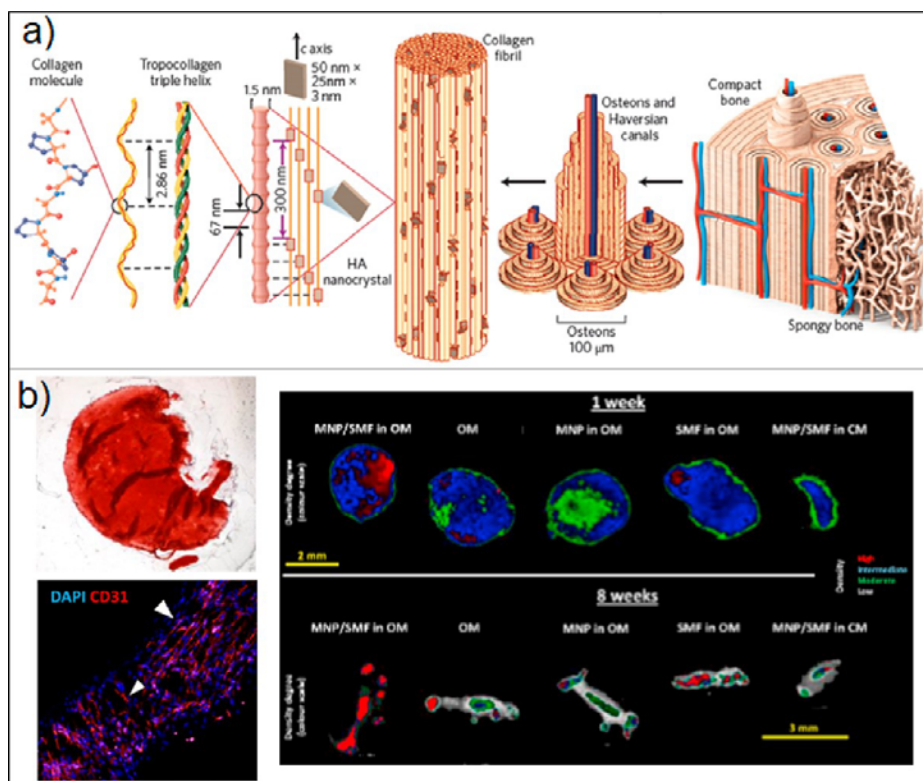


**Figure 8.** (a) Schematic illustration of the hierarchical organization of bone tissues from the macro- to the nanoscale (Reproduced with permission from ref 251. Copyright 2016 Wiley-VCH). (b) Application of magnetic hydrogels in bone TE. After 3 weeks in culture under the application of a static magnetic field (SMF), PEG-based cell-laden hydrogels with incorporated MNPs showed high levels of calcium deposition (alizarin red staining image). Confocal microscopy image also demonstrates that magnetic stimulation promotes an increase of CD31+ cells population, indicating the vasculogenic potential of the designed composites. The composites were implanted subcutaneously into nude mice, observing from  $\mu$ CT images different density gradients in the tissues generated *in vivo*. The highest degree of mineralization (red color) was observed in MNPs-loaded hydrogels previously cultured in osteogenic medium under magnetic stimulation (MNP/SFM in OM), with a significant increase from week 1 to week 8. The decrease in the overall volume of tissues with time *in vivo* was attributed to degradation of hydrogels/tissue remodeling (Adapted with permission from ref 247. Copyright 2019 Elsevier).

effective approach. For example, Huang *et al.*<sup>30</sup> prepared reinforced nanocomposite magnetic hydrogels using PVA, hydroxyapatite particles and maghemite MNPs. The incorporation of MNPs enhanced the mechanical properties of the scaffolds and promoted the proliferation and the chondrocyte-related gene expression of the seeded bone mesenchymal stem cells. In another work, commercially available MNPs and human hyaline chondrocytes were incorporated within a fibrin–agarose hydrogel.<sup>227</sup> The presence of magnetic materials increased the values of the storage and loss moduli in the designed composites, although they were still much weaker than native cartilage tissue. Moreover, the inclusion of MNPs did not have a negative effect over the expression of collagen type II by chondrocytes and the cytocompatibility of the designed biomaterials, constituting a promising approach to engineer cartilage tissues. Further *et al.*<sup>185</sup> combined the use of magnetic materials with the application of external magnetic fields for the magnetomechanical stimulation of the cells. These authors designed magnetic hydrogels through the addition of MNPs to a styrene maleic anhydride copolymer solution before the gelation step. Human mesenchymal stem cells were seeded on the scaffolds and a noncontinuous 800 mT magnetic field was applied (2 s on followed by 10–225 s off), which promoted the chondrogenic differentiation of the cells without any additional chondrogenesis stimulating growth factor. In this way, it was demonstrated that a pure mechanical stimulation derived from the deformation of the magnetic

scaffolds under the application of external magnetic fields allows the desired cell differentiation for cartilage TE. In a slightly different approach, commercially available dextran-coated MNPs were blended with agarose hydrogels.<sup>228</sup> In order to recreate the mechanical properties and architecture of native cartilage, three hydrogel layers with different agarose concentrations (1, 2, and 2.5% (w/w)) were integrated, resulting in a scaffold with decreasing compressive moduli from top to bottom. Bovine chondrocytes were then seeded into the different layers of the composite and cultured in chondrogenic medium under the application of a 500 mT magnetic field. After 14 days, the scaffolds exhibited depth-dependent strain and a biochemical gradient of sulfated glycosaminoglycans similar to native cartilage tissues.

In the aforementioned works, MNPs were only exploited to stimulate cells encapsulated within the magnetic hydrogels. However, magnetic materials can also be used to create hydrogels with anisotropic architectures, which is of great interest for the correct mimicking of cartilage tissues. For example, magnetically assisted 3D printing technique was exploited to produce anisotropic bilayer composites using collagen–agarose hydrogels containing iron oxide nanoparticles under extremely weak 2 mT magnetic fields.<sup>148</sup> The collagen fibers were forced to align in the desired direction due to the unidirectional traveling motion of MNPs across the hydrogel, allowing one to obtain random-to-aligned collagen fibers

organization (Figure 7b). Due to this anisotropic structure, the generated scaffolds showed reinforced directional mechanical properties in comparison with monolayer composites. Moreover, when chondrocytes were loaded into these scaffolds, they expressed more collagen type II in comparison to solely randomly orientated fiber constructs, suggesting that the proposed concept might have the potential to be applied in cartilage TE.

**Bone.** Bones are mineralized connective tissues that compose the skeleton of vertebrates, harboring the bone marrow. The ECM of bones consists of hydroxyapatite nanocrystals deposited periodically along collagen fibers forming complex composite structures hierarchically organized from the nano- to the macroscale.<sup>229,230</sup> The bone cells, located between the collagen fibers, are the living elements responsible for bone homeostasis and response to external stimuli. Morphologically, the bone can be classified into cortical or trabecular bone. Cortical bone is more compact and solid (<20% porosity) and consists of cylindrical structures (Haversian canals) with a central channel enclosing a blood vessel and surrounding it by concentric rings of bone matrix, whereas trabecular bone (>90% porosity) is structured in plates (trabeculae) offering a larger surface area to mass ratio, making it an effective structure for ion exchange (homeostasis) and imparting flexibility in load-bearing bones.<sup>231</sup> Cortical bones are characterized by highly anisotropic mechanical properties, presenting an elastic modulus close to 20 GPa when the force is applied along the Haversian system which decreases to 8 GPa along the transverse axis. On the other hand, trabecular bone is softer and more flexible and presents more isotropic mechanical stiffness, with elastic moduli between 50 and 100 MPa (Figure 8a).<sup>232</sup>

The characteristic very high toughness and stiffness of bone tissues limit the potential use of hydrogels in bone TE, particularly for the regeneration of critical size defects in load-bearing bones.<sup>233,234</sup> Notwithstanding, many composite hydrogel-based systems containing osteopromotive and reinforcing ceramic particles have been proposed for bone TE.<sup>235–237</sup> For example, the incorporation of hydroxyapatite microparticles<sup>238</sup> or disk-shaped nanosilicates<sup>239</sup> within GelMA hydrogels has been analyzed, observing high increases on the storage modulus of the scaffolds by the sole influence of the particles in the first case and the proliferation and osteogenic differentiation of the encapsulated stem cells in both.

The incorporation of magnetic materials and the subsequent application of magnetic fields may present different advantages for bone TE strategies. First, although it is a low-explored strategy, MNPs can be used to provide the biomaterials with the anisotropic hierarchical architecture observed in native bone tissues. Moreover, the magnetic forces at the interface between cells and hybrid composites have been shown to activate sensitive receptors of the cell's surface, enhancing cell activity and promoting the bone formation process and the integration of scaffolds into the host bone.<sup>240–242</sup> On the other hand, MNPs present high specific stiffness and strength, which can be leveraged to improve mechanical properties of bone-engineered constructs.<sup>162</sup> In this regard, magnetic PCL-based matrices have been commonly used as support for bone-mimicking scaffolds due to their low toxicity and high toughness and strength.<sup>243–245</sup>

Although hydrogels are not the first choice for developing bone scaffolds, there are a few, but promising, reports using magnetic hydrogels in the field. For example, magnetite MNPs modified with basic fibroblast growth factor were incorporated within the structure of silk fibroin-based hydrogels.<sup>246</sup> The

presence of MNPs induced significant increases in the water uptake and the stiffness of the composites. *In vitro* studies performed under the effect of a 240 mT magnetic field showed that the designed composites maintain the viability of human osteoblasts-like cells and enhance alkaline phosphatase (ALP) activity, one of the main markers of osteoblasts differentiation and bone formation. In a recent work, PEG-based hydrogels incorporating MNPs were used to magnetomechanically actuate the encapsulated cells from the stromal vascular fraction (SVF) of human adipose tissue.<sup>247</sup> Magnetic actuation of the constructs with external magnetostatic fields significantly increased the expression of different osteogenic markers and deposition of the mineralized matrix while simultaneously inducing a strong activation of endothelial, pericytic, and perivascular genes, as well as an enrichment in the CD31+ cells population, suggesting that besides promoting osteogenesis progenitor cells it also favors vasculogenesis, both critical events for bone regeneration.<sup>248</sup> Interestingly, the stimulation of cell signaling pathways involved in the mechanotransduction suggested that these effects are mediated by the mechanical stimuli applied through magnetic actuation of the constructs. Overall, these results indicate that magnetomechanical actuation is a promising strategy to improve the functionality of bioengineered bone tissue grafts (Figure 8b).

As mentioned, the use of osteoinductive nano- and micro-particles is a widely explored approach in bone TE, having also been evaluated for its combination with the incorporation of MNPs. For instance, Huang and Chu<sup>249</sup> integrated magnetite MNPs and hydroxyapatite NPs within injectable methoxy-(PEG)-polyalanine hydrogels. MC3T3-E1 rat preosteoblasts were encapsulated within the composites and cultured under the application of 400 mT magnetostatic or moving fields. The designed scaffolds up-regulated osteoblasts' proliferation and differentiation markers such as alkaline phosphatase and osteocalcin, indicating an osteogenic commitment. In a slightly different approach, maghemite MNPs were synthesized and then coated with hydroxyapatite shells.<sup>250</sup> The hybrid ceramic–magnetic particles were composited with PVA hydrogels, increasing the porosity and compressive strength (up to 29 MPa) of the resulting structures. The hydrogels with both magnetic and ceramic phases promoted higher degrees of cells adhesion and proliferation of human SV40 osteoblasts than pure PVA and hydroxyapatite–PVA formulations.

**Tendon and Tendon-to-Bone.** Tendons consist of dense networks of collagen type I fibers aligned in the direction of the long axis of the tissue, connecting bones, and muscles. In addition to collagen I (70%–80% dry weight of normal tendon), collagen types III, V, or XII are also present, as well as proteoglycans and glycoproteins such as elastin or fibronectin.<sup>15</sup> Tendon tissues are loaded in the direction parallel to fibers and display anisotropic and viscoelastic properties at all levels of hierarchy. The complex structure of tendons' ECM allows fibrils (nanometric scales), fibers (small groups of fibrils), and fascicles (micrometric scale) to slide side by side, giving rise to singular mechanical properties. Moreover, the mechanical properties also depend on the nature of the tendon tissue and the aging. Thus, human patellar tendon characterized by a Young's modulus of around 650 MPa, while in tibialis anterior tendon it increases to 1200 MPa.<sup>252</sup> Regarding the biological component, the ECM surrounds a scarce resident cell population, mainly composed of tenocytes, which are typically found in rows between collagen bundles showing elongated morphologies.<sup>253,254</sup>



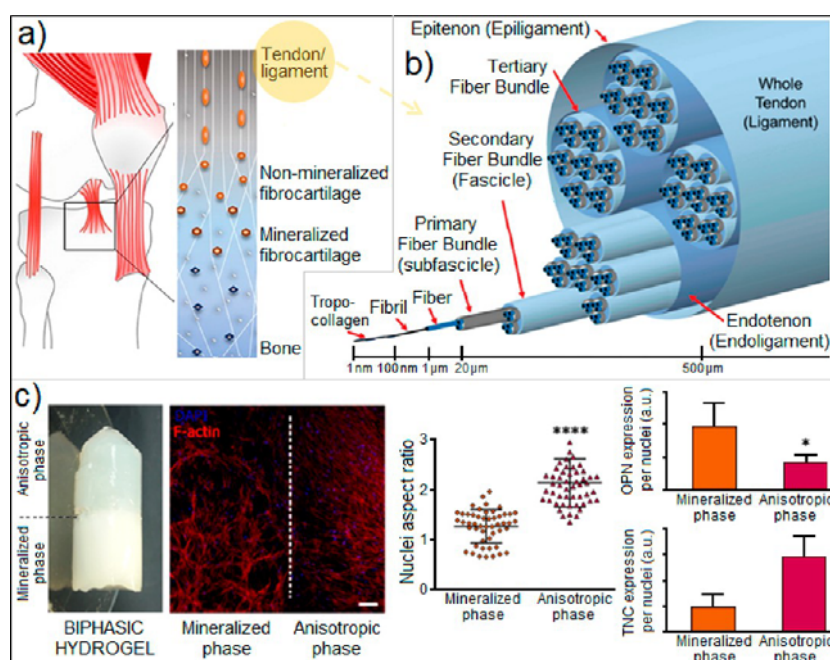


**Figure 9.** Schematic illustration of (a) tendon-to-bone interface (Adapted with permission from ref 35. Copyright 2015 Elsevier) and (b) tendon/ligament tissues (Adapted with permission from ref 265. Copyright 2018 The Authors under a Creative Commons CC BY License (<https://creativecommons.org/licenses/by/4.0/>), published by MDPI). (c) Application of magnetic hydrogels in tendon-to-bone TE: development of biphasic hydrogels with well-differentiated anisotropic (incorporation and magnetic alignment of cellulose nanocrystals) and mineralized (incorporation of hydroxyapatite NPs) phases. From confocal images, it can be observed that anisotropic phase induces higher aspect ratio of the nucleus of encapsulated cells (scale bars = 100 μm). Moreover, osteogenic differentiation-related marker osteopontin (OPN) is highly expressed in mineralized phase, while tendon-related marker tenascin (TNC) is highly expressed in anisotropic phase (Adapted with permission from ref 178. Copyright 2019 American Chemical Society).

Furthermore, the interface between tendon and bone (also called enthesis) is a biomechanical buffering region mainly composed by collagen II and aggrecan and characterized by complex gradients in composition, organization, mechanical properties, and cells phenotype.<sup>255</sup> From tendon to bone, there is a gradual transition from soft to stiff, from unmineralized to mineralized, from low to high cellularization, and in the anisotropy degree of the ECM/cell alignment (Figure 9a,b).<sup>210</sup>

Several works show the relevance of the highly anisotropic uniaxial architecture in order to mimic the structure of tendon tissues and provide cells the cues for their tenogenic differentiation.<sup>256–258</sup> Although electrospinning and wet-spinning are the preferred techniques to prepare nano- and microfiber-based scaffolds to mimic tendon, their lack of 3D structure is a limitation, which has fostered the development of innovative strategies to incorporate these fibers into hydrogels. For instance, hydrogels prepared with aligned electrospun PCL nanofibers<sup>259</sup> or wet-spun GelMA microfibers<sup>260</sup> showed the desirable anisotropic architectures, which induced an elongated morphology and the differentiation of the encapsulated stem cells into the tenocyte lineage.

As mechanosensitive tissues, the development of magnetic responsive hydrogels capable of stimulating cells and/or showing anisotropic architecture might be an important progress to achieve functional tendon TE constructs, which has been mainly investigated by our team. In order to remotely stimulate cells, iron oxide MNPs were added to tropoelastin-based hydrogels through an *in situ* precipitation method, observing a highly uniform distribution of the magnetic material in the 3D network.<sup>261</sup> Interestingly, the presence of MNPs changed the secondary structure of tropoelastin, leading to

spongy-like hydrogels with quasi-anisotropic lamellar-like structures with smaller pore sizes and lower swelling extents than nonmagnetic hydrogels. Human tendon-derived cells were seeded on the magnetic scaffolds, which were exposed to an oscillating magnetic field (350 mT; oscillation, 2 Hz; 0.2 mm). After 14 days in culture, the magnetic scaffolds improved the adhesion and viability of tendon cells, providing evidence of their potential for tendon tissue regeneration.

The use of magnetism to fabricate anisotropic hydrogels for tendon TE was explored by Araújo-Custódio *et al.*<sup>29</sup> in a recent work. Here, rod-shaped cellulose NPs were co-precipitated with iron oxide MNPs, which aligned within gelatin-based hydrogels through the application of 108 mT magnetic fields. The microstructural pattern derived from NPs distribution provided hydrogels with highly anisotropic mechanical properties (maximum storage modulus in the direction parallel to the main axis of alignment). Moreover, the anisotropic characteristics induced an elongated morphology and directional growth of the hASCs encapsulated or seeded in the hydrogels. Nevertheless, we did not test stem cells' tenogenic commitment, which only allows one to suggest the potential application of this concept to mimic highly anisotropic tissues such as tendons.

The engineering of tendon-to-bone interfaces has mainly relied on the development of fiber-based scaffolds showing gradients of fibers' alignment and/or mineralization degree.<sup>262–264</sup> As more biomimetic alternative, similar to tendon, strategies, magnetically responsive hydrogels have been proposed as potential supports for the design of enthesis-like composites. For instance, magnetic hydrogels were used to remotely stimulate the encapsulated cells and induce the biological characteristics of enthesis.<sup>28</sup> For that, iron oxide

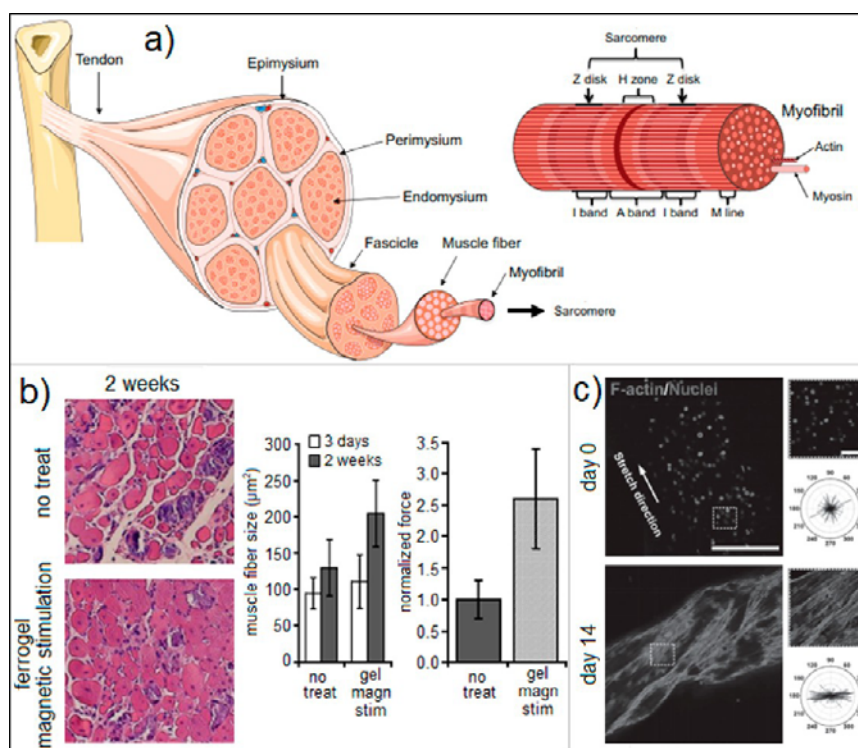


**Figure 10.** (a) Schematic illustration of the organization of skeletal muscle tissues (Adapted with permission from ref 276. Copyright 2019 Elsevier). (b) Application of magnetic hydrogels in skeletal muscle TE. Evaluation of magnetic alginate-based hydrogels for the *in vivo* regeneration of tibial anterior muscles of mice; histological cross-section images of muscles show that after 2 weeks mean muscle fiber size is greater in muscles treated with ferrogels under magnetic stimulation compared with no-treatment controls. Moreover, injured muscles treated with stimulated ferrogels showed significant increases in specific peak contractile force after 2 weeks, 2.6-fold over no-treatment controls (Adapted with permission from ref 274). (c) Application of magnetic hydrogels in skeletal muscle TE. Confocal images of C2C12 myoblasts encapsulated in microfiber-shaped magnetic hydrogels showed that cells in unstrained hydrogels present random orientation after encapsulation. However, cells in hydrogels magnetically stretched at 10% for 14 days present an increasing polarization parallel to the stretch direction. This observation indicates the alignment of the encapsulated cells within the designed 3D matrix as a function of the uniaxial stretching time, mimicking in this way native muscle tissues (Adapted with permission from ref 275. Copyright 2015 Wiley-VCH).

MNPs were prepared through a co-precipitation method and, then, incorporated into methacrylated chondroitin sulfate hydrogels together with tendon-derived cells and osteogenically differentiated stem cells. The application of an oscillating magnetostatic field modulated the intrinsic properties of the magnetically responsive composites, allowing the replication of the forces exerted on cells in native tissues. Although this strategy did not mimic the characteristic anisotropy of enthesis tissues, magnetic stimulation enabled achieving a control on the cell response, creating the desired biological gradients within the hydrogels.

For the purpose of recreating the characteristic gradients of the enthesis, gelatin hydrogels incorporating hydroxyapatite microparticles or diamagnetic rod-shaped cellulose nanocrystals were used to engineer constructs with two different phases, mimicking the bone and tendon, respectively.<sup>178</sup> In the bone-like phase, the presence of hydroxyapatite particles increased the stiffness of the composites and induced the differentiation of the encapsulated hASCs to osteogenic lineages, increasing the alkaline phosphatase activity and up-regulating the expression of bone markers such as osteopontin. In the other phase, the application of a 400 mT magnetostatic field during gelatin cross-linking resulted in the alignment of the cellulose crystals, which induced cell elongation and alignment and increased the deposition of tenascin (tendon marker). Thus, these authors obtained magnetic scaffolds with gradients on their structure, mineralization degree and cellular organization/differentiation

similar to those observed on tendon-to-bone native interfaces (Figure 9c).

**Skeletal Muscle.** Skeletal muscle represents more than 40% of total body weight. Its structure consists on multinucleated cell fibers (myofibers) with highly uniaxial alignment degree along the main axis of the tissue. Individual myofibers are hierarchically organized and wrapped by a thin connective tissue mainly composed of laminin and collagen types I and IV.<sup>266</sup> Skeletal muscles are populated by myocytes, cells characterized by an elongated morphology and tubular structure, which are fused to form the myofibers (a process known as myogenesis).<sup>267</sup> Skeletal muscles are considered soft tissues, with maximum elastic modulus in the range of several tens of kPa.<sup>268</sup> Their anisotropic mechanical response is observed, for instance, in the elasticity of porcine tracheal muscle, which is 31 and 8 kPa in the axial and circumferential directions of fibers, respectively.<sup>269</sup> Moreover, skeletal muscle tissues also present anisotropic electrical behavior, being able to carry higher electric current flows along the main axis of muscle fibers than in other directions (Figure 10a).<sup>270</sup>

Muscle TE strategies are focused on the design of anisotropic scaffolds that provide cells the adequate features for their alignment, elongated growth, and fusion. Natural and synthetic polymers prepared in the form of micro-/nanofibrous or porous-aligned scaffolds have been proposed as supports for muscle-engineered composites.<sup>266</sup> In order to provide them with the desired mechanical/electrical properties, the use of different

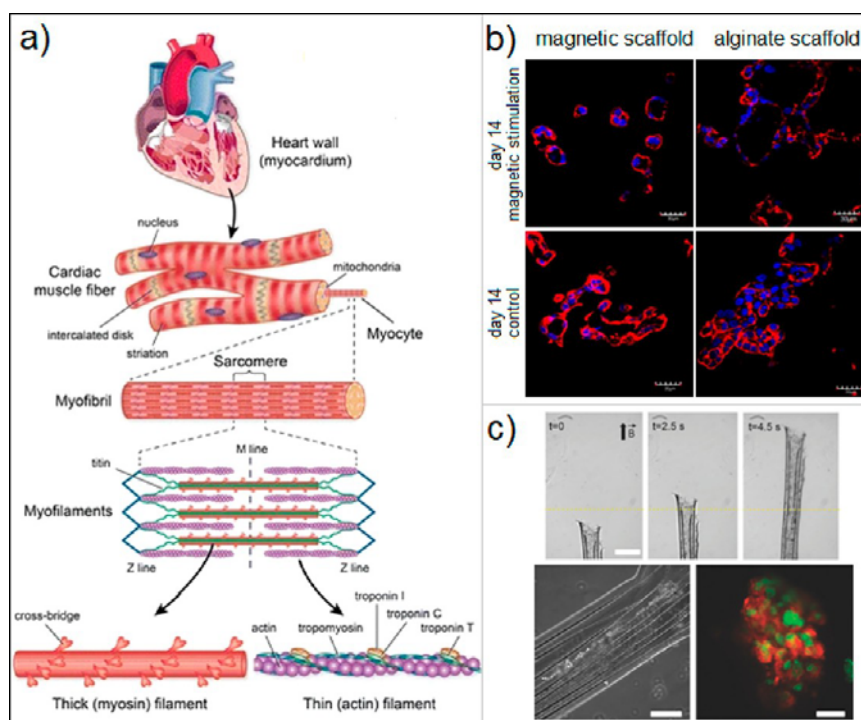


**Figure 11.** (a) Schematic illustration of the anisotropic architecture of cardiac tissue (Reproduced with permission from ref 293. Copyright 2014 Springer Nature). (b) Application of magnetic hydrogels in cardiac TE. Magnetic stimulus promotes a morphological change in the endothelial cells seeded onto alginate hydrogels modified with MNPs after 14 days of culture. Stimulated cells in magnetic scaffolds were mostly found in separated looplike structures similar to those observed for native cardiac tissues, instead of a massive interconnected structure (Scale bars = 30  $\mu\text{m}$ . Adapted with permission from ref 151. Copyright 2012 Elsevier). (c) Application of magnetic hydrogels in cardiac TE. Anisotropic PEG-based hydrogels were prepared by stacking two layers in the form of a 3D tube. Image sequence shows that the incorporation of MNPs within the constructs enabled the magnetic gradient pulling-based actuation of the folded structures using a neodymium magnet (scale bar = 1 mm). The Cor4u cardiomyocytes incorporated inside the tubes exhibit high viability and preserve their contractile function over the course of 7 days (scale bar = 20  $\mu\text{m}$ ). (Adapted with permission from ref 291. Copyright 2018 Wiley-VCH).

structures such as carbon nanotubes<sup>271</sup> or electrospun conductive fibers<sup>272</sup> has been evaluated.

Magnetically responsive hydrogels have also been studied as potential scaffolding materials to provide the contractions necessary to engineer skeletal muscle tissues. In a very recent work, magnetic polyacrylamide hydrogels were prepared through a grafting-onto method.<sup>273</sup> For that, magnetite MNPs were coated with 3-(trimethoxysilyl)propyl methacrylate, this compound acting as cross-linker and generating covalent bonds between MNPs and hydrogel monomers, thus preventing their loss or leaching. The high magnetic content of the composites (60% of the weight of polymer and water) allowed fast responses to the application of an external magnetic field, also providing them high tensile strength and fracture toughness. Through the application of a non-uniform magnetic field with maximum intensity of 335 mT created by an electromagnet, contractions along the axial directions of the hydrogels up to 22% of their original lengths can be reached, which highlighted their potential use as artificial muscles. Similarly, hydrogels prepared with high content of cobalt NPs covalently bonded to the polymer network were tested for their potential as artificial muscles.<sup>150</sup> Elongation and contraction movements were induced using a parallel arrangement of the magnetic hydrogel and the magnetic field gradient provided by a simple electromagnetic coil. The designed magnetic hydrogels showed long-term stability and flexibility, as well as a stretching up to 123% of their initial length, being promising candidates for their use in muscle TE applications. In a different work from Mooney's group, iron

oxide MNPs were incorporated in RGD-modified alginate hydrogels, which were tested *in vivo* in injured tibial anterior muscles of mice.<sup>274</sup> The magnetic ferrogels showed high fatigue resistance and the application of an external AMF (651 mT, 1 Hz) resulted in uniform cyclic compressions that led to reduced fibrous capsule formation around the implant, as well as reduced fibrosis and inflammation in the injured muscle. In contrast, no significant effect of ferrogel actuation on muscle vascularization or perfusion was found. Thus, it was demonstrated that the designed magnetic scaffolds can mechanically stimulate injured skeletal muscles and promote their regeneration (Figure 10b). Microfiber-based constructs composed of GelMA and dimethylacrylated PEG modified with magnetic iron microspheres were also evaluated to engineer skeletal muscle tissues.<sup>275</sup> The magnetically responsive hydrogels were stretched using the magnetostatic field created by a single neodymium magnet, observing that the applied tensile force induce the spreading, proliferation and differentiation of the encapsulated C2C12 myoblasts. The cells showed significant alignment parallel to the stretch direction and myosin heavy chain formation after 14 days in culture. The structural maturation of the composites was evident from the progressive increases in the myotubes diameter and in the expression of skeleton muscle-specific proteins with the time of culture (Figure 10c).

**Cardiac Tissue.** Cardiac tissue is a specialized type of muscle that constitutes the walls of the heart. The ECM is composed mainly by collagen type I and collagen type III, with elastin, fibronectin, laminin, or different glycoproteins also present in



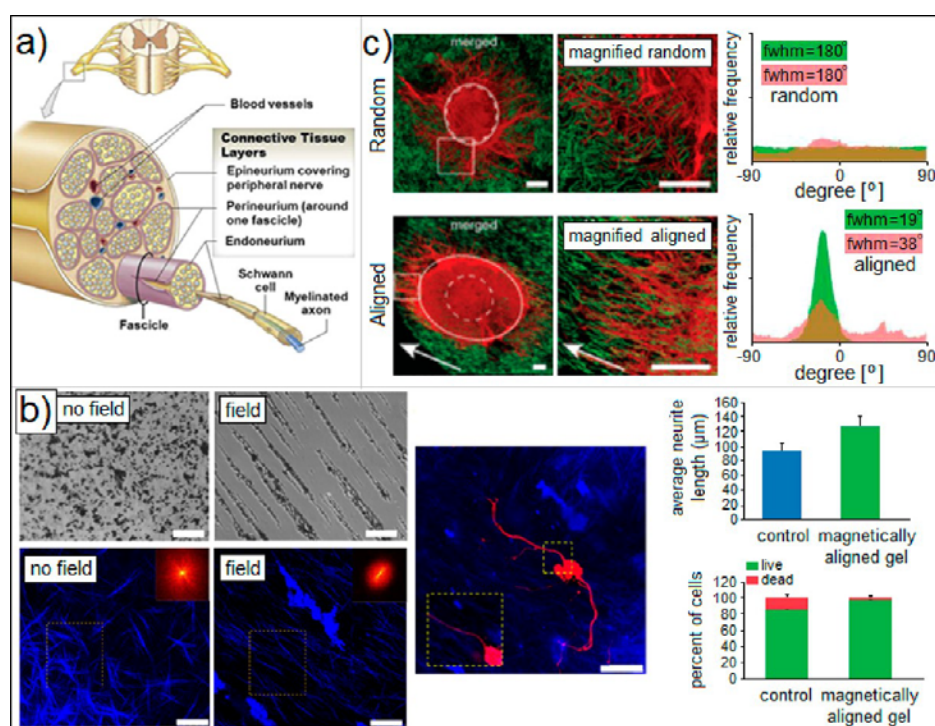


**Figure 12.** (a) Schematic illustration of the cross-sectional view of a spinal nerve showing its different layers (Adapted with permission from ref 298. Copyright 2019 Elsevier). (b) Application of magnetic hydrogels in neural TE. SEM images of magnetically modified collagen hydrogels demonstrate that applied magnetic fields during gelation promote the aggregation of MNPs in the form of magnetic strings. From confocal images, it can be observed that the created magnetic anisotropy induces the alignment of collagen fibers (in blue) and induces the elongation of the encapsulated neurons (in red), also enhancing their viability (Scale bars = 100  $\mu\text{m}$ . Adapted with permission from ref 296. Copyright 2016 American Chemical Society). (c) Application of magnetic hydrogels in neural TE (spinal cord): nerve cells distribution in hydrogels containing randomly oriented and magnetically aligned rod-shaped magnetic microgels (in green).  $\beta$ -Tubulin staining (in red) indicates neurites growth and orientation parallel to magnetically aligned microgels, mimicking native neural tissue (Scale bars = 200  $\mu\text{m}$ . Adapted with permission from ref 196. Copyright 2017 American Chemical Society).

lower percentage, lending high viscoelastic properties.<sup>277</sup> These molecules are anisotropically organized, allowing direction of the force generated by cardiac contractions and expansions in the same direction.<sup>278</sup> Furthermore, the bioelectrical signals generated by the heart are transmitted through cardiac tissue as a result of its conductive and contractile properties originated by the alignment and coupling of cardiomyocytes (Figure 11a).<sup>279</sup>

The scaffolds for cardiac TE have to mimic the mechanical properties of the native tissue, provide cells with cues for their correct orientation and elongation in order to recreate their specific contractile properties, and allow electrical conductivity.<sup>280</sup> The use of conductive polymers, such as polyaniline<sup>281</sup> or polypyrrole,<sup>282</sup> as well as the incorporation of noble metals<sup>283</sup> or carbon-based particles<sup>284</sup> has been evaluated for cardiac TE strategies. Among the latter, the rod-shaped morphology of carbon nanotubes makes them especially suited to aim for cardiac TE applications. These kinds of NPs have been used to create highly conductive scaffolds with anisotropic architecture that promoted the growth of elongated cells similar to those observed in cardiac native tissues.<sup>285,286</sup>

Although the use of electric fields<sup>286</sup> or acoustic waves<sup>287</sup> have been more explored in the field of cardiac TE, magnetic strategies for fabrication and stimulation can be applied to mimic the physical/biological organization of cardiac tissues, as well as a tool to reproduce the cardiac contraction–expansion rhythm in the designed hydrogels.<sup>288,289</sup> For example, Sapir *et al.*<sup>151</sup> explored the use of MNPs for the remote stimulation of cells in cardiac-engineered constructs. For that, co-precipitated magnet-

ite MNPs were blended with alginate macroporous hydrogels fabricated by a freeze-drying technique. Bovine aortic endothelial cells were seeded onto the scaffolds, and an extremely weak AFM generated by Helmholtz coils (1.5 mT, 40 Hz) was applied. The exposure of magnetic scaffolds to AFM and the consequent mechanical stimulation promoted the organization of the endothelial cells into early capillary-like structures, mimicking the biological architecture of native cardiac tissue (Figure 11b).

As an example of the use of magnetism for biofabrication of scaffolds for cardiac TE, paramagnetic iron oxide nanoparticles synthesized by co-precipitation were incorporated into collagen films.<sup>290</sup> Through the application of external magnetostatic fields (obtained by two parallel magnets or current wire setups), it was possible to obtain micropatterns of MNPs within the collagen matrices. This strategy allowed an increase of the electrical conductivity of the designed scaffolds without adding highly conductive compounds. In this way, the authors demonstrated the importance of the anisotropy to mimic properly the electroconductive properties of cardiac tissues, designing a useful tool in order to trigger stem cells' cardiac differentiation. In another interesting work, PEG diacrylate-based hydrogels consisting of two stacked 2D layers modified with commercially available MNPs were also evaluated as potential scaffolds for cardiac and muscle TE.<sup>291</sup> For that, the layers were folded into 3D tubes and cardiomyocytes were seeded inside, exhibiting high adhesion and viability and preserving their contractile function over the course of 7 days.

The presence of MNPs enabled the remote movement of the composites under the application of a 150 mT generated by a single magnet setup, envisioning not only the desired uniaxial organization of cells but also a fine positioning in the implantation site (Figure 11c). Magnetically responsive cryogels based on GelMA and methacrylated elastin modified with carbon nanotubes and magnetite MNPs were also evaluated for cardiac TE purposes.<sup>292</sup> The resultant scaffolds combined excellent elasticity, flexibility, and stress-dependent conductivity under the application of external magnetic fields in the mT range, thus being excellent candidates to be used as remotely controlled conductive bioactuators for cardiac TE. However, these authors also did not encapsulate/seed cells in order to evaluate the biological behavior of the designed composites.

**Neural Tissue.** Neural tissue is the specialized part of the nervous system that receives and transmits the nerve impulse across the body. Neurons, the most common cells in neural tissues, present a cell body and elongated extensions (axon and dendrites), thus showing highly anisotropic characteristics. In contrast with other anisotropic tissues, such as bone or cartilage, neural tissues are among of the softest of the human body and are characterized by elastic moduli lower than 1 kPa.<sup>294</sup> To reach these values, soft hydrogels are typically used as templates to mimic this tissue, in almost all cases combined with other biophysical and biological cues that guide and stimulate oriented neural tissue growth (Figure 11a).<sup>295</sup>

In a very interesting approach, the effect of magneto-mechanical stimulation of neuron cells was analyzed using magnetic microparticles blended into high molecular weight hyaluronic acid hydrogels.<sup>165</sup> The resultant composites mimicked the mechanical properties of the spinal cord ECM, showing a storage modulus of 0.14 kPa. Moreover, the magnetic hydrogels facilitated the healthy growth of the encapsulated dorsal root ganglion neurons as well as the expression of excitatory and inhibitory ion channels. In this sense, the authors studied the effect of magnetomechanical stimulation of the composites using a 2 T permanent magnet. While short-term “acute” stimulation enhanced the opening of endogenous mechanosensitive ion channels allowing calcium influx, long-term “chronic” stimulation reduced the expression of these channels. Thus, these hydrogels are a versatile tool to study not only the effects of magnetomechanical stimulation but as well a possible therapeutic strategy to reduce the expression of mechanosensitive channels typically overexpressed in patients suffering from chronic pain.

Other works explored the use of magnetism to fabricate hydrogels with anisotropic architecture, mimicking the properties of native neural tissues and providing cells the adequate cues for their elongated growth and/or neuronal differentiation. For example, Antman-Passig *et al.*<sup>296</sup> added magnetite and maghemite MNPs to a collagen solution and applied a weak magnetic field (25.5 mT) during polymer gelation. This external stimulus resulted in MNPs aggregation in the form of magnetic strings along the lines of the applied magnetic field within the hydrogels. In addition, the anisotropic distribution of the magnetic material also led to an alignment of the collagen fibers. The physical cues provided by the scaffolds induced the elongation (aspect ratio twice as high as control) and directional growth of the encapsulated primary neurons derived from the medicinal leech (a type of worm), mimicking in this way the characteristic cellular features of native neural tissues. To validate the capacity of the ferrogels to direct neuronal growth, the authors also analyzed the behavior PC12 cells (derived from

rat adrenal medulla). Following treatment with nerve growth factor (NGF), it was observed that PC12 cells showed oriented growth within the anisotropic hydrogels and developed co-oriented neurites (Figure 12b).

Since high concentrations of magnetic iron oxide particles can decrease cell viability (especially of very sensitive cells such as neurons),<sup>297</sup> lowering the amount of magnetic materials necessary to obtain anisotropy within hydrogels has been investigated using MNPs incorporated within rod-shaped micro- and nanoelements. For example, PEG-based rod-shaped microgels loaded with commercially available SPIONs were aligned within a hydrogel matrix through the application of a 130 mT magnetic field, which resulted in anisotropic scaffolds with low elastic moduli (kPa range).<sup>196</sup> Chicken-derived primary dorsal root ganglions were encapsulated into NGF-supplemented anisotropic hydrogels, which oriented neurite growth and blocked their extension in the perpendicular direction (Figure 12c). In another relevant example, 12 nm SPIONs were incorporated into electrospun poly-L-lactic acid nanofibers, which were used in combination with collagen and fibrinogen solutions to form hydrogels.<sup>144</sup> Under the application of magnetostatic fields, generated by two parallel magnets configuration, the SPIONs-loaded fibers were aligned within the hydrogels. The anisotropy created in the hybrid composites provided directional nanotopographic cues for the alignment of the encapsulated primary dorsal root ganglions. The average length of the cells increased 3-fold in fibrin hydrogels and 1.4-fold in collagen hydrogels modified with magnetic fibers in comparison with cells grown in nonmagnetic isotropic hydrogels.

## CONCLUSIONS AND OUTLOOK

Anisotropic magnetically responsive hydrogels have been confirmed as promising support materials to engineer different tissues of the human body. By controlling the properties of the magnetic materials incorporated into the hydrogels made of different polymers and adjusting the applied magnetic fields, the response of the hydrogels can be tunable, providing these hybrid composites with the desired physical properties and biological cues to mimic native tissues. In this way, the use of magnetically responsive hydrogels has allowed impressive advances in the field of TE in the past few years.

Although the magnetic manipulation of diamagnetic nanomaterials with weak magnetic response has been proposed as a strategy to control the microstructural properties of nanocomposite hydrogels, the addition of MNPs with much higher magnetic susceptibility has been the preferential strategy followed to improve the magnetic control over tissue-engineered constructs and decrease the amplitude of the magnetic fields required for their manipulation. In this sense, the incorporation of highly sensitive MNPs that can be remotely controlled through the application of low-intensity magnetic fields is one of the most important key factors in the preparation of magnetic hydrogels. In this context, the choice of the adequate synthetic method is critical, as is the careful design of the MNPs in terms of size, shape, or composition, among other features to provide them with high magnetic power and predicting their response when an external magnetic field is applied.

The ability to arrange the magnetic materials within the polymeric hydrogels in the desired form is crucial to engineer tissues with highly anisotropic architecture. However, in most cases, it is difficult to reach a high control over the interdistances/aggregation state of free MNPs directly incorpo-

rated within the hydrogels, hindering the creation of composites with global anisotropy. In this sense, the design of anisotropic nano- or microstructures, such as fibers or rod-shaped microgels, and their subsequent modification with MNPs before their incorporation within hydrogels has been revealed to be among the most successful alternatives to fabricate constructs with magnetic responsiveness and high degrees of anisotropic microarchitectural organization.

The application of magnetically responsive hydrogels to engineer specific human tissues such as tendon, bone, cartilage, or skeletal muscle has seen an impressive increase during the recent past years. In some cases, the magnetic materials incorporated within polymeric networks have been combined with other components such as ceramic particles or conductive structures to properly mimic the native tissues. In this way, the combination of cells with the hybrid nanocomposite hydrogels under the control of programmed external magnetic fields allows the design of biomaterials with tissue-mimetic characteristics in terms of anisotropy and mechanical properties. These properties have shown positive effects over the behavior of encapsulated cells (*e.g.*, directed migration, differentiation) in constructs designed for different TE applications.

However, there are still many challenges related to the application of magnetic hydrogels in the biomedical field. The use of magnetic materials presents several problems related with their non-negligible cytotoxicity, as well as with the safety risks associated with the application of high-intensity magnetic fields. On the other hand, the importance of the actual dimensions and spacing between magnetically aligned particles in the hydrogel matrix or the specific “design rules” of anisotropic hydrogels for achieving the aimed biological responses are often not sufficiently understood and need further systematic investigation. In addition, although improved, the mechanical properties of the majority of magnetic hydrogels obtained following the proposed synthetic routes are still not completely satisfactory for their successful implementation in many TE strategies requiring mechanical support, particularly for high-load-bearing tissues. The design of magnetic composite hydrogels that combine controlled magnetic properties with the required mechanical and biological performance has, therefore, considerable room for improvement.

The development of the next generation of magnetic hydrogel biomaterials would definitely benefit from an increased integration of bioengineering and physical science knowledge. The design of MNPs with high magnetic power, which can be synthesized following the available strategies discussed here, would allow one to decrease the required amount of magnetic material and the intensity of the applied magnetic fields for achieving the targeted responsiveness, minimizing the aforementioned associated risks. Therefore, we expect that the incorporation of rationally designed MNPs into hydrogels' matrices will allow a greater control over their resulting mechanical/biological properties and will also contribute to facilitate the implementation of this kind of biomaterials in clinical practice.

The use of magnetic hydrogels has been suggested for TE strategies of many different tissues, particularly for mechanosensitive tissues of the musculoskeletal system that present characteristic uniaxial anisotropic architectures in their cell and ECM organization, which are crucial for their function, including, *e.g.*, bone, cartilage, or skeletal muscle. Nevertheless, most human body tissues have hierarchical architectures organized in anisotropic structures. The additional design

control allowed by magnetic materials and fabrication technologies could thus be leveraged for improving the regenerative outcome of a much wider range of TE strategies. On the other hand, besides being used for the uniaxial alignment of magnetic elements to produce hydrogels with uniform microarchitectures, experimental setups that allow for the generation of magnetic field gradients or defined magnetic patterns could be applied to engineer tissues that present regions with different anisotropic patterns on their structural organization, such as cartilage or cornea.

In terms of fabrication technologies, the recently introduced magnetically assisted 3D printing technique has the potential to significantly increase the level of control and to widen the available design space of hybrid magnetic composites. However, as mentioned throughout the review, just a few works have used this technique in the field of TE.<sup>147,148</sup> Significant hardware configuration evolutions are still needed to fully explore the design liberty that this technology promises, making it a field with many possibilities to be explored. In this sense, we expect that the strategies for the preparation of advanced magnetic materials detailed here, combined with the progress on the required setups for the generation of tunable external magnetic fields, will contribute to increase the fabrication with nano- to macroscale precision of hydrogel-based constructs.

Beyond the fabrication and design aspects of the materials, the possibilities that magnetic hydrogels offer for remote actuation are intrinsic characteristics that can be explored in multiple ways. Several works have explored the responsiveness of magnetic hydrogels to magnetomechanically stimulate encapsulated cells and improve the overall performance of the proposed TE strategy. However, this concept can be further evolved to incorporate into magnetic hydrogels additional stimulation possibilities besides the magnetic and mechanical ones allowed by the current systems.

For example, the combination of electrical and magnetic responses has attracted intensive research efforts in the past few years. Among these, the incorporation of electrically responsive elements within the internal structure of the MNPs<sup>302</sup> or the formation of external shells around them<sup>303</sup> have been the most common design approaches. These types of nanostructures could be particularly useful to improve the regenerative potential of TE strategies proposed for tissues that not only require anisotropic structure for function but are also responsive to electrical stimuli, such as cardiac tissues or nerves.

Several unpredicted directions for future regenerative strategies might also arise from the intersection of TE with other biomedical branches that are showing exciting developments with magnetic hydrogels. In this sense, biodegradable magnetic “milli-robots” (microfabricated hydrogels with anisotropic armaments of MNPs whose motion can be controlled by external magnetic fields) are being proposed as potential devices for minimally invasive medical applications inside the human body.<sup>304</sup> The questions of whether these milli-robots can transport cells as cargo to an injury site and/or anchor on it to stimulate endogenous regenerative mechanisms remain to be tested and answered. However, these questions also suggest that the potential of magnetic hydrogels with bioinspired ordered structures in the field of TE is wide-ranging and in many aspects still quite unexplored. Therefore, we foresee the surge of many exciting developments in this field in the near future.



## AUTHOR INFORMATION

## Corresponding Authors

**Manuela E. Gomes** – 3B's Research Group, I3Bs – Research Institute on Biomaterials, Biodegradables and Biomimetics, University of Minho, 4805-017 Barco-Guimarães, Portugal; ICVS/3B's-PT Government Associate Laboratory, 4805-017 Braga/Guimarães, Portugal; [orcid.org/0000-0002-2036-6291](https://orcid.org/0000-0002-2036-6291); Email: [megomes@i3bs.uminho.pt](mailto:megomes@i3bs.uminho.pt)

**Rui M. A. Domingues** – 3B's Research Group, I3Bs – Research Institute on Biomaterials, Biodegradables and Biomimetics, University of Minho, 4805-017 Barco-Guimarães, Portugal; ICVS/3B's-PT Government Associate Laboratory, 4805-017 Braga/Guimarães, Portugal; [orcid.org/0000-0002-3654-9906](https://orcid.org/0000-0002-3654-9906); Email: [rui.domingues@i3bs.uminho.pt](mailto:rui.domingues@i3bs.uminho.pt)

## Authors

**Alberto Pardo** – 3B's Research Group, I3Bs – Research Institute on Biomaterials, Biodegradables and Biomimetics, University of Minho, 4805-017 Barco-Guimarães, Portugal; ICVS/3B's-PT Government Associate Laboratory, 4805-017 Braga/Guimarães, Portugal; [orcid.org/0000-0003-4011-4232](https://orcid.org/0000-0003-4011-4232)

**Manuel Gómez-Florit** – 3B's Research Group, I3Bs – Research Institute on Biomaterials, Biodegradables and Biomimetics, University of Minho, 4805-017 Barco-Guimarães, Portugal; ICVS/3B's-PT Government Associate Laboratory, 4805-017 Braga/Guimarães, Portugal; [orcid.org/0000-0001-7758-1251](https://orcid.org/0000-0001-7758-1251)

**Silvia Barbosa** – Colloids and Polymers Physics Group, Condensed Matter Physics Area and Health Research Institute of Santiago de Compostela (IDIS), Universidade de Santiago de Compostela, 15782 Santiago de Compostela, Spain; [orcid.org/0000-0003-1831-1686](https://orcid.org/0000-0003-1831-1686)

**Pablo Taboada** – Colloids and Polymers Physics Group, Condensed Matter Physics Area and Health Research Institute of Santiago de Compostela (IDIS), Universidade de Santiago de Compostela, 15782 Santiago de Compostela, Spain; [orcid.org/0000-0002-2903-7857](https://orcid.org/0000-0002-2903-7857)

Complete contact information is available at:  
<https://pubs.acs.org/10.1021/acsnano.0c08253>

## Notes

The authors declare no competing financial interest.

## ACKNOWLEDGMENTS

We acknowledge European Union's Horizon 2020 Research and Innovation Programme—European Research Council Consolidator Grant MagTendon (Agreement No. 772817) and Project Achilles (Agreement No. 810850) and Fundação para a Ciência e Tecnologia (FCT) for Project SmarTendon-PTDC/NAN-MAT/30595/2017 and Project MagTT-PTDC/CTM-CTM/29930/2017, from NORTE-01-0145-FEDER-000021 supported by Norte Portugal Regional Operational Programme (NORTE 2020). We also thank Agencia Estatal de Investigación by Project MAT2016-80266-R and Xunta de Galicia (Grupo de Referencia Competitiva ED431C 2018/26 and ED431C 2018/09; Agrupación Estratégica en Materiales ED431E 2018/08). A.P. is grateful to Xunta de Galicia for his postdoctoral fellowship ED481B2019/025. ERDF funds are also acknowledged.

## VOCABULARY

**Tissue engineering**, interdisciplinary field that involves the use of knowledge and technology from life sciences and engineering to develop biological substitutes that restore, maintain, or improve tissue function or a whole organ; **Nanoparticles**, particles with their three size dimensions below 100 nm that usually display physicochemical properties different from those observed on their bulk materials counterparts; **Magnetic biomaterials**, natural or synthetic magnetically responsive substances that present the suitable characteristics to be introduced into living tissues for biomedical purposes (the magnetic behavior is typically provided through the incorporation of magnetic materials); **Anisotropic hydrogels**, hydrogels that present directionally dependent properties (one or more physical, chemical and/or biological properties change with direction along these types of hydrogels); **Magnetic field**, vector field originated around magnets, electric currents, or changing electric fields (moving charged particles) and which makes a magnetic force move electric charges and magnetic dipoles; **Remote actuation**, use of remote stimuli, such as light or magnetic/electric fields, to manipulate constructs that have parts with responsive properties to these external stimuli in the desired way; **Magnetomechanical stimulation**, use of remote magnetic fields to produce mechanical stimuli in the designed constructs on the basis of the movement/physical change of the previously incorporated magnetic materials.

## REFERENCES

- (1) Stratton, S.; Shelke, N. B.; Hoshino, K.; Rudraiah, S.; Kumbar, S. G. Bioactive Polymeric Scaffolds for Tissue Engineering. *Bioact. Mater.* **2016**, *1* (2), 93–108.
- (2) O'Brien, F. J. Biomaterials & Scaffolds for Tissue Engineering. *Mater. Today* **2011**, *14* (3), 88–95.
- (3) Lu, T.; Li, Y.; Chen, T. Techniques for Fabrication and Construction of Three-Dimensional Scaffolds for Tissue Engineering. *Int. J. Nanomed.* **2013**, *8*, 337–350.
- (4) Sivashanmugam, A.; Arun Kumar, R.; Vishnu Priya, M.; Nair, S. V.; Jayakumar, R. An Overview of Injectable Polymeric Hydrogels for Tissue Engineering. *Eur. Polym. J.* **2015**, *72*, 543–565.
- (5) Van Vlierberghe, S.; Dubrue, P.; Schacht, E. Biopolymer-Based Hydrogels as Scaffolds for Tissue Engineering Applications: A Review. *Biomacromolecules* **2011**, *12* (5), 1387–1408.
- (6) Tan, H.; Marra, K. G. Injectable, Biodegradable Hydrogels for Tissue Engineering Applications. *Materials* **2010**, *3* (3), 1746–1767.
- (7) Khademhosseini, A.; Langer, R. Microengineered Hydrogels for Tissue Engineering. *Biomaterials* **2007**, *28* (34), 5087–5092.
- (8) Taylor, D. L.; in het Panhuis, M. Self-Healing Hydrogels. *Adv. Mater.* **2016**, *28* (41), 9060–9093.
- (9) Rose, J. C.; De Laporte, L. Hierarchical Design of Tissue Regenerative Constructs. *Adv. Healthcare Mater.* **2018**, *7* (6), 1701067.
- (10) Möller, L.; Krause, A.; Dahmann, J.; Gruh, I.; Kirschning, A.; Dräger, G. Preparation and Evaluation of Hydrogel-Composites from Methacrylated Hyaluronic Acid, Alginate, and Gelatin for Tissue Engineering. *Int. J. Artif. Organs* **2011**, *34* (2), 93–102.
- (11) Florencio-Silva, R.; Sasso, G. R. D. S.; Sasso-Cerri, E.; Simões, M. J.; Cerri, P. S. Biology of Bone Tissue: Structure, Function, and Factors That Influence Bone Cells. *BioMed Res. Int.* **2015**, *2015*, 421746.
- (12) Chung, C.; Beecham, M.; Mauck, R. L.; Burdick, J. A. The Influence of Degradation Characteristics of Hyaluronic Acid Hydrogels on *in Vitro* Neocartilage Formation by Mesenchymal Stem Cells. *Biomaterials* **2009**, *30* (26), 4287–4296.
- (13) Schmidt, C. E.; Leach, J. B. Neural Tissue Engineering: Strategies for Repair and Regeneration. *Annu. Rev. Biomed. Eng.* **2003**, *5* (1), 293–347.

- (14) Vunjak-Novakovic, G.; Tandon, N.; Godier, A.; Maidhof, R.; Marsano, A.; Martens, T. P.; Radisic, M. Challenges in Cardiac Tissue Engineering. *Tissue Eng., Part B* **2010**, *16*, 169–187.
- (15) Wang, J. H. C.; Guo, Q.; Li, B. Tendon Biomechanics and Mechanobiology - A Minireview of Basic Concepts and Recent Advancements. *J. Hand Ther.* **2012**, *25* (2), 133–141.
- (16) Mehrali, M.; Thakur, A.; Pennisi, C. P.; Talebian, S.; Arpanaei, A.; Nikkhal, M.; Dolatshahi-Pirouz, A. Nanoreinforced Hydrogels for Tissue Engineering: Biomaterials That Are Compatible with Load-Bearing and Electroactive Tissues. *Adv. Mater.* **2017**, *29* (8), 1603612.
- (17) Sydney Gladman, A.; Matsumoto, E. A.; Nuzzo, R. G.; Mahadevan, L.; Lewis, J. A. Biomimetic 4D Printing. *Nat. Mater.* **2016**, *15* (4), 413–418.
- (18) Salehi, M.; Naseri-Nosar, M.; Ebrahimi-Barough, S.; Nourani, M.; Vaez, A.; Farzamfar, S.; Ai, J. Regeneration of Sciatic Nerve Crush Injury by a Hydroxyapatite Nanoparticle-Containing Collagen Type I Hydrogel. *J. Physiol. Sci.* **2018**, *68* (5), 579–587.
- (19) Castilho, M.; Mouser, V.; Chen, M.; Malda, J.; Ito, K. Bi-Layered Micro-Fibre Reinforced Hydrogels for Articular Cartilage Regeneration. *Acta Biomater.* **2019**, *95*, 297–306.
- (20) Wu, S.; Duan, B.; Lu, A.; Wang, Y.; Ye, Q.; Zhang, L. Biocompatible Chitin/Carbon Nanotubes Composite Hydrogels as Neuronal Growth Substrates. *Carbohydr. Polym.* **2017**, *174*, 830–840.
- (21) Gila-Vilchez, C.; Manas-Torres, M. C.; Contreras-Montoya, R.; Alaminos, M.; Duran, J. D. G.; De Cienfuegos, L. A.; Lopez-Lopez, M. T. Anisotropic Magnetic Hydrogels: Design, Structure and Mechanical Properties. *Philos. Trans. R. Soc., A* **2019**, *377*, 20180217.
- (22) Lee, E. A.; Yim, H.; Heo, J.; Kim, H.; Jung, G.; Hwang, N. S. Application of Magnetic Nanoparticle for Controlled Tissue Assembly and Tissue Engineering. *Arch. Pharmacol. Res.* **2014**, *37* (1), 120–128.
- (23) Li, Y.; Huang, G.; Zhang, X.; Li, B.; Chen, Y.; Lu, T.; Lu, T. J.; Xu, F. Magnetic Hydrogels and Their Potential Biomedical Applications. *Adv. Funct. Mater.* **2013**, *23* (6), 660–672.
- (24) Santos, L. J.; Reis, R. L.; Gomes, M. E. Harnessing Magnetic-Mechano Actuation in Regenerative Medicine and Tissue Engineering. *Trends Biotechnol.* **2015**, *33* (8), 471–479.
- (25) Huang, Q.; Zou, Y.; Arno, M. C.; Chen, S.; Wang, T.; Gao, J.; Dove, A. P.; Du, J. Hydrogel Scaffolds for Differentiation of Adipose-Derived Stem Cells. *Chem. Soc. Rev.* **2017**, *46* (20), 6255–6275.
- (26) Rose, J. C.; Gehlen, D. B.; Haraszti, T.; Köhler, J.; Licht, C. J.; De Laporte, L. Biofunctionalized Aligned Microgels Provide 3D Cell Guidance to Mimic Complex Tissue Matrices. *Biomaterials* **2018**, *163*, 128–141.
- (27) Santo, V. E.; Rodrigues, M. T.; Gomes, M. E. Contributions and Future Perspectives on the Use of Magnetic Nanoparticles as Diagnostic and Therapeutic Tools in the Field of Regenerative Medicine. *Expert Rev. Mol. Diagn.* **2013**, *13* (6), 553–566.
- (28) Silva, E. D.; Babo, P. S.; Costa-Almeida, R.; Domingues, R. M. A.; Mendes, B. B.; Paz, E.; Freitas, P.; Rodrigues, M. T.; Granja, P. L.; Gomes, M. E. Multifunctional Magnetic-Responsive Hydrogels to Engineer Tendon-to-Bone Interface. *Nanomedicine* **2018**, *14* (7), 2375–2385.
- (29) Araújo-Custódio, S.; Gomez-Florit, M.; Tomás, A. R.; Mendes, B. B.; Babo, P. S.; Mithieux, S. M.; Weiss, A.; Domingues, R. M. A.; Reis, R. L.; Gomes, M. E. Injectable and Magnetic Responsive Hydrogels with Bioinspired Ordered Structures. *ACS Biomater. Sci. Eng.* **2019**, *5* (3), 1392–1404.
- (30) Huang, J.; Liang, Y.; Jia, Z.; Chen, J.; Duan, L.; Liu, W.; Zhu, F.; Liang, Q.; Zhu, W.; You, W.; Xiong, J.; Wang, D. Development of Magnetic Nanocomposite Hydrogel with Potential Cartilage Tissue Engineering. *ACS Omega* **2018**, *3* (6), 6182–6189.
- (31) Rao, K. M.; Kumar, A.; Han, S. S. Polysaccharide-Based Magnetically Responsive Polyelectrolyte Hydrogels for Tissue Engineering Applications. *J. Mater. Sci. Technol.* **2018**, *34* (8), 1371–1377.
- (32) Bolonduro, O. A.; Duffy, B. M.; Rao, A. A.; Black, L. D.; Timko, B. P. From Biomimicry to Bioelectronics: Smart Materials for Cardiac Tissue Engineering. *Nano Res.* **2020**, *13* (5), 1253–1267.
- (33) McDonald, J. W.; Belegu, V.; Becker, D. Spinal Cord. In *Principles of Tissue Engineering*, 4th ed.; Lanza, R., Langer, R., Vacanti, J., Eds.; Elsevier: Amsterdam, The Netherlands, 2013; pp 1353–1373, DOI: 10.1016/B978-0-12-398358-9.00064-1.
- (34) Zhao, Z.; Fang, R.; Rong, Q.; Liu, M. Bioinspired Nanocomposite Hydrogels with Highly Ordered Structures. *Adv. Mater.* **2017**, *29* (45), 1703045.
- (35) Font Tellado, S.; Balmayor, E. R.; Van Griensven, M. Strategies to Engineer Tendon/Ligament-to-Bone Interface: Biomaterials, Cells and Growth Factors. *Adv. Drug Delivery Rev.* **2015**, *94*, 126–140.
- (36) Indira, T. K.; Lakshmi, P. K. Magnetic Nanoparticles - A Review. *Int. J. Pharm. Sci. Nanotechnol.* **2010**, *3* (3), 1035–1042.
- (37) Lisjak, D.; Mertelj, A. Anisotropic Magnetic Nanoparticles: A Review of Their Properties, Syntheses and Potential Applications. *Prog. Mater. Sci.* **2018**, *95*, 286–328.
- (38) Mohammed, L.; Gomaa, H. G.; Ragab, D.; Zhu, J. Magnetic Nanoparticles for Environmental and Biomedical Applications: A Review. *Particuology* **2017**, *30* (30), 1–14.
- (39) Kolosnjaj-Tabi, J.; Lartigue, L.; Javed, Y.; Luciani, N.; Pellegrino, T.; Wilhelm, C.; Alloyeau, D.; Gazeau, F. Biotransformation of Magnetic Nanoparticles in the Body. *Nano Today* **2016**, *11* (3), 280–284.
- (40) Zaki, H. M.; Al-Heniti, S. H.; Hashhash, A. Effect of Al<sup>3+</sup> Ion Addition on the Magnetic Properties of Cobalt Ferrite at Moderate and Low Temperatures. *J. Magn. Magn. Mater.* **2016**, *401*, 1027–1032.
- (41) Gu, H.; Huang, Y.; Zhang, X.; Wang, Q.; Zhu, J.; Shao, L.; Haldolaarachchige, N.; Young, D. P.; Wei, S.; Guo, Z. Magneto-resistant Polyaniline-Magnetite Nanocomposites with Negative Dielectric Properties. *Polymer* **2012**, *53* (3), 801–809.
- (42) Chandra, S.; Patel, M. D.; Lang, H.; Bahadur, D. Dendrimer-Functionalized Magnetic Nanoparticles: A New Electrode Material for Electrochemical Energy Storage Devices. *J. Power Sources* **2015**, *280*, 217–226.
- (43) Liu, F.; Zhu, J.; Yang, W.; Dong, Y.; Hou, Y.; Zhang, C.; Yin, H.; Sun, S. Building Nanocomposite Magnets by Coating a Hard Magnetic Core with a Soft Magnetic Shell. *Angew. Chem., Int. Ed.* **2014**, *53* (8), 2176–2180.
- (44) Mou, X.; Ali, Z.; Li, S.; He, N. Applications of Magnetic Nanoparticles in Targeted Drug Delivery System. *J. Nanosci. Nanotechnol.* **2015**, *15* (1), 54–62.
- (45) Ulbrich, K.; Holá, K.; Šubr, V.; Bakandritsos, A.; Tuček, J.; Zbořil, R. Targeted Drug Delivery with Polymers and Magnetic Nanoparticles: Covalent and Noncovalent Approaches, Release Control, and Clinical Studies. *Chem. Rev.* **2016**, *116* (9), 5338–5431.
- (46) Hedayatnasab, Z.; Abnisa, F.; Daud, W. M. A. W. Review on Magnetic Nanoparticles for Magnetic Nanofluid Hyperthermia Application. *Mater. Des.* **2017**, *123*, 174–196.
- (47) Obaidat, I.; Issa, B.; Haik, Y. Magnetic Properties of Magnetic Nanoparticles for Efficient Hyperthermia. *Nanomaterials* **2015**, *5* (1), 63–89.
- (48) Lee, N.; Hyeon, T. Designed Synthesis of Uniformly Sized Iron Oxide Nanoparticles for Efficient Magnetic Resonance Imaging Contrast Agents. *Chem. Soc. Rev.* **2012**, *41* (7), 2575–2589.
- (49) Shin, T.-H.; Choi, Y.; Kim, S.; Cheon, J. Recent Advances in Magnetic Nanoparticle-Based Multi-Modal Imaging. *Chem. Soc. Rev.* **2015**, *44* (14), 4501–4516.
- (50) Hasan, A.; Morshed, M.; Memic, A.; Hassan, S.; Webster, T. J.; Marei, H. E. S. Nanoparticles in Tissue Engineering: Applications, Challenges and Prospects. *Int. J. Nanomed.* **2018**, *13*, 5637–5655.
- (51) Leslie-Pelecky, D. L.; Rieke, R. D. Magnetic Properties of Nanostructured Materials. *Chem. Mater.* **1996**, *8* (8), 1770–1783.
- (52) del Pino, P.; Pelaz, B. Hyperthermia Using Inorganic Nanoparticles. In *Nanobiotechnology: Inorganic Nanoparticles vs Organic Nanoparticles*; de la Fuente, J. M., Grazu, V., Eds.; Frontiers of Nanoscience, Vol. 4; Elsevier: Amsterdam, The Netherlands, 2012; pp 309–335, DOI: 10.1016/B978-0-12-415769-9.00013-3.
- (53) Arruebo, M.; Fernández-Pacheco, R.; Ibarra, M. R.; Santamaría, J. Magnetic Nanoparticles for Drug Delivery. *Nano Today* **2007**, *2* (3), 22–32.



- (54) Serantes, D.; Balmir, D. Superparamagnetism and Monte Carlo Simulations. *Open Surf. Sci. J.* **2012**, *4*, 71.
- (55) Li, Q.; Kartikowati, C. W.; Horie, S.; Ogi, T.; Iwaki, T.; Okuyama, K. Correlation between Particle Size/Domain Structure and Magnetic Properties of Highly Crystalline Fe<sub>3</sub>O<sub>4</sub> Nanoparticles. *Sci. Rep.* **2017**, *7* (1), 9894.
- (56) Dennis, C. L.; Ivkov, R. Physics of Heat Generation Using Magnetic Nanoparticles for Hyperthermia. *Int. J. Hyperthermia* **2013**, *29* (8), 715–729.
- (57) Kandasamy, G.; Maity, D. Recent Advances in Superparamagnetic Iron Oxide Nanoparticles (SPIONs) for *in Vitro* and *in Vivo* Cancer Nanotheranostics. *Int. J. Pharm.* **2015**, *496* (2), 191–218.
- (58) Wu, W.; Wu, Z.; Yu, T.; Jiang, C.; Kim, W. S. Recent Progress on Magnetic Iron Oxide Nanoparticles: Synthesis, Surface Functional Strategies and Biomedical Applications. *Sci. Technol. Adv. Mater.* **2015**, *16* (2), No. 023501.
- (59) Parkinson, G. S. Iron Oxide Surfaces. *Surf. Sci. Rep.* **2016**, *71* (1), 272–365.
- (60) Roca, A. G.; Costo, R.; Rebolledo, A. F.; Veintemillas-Verdaguer, S.; Tartaj, P.; González-Carreño, T.; Morales, M. P.; Serna, C. J. Progress in the Preparation of Magnetic Nanoparticles for Applications in Biomedicine. *J. Phys. D: Appl. Phys.* **2009**, *42* (22), 224002.
- (61) Majidi, S.; Zeinali Sehrig, F.; Farkhani, S. M.; Soleymani Goloujeh, M.; Akbarzadeh, A. Current Methods for Synthesis of Magnetic Nanoparticles. *Artif. Cells, Nanomed., Biotechnol.* **2016**, *44* (2), 722–734.
- (62) Zanella, R. Methodologies for the Synthesis of Nanoparticles Controlling Shape and Size. *Mundo Nano. Interdiscip. J. Nanosci. Nanotechnol.* **2014**, *5* (1), DOI: 10.22201/ceiich.24485691e.2012.1.45167.
- (63) Ansari, F.; Sobhani, A.; Salavati-Niasari, M. Simple Sol-Gel Synthesis and Characterization of New CoTiO<sub>3</sub>/CoFe<sub>2</sub>O<sub>4</sub> Nanocomposite by Using Liquid Glucose, Maltose and Starch as Fuel, Capping and Reducing Agents. *J. Colloid Interface Sci.* **2018**, *514*, 723–732.
- (64) Daou, T. J.; Pourroy, G.; Bégin-Colin, S.; Grenèche, J. M.; Ulhaq-Bouillet, C.; Legaré, P.; Bernhardt, P.; Leuvrey, C.; Rogez, G. Hydrothermal Synthesis of Monodisperse Magnetite Nanoparticles. *Chem. Mater.* **2006**, *18* (18), 4399–4404.
- (65) Lin, S.; Lin, K.; Lu, D.; Liu, Z. Preparation of Uniform Magnetic Iron Oxide Nanoparticles by Co-Precipitation in a Helical Module Microchannel Reactor. *J. Environ. Chem. Eng.* **2017**, *5* (1), 303–309.
- (66) Unni, M.; Uhl, A. M.; Savliwala, S.; Savitzky, B. H.; Dhavalikar, R.; Garraud, N.; Arnold, D. P.; Kourkoutis, L. F.; Andrew, J. S.; Rinaldi, C. Thermal Decomposition Synthesis of Iron Oxide Nanoparticles with Diminished Magnetic Dead Layer by Controlled Addition of Oxygen. *ACS Nano* **2017**, *11* (2), 2284–2303.
- (67) Xu, J.; Sun, J.; Wang, Y.; Sheng, J.; Wang, F.; Sun, M. Application of Iron Magnetic Nanoparticles in Protein Immobilization. *Molecules* **2014**, *19* (8), 11465–11486.
- (68) Verma, J.; Lal, S.; Van Noorden, C. J. F. Nanoparticles for Hyperthermic Therapy: Synthesis Strategies and Applications in Glioblastoma. *Int. J. Nanomed.* **2014**, *9* (1), 2863–2877.
- (69) Ali, A.; Zafar, H.; Zia, M.; ul Haq, I.; Phull, A. R.; Ali, J. S.; Hussain, A. Synthesis, Characterization, Applications, and Challenges of Iron Oxide Nanoparticles. *Nanotechnol., Sci. Appl.* **2016**, *9*, 49–67.
- (70) Getzlaff, M. Magnetism in Reduced Dimensions – Single Thin Films. *Fundamentals of Magnetism*; Springer: Berlin, Heidelberg, 2007; pp 223–238. DOI: 10.1007/978-3-540-31152-2\_14.
- (71) Pardo, A.; Yáñez, S.; Piñeiro, Y.; Iglesias-Rey, R.; Al-Modlej, A.; Barbosa, S.; Rivas, J.; Taboada, P. Cubic Anisotropic Co- and Zn-Substituted Ferrite Nanoparticles as Multimodal Magnetic Agents. *ACS Appl. Mater. Interfaces* **2020**, *12* (8), 9017–9031.
- (72) Zhou, Z.; Zhu, X.; Wu, D.; Chen, Q.; Huang, D.; Sun, C.; Xin, J.; Ni, K.; Gao, J. Anisotropic Shaped Iron Oxide Nanostructures: Controlled Synthesis and Proton Relaxation Shortening Effects. *Chem. Mater.* **2015**, *27* (9), 3505–3515.
- (73) Lentijo-Mozo, S.; Tan, R. P.; Garcia-Marcelot, C.; Altantzis, T.; Fazzini, P. F.; Hungria, T.; Cormary, B.; Gallagher, J. R.; Miller, J. T.; Martinez, H.; Schrittwieser, S.; Schotter, J.; Respaud, M.; Bals, S.; Van Tendeloo, G.; Gatel, C.; Soullantica, K. Air- and Water-Resistant Noble Metal Coated Ferromagnetic Cobalt Nanorods. *ACS Nano* **2015**, *9* (3), 2792–2804.
- (74) Xia, A.; Zuo, C.; Chen, L.; Jin, C.; Lv, Y. Hexagonal SrFe<sub>2</sub>O<sub>19</sub> Ferrites: Hydrothermal Synthesis and Their Sintering Properties. *J. Magn. Magn. Mater.* **2013**, *332*, 186–191.
- (75) Lu, L. T.; Dung, N. T.; Tung, L. D.; Thanh, C. T.; Quy, O. K.; Chuc, N. V.; Maenosono, S.; Thanh, N. T. K. Synthesis of Magnetic Cobalt Ferrite Nanoparticles with Controlled Morphology, Monodispersity and Composition: The Influence of Solvent, Surfactant, Reductant and Synthetic Conditions. *Nanoscale* **2015**, *7* (46), 19596–19610.
- (76) Guardia, P.; Labarta, A.; Batlle, X. Tuning the Size, the Shape, and the Magnetic Properties of Iron Oxide Nanoparticles. *J. Phys. Chem. C* **2011**, *115* (2), 390–396.
- (77) Noh, S. H.; Na, W.; Jang, J. T.; Lee, J. H.; Lee, E. J.; Moon, S. H.; Lim, Y.; Shin, J. S.; Cheon, J. Nanoscale Magnetism Control via Surface and Exchange Anisotropy for Optimized Ferrimagnetic Hysteresis. *Nano Lett.* **2012**, *12* (7), 3716–3721.
- (78) Bordet, A.; Landis, R. F.; Lee, Y. W.; Tonga, G. Y.; Asensio, J. M.; Li, C. H.; Fazzini, P. F.; Soullantica, K.; Rotello, V. M.; Chaudret, B. Water-Dispersible and Biocompatible Iron Carbide Nanoparticles with High Specific Absorption Rate. *ACS Nano* **2019**, *13* (3), 2870–2878.
- (79) Chen, M.; Yang, B.; Zhu, J.; Liu, H.; Zhang, X.; Zheng, X.; Liu, Q. FePt Nanoparticles-Decorated Graphene Oxide Nanosheets as Enhanced Peroxidase Mimics for Sensitive Response to H<sub>2</sub>O<sub>2</sub>. *Mater. Sci. Eng., C* **2018**, *90*, 610–620.
- (80) Salati, A.; Ramazani, A.; Almasi Kashi, M. Deciphering Magnetic Hyperthermia Properties of Compositionally and Morphologically Modulated FeNi Nanoparticles Using First-Order Reversal Curve Analysis. *Nanotechnology* **2019**, *30* (2), No. 025707.
- (81) Pardo, A.; Pelaz, B.; Gallo, J.; Bañobre-López, M.; Parak, W. J.; Barbosa, S.; del Pino, P.; Taboada, P. Synthesis, Characterization, and Evaluation of Superparamagnetic Doped Ferrites as Potential Therapeutic Nanotools. *Chem. Mater.* **2020**, *32* (6), 2220–2231.
- (82) Liang, X.; Zhong, Y.; Zhu, S.; He, H.; Yuan, P.; Zhu, J.; Jiang, Z. The Valence and Site Occupancy of Substituting Metals in Magnetite Spinel Structure Fe<sub>3-x</sub>M<sub>x</sub>O<sub>4</sub> (M = Cr, Mn, Co and Ni) and Their Influence on Thermal Stability. *Solid State Sci.* **2013**, *15*, 115–122.
- (83) Fantechi, E.; Innocenti, C.; Albino, M.; Lottini, E.; Sangregorio, C. Influence of Cobalt Doping on the Hyperthermic Efficiency of Magnetite Nanoparticles. *J. Magn. Magn. Mater.* **2015**, *380*, 365–371.
- (84) Sathya, A.; Guardia, P.; Brescia, R.; Silvestri, N.; Pugliese, G.; Nitti, S.; Manna, L.; Pellegrino, T. CoFe<sub>3</sub>XO<sub>4</sub> Nanocubes for Theranostic Applications: Effect of Cobalt Content and Particle Size. *Chem. Mater.* **2016**, *28* (6), 1769–1780.
- (85) Larumbe, S.; Gomez-Polo, C.; Pérez-Landazábal, J. I.; García-Prieto, A.; Alonso, J.; Fdez-Gubieda, M. L.; Cordero, D.; Gómez, J. Ni Doped Fe<sub>3</sub>O<sub>4</sub> Magnetic Nanoparticles. *J. Nanosci. Nanotechnol.* **2012**, *12* (3), 2652–2660.
- (86) Ghosh Chaudhuri, R.; Paria, S. Core/Shell Nanoparticles: Classes, Properties, Synthesis Mechanisms, Characterization, and Applications. *Chem. Rev.* **2012**, *112* (4), 2373–2433.
- (87) Zhang, Q.; Castellanos-Rubio, I.; Munshi, R.; Orue, I.; Pelaz, B.; Gries, K. I.; Parak, W. J.; Del Pino, P.; Pralle, A. Model Driven Optimization of Magnetic Anisotropy of Exchange-Coupled Core-Shell Ferrite Nanoparticles for Maximal Hysteretic Loss. *Chem. Mater.* **2015**, *27* (21), 7380–7387.
- (88) Lee, J. H.; Jang, J. T.; Choi, J. S.; Moon, S. H.; Noh, S. H.; Kim, J. W.; Kim, J. G.; Kim, I. S.; Park, K. I.; Cheon, J. Exchange-Coupled Magnetic Nanoparticles for Efficient Heat Induction. *Nat. Nanotechnol.* **2011**, *6* (7), 418–422.
- (89) Jang, J. T.; Nah, H.; Lee, J. H.; Moon, S. H.; Kim, M. G.; Cheon, J. Critical Enhancements of MRI Contrast and Hyperthermic Effects by Dopant-Controlled Magnetic Nanoparticles. *Angew. Chem., Int. Ed.* **2009**, *48* (7), 1234–1238.
- (90) Guardia, P.; Riedinger, A.; Nitti, S.; Pugliese, G.; Marras, S.; Genovese, A.; Materia, M. E.; Lefevre, C.; Manna, L.; Pellegrino, T.



One Pot Synthesis of Monodisperse Water Soluble Iron Oxide Nanocrystals with High Values of the Specific Absorption Rate. *J. Mater. Chem. B* **2014**, *2* (28), 4426–4434.

(91) Pazos-Pérez, N.; Rodríguez-González, B.; Hilgendorff, M.; Giersig, M.; Liz-Marzán, L. M. Gold Encapsulation of Star-Shaped FePt Nanoparticles. *J. Mater. Chem.* **2010**, *20* (1), 61–64.

(92) Ling, D.; Lee, N.; Hyeon, T. Chemical Synthesis and Assembly of Uniformly Sized Iron Oxide Nanoparticles for Medical Applications. *Acc. Chem. Res.* **2015**, *48* (5), 1276–1285.

(93) Arami, H.; Khandhar, A.; Liggitt, D.; Krishnan, K. M. *In Vivo* Delivery, Pharmacokinetics, Biodistribution and Toxicity of Iron Oxide Nanoparticles. *Chem. Soc. Rev.* **2015**, *44* (23), 8576–8607.

(94) Crist, R. M.; Grossman, J. H.; Patri, A. K.; Stern, S. T.; Dobrovolskaia, M. A.; Adisheshaiah, P. P.; Clogston, J. D.; McNeil, S. E. Common Pitfalls in Nanotechnology: Lessons Learned from NCI's Nanotechnology Characterization Laboratory. *Integr. Biol. (United Kingdom)* **2013**, *5* (1), 66–73.

(95) Soenen, S. J.; Rivera-Gil, P.; Montenegro, J. M.; Parak, W. J.; De Smedt, S. C.; Braeckmans, K. Cellular Toxicity of Inorganic Nanoparticles: Common Aspects and Guidelines for Improved Nanotoxicity Evaluation. *Nano Today* **2011**, *6* (5), 446–465.

(96) Joris, F.; Manshian, B. B.; Peynshaert, K.; De Smedt, S. C.; Braeckmans, K.; Soenen, S. J. Assessing Nanoparticle Toxicity in Cell-Based Assays: Influence of Cell Culture Parameters and Optimized Models for Bridging the *in Vitro-in Vivo* Gap. *Chem. Soc. Rev.* **2013**, *42* (21), 8339–8359.

(97) Levy, M.; Luciani, N.; Alloeyau, D.; Elgrabli, D.; Deveaux, V.; Pechoux, C.; Chat, S.; Wang, G.; Vats, N.; Gendron, F.; Factor, C.; Lotersztajn, S.; Luciani, A.; Wilhelm, C.; Gazeau, F. Long Term *in Vivo* Biotransformation of Iron Oxide Nanoparticles. *Biomaterials* **2011**, *32* (16), 3988–3999.

(98) Weissleder, R.; Stark, D. D.; Engelstad, B. L.; Bacon, B. R.; Compton, C. C.; White, D. L.; Jacobs, P.; Lewis, J. Superparamagnetic Iron Oxide: Pharmacokinetics and Toxicity. *AJR, Am. J. Roentgenol.* **1989**, *152* (1), 167–173.

(99) Soenen, S. J.; Parak, W. J.; Rejman, J.; Manshian, B. (Intra)Cellular Stability of Inorganic Nanoparticles: Effects on Cytotoxicity, Particle Functionality, and Biomedical Applications. *Chem. Rev.* **2015**, *115* (5), 2109–2135.

(100) Calero, M.; Chiappi, M.; Lazaro-Carrillo, A.; Rodríguez, M. J.; Chichón, F. J.; Crosbie-Staunton, K.; Prina-Mello, A.; Volkov, Y.; Villanueva, A.; Carrascosa, J. L. Characterization of Interaction of Magnetic Nanoparticles with Breast Cancer Cells. *J. Nanobiotechnol.* **2015**, *13* (1), 16.

(101) Sakhtianchi, R.; Minchin, R. F.; Lee, K. B.; Alkilany, A. M.; Serpooshan, V.; Mahmoudi, M. Exocytosis of Nanoparticles from Cells: Role in Cellular Retention and Toxicity. *Adv. Colloid Interface Sci.* **2013**, *201*–202, 18–29.

(102) Kim, J.; Staunton, J. R.; Tanner, K. Independent Control of Topography for 3D Patterning of the ECM Microenvironment. *Adv. Mater.* **2016**, *28* (1), 132–137.

(103) Huang, D. M.; Hsiao, J. K.; Chen, Y. C.; Chien, L. Y.; Yao, M.; Chen, Y. K.; Ko, B. S.; Hsu, S. C.; Tai, L. A.; Cheng, H. Y.; Wang, S. W.; Yang, C. S.; Chen, Y. C. The Promotion of Human Mesenchymal Stem Cell Proliferation by Superparamagnetic Iron Oxide Nanoparticles. *Biomaterials* **2009**, *30* (22), 3645–3651.

(104) Han, J.; Kim, B.; Shin, J. Y.; Ryu, S.; Noh, M.; Woo, J.; Park, J. S.; Lee, Y.; Lee, N.; Hyeon, T.; Choi, D.; Kim, B. S. Iron Oxide Nanoparticle-Mediated Development of Cellular Gap Junction Cross-talk to Improve Mesenchymal Stem Cells' Therapeutic Efficacy for Myocardial Infarction. *ACS Nano* **2015**, *9* (3), 2805–2819.

(105) Joris, F.; Valdepérez, D.; Pelaz, B.; Wang, T.; Doak, S. H.; Manshian, B. B.; Soenen, S. J.; Parak, W. J.; De Smedt, S. C.; Raemdonck, K. Choose Your Cell Model Wisely: The *in Vitro* Nanoneurotoxicity of Differentially Coated Iron Oxide Nanoparticles for Neural Cell Labeling. *Acta Biomater.* **2017**, *55*, 204–213.

(106) Hohnholt, M. C.; Geppert, M.; Dringen, R. Treatment with Iron Oxide Nanoparticles Induces Ferritin Synthesis but Not Oxidative

Stress in Oligodendroglial Cells. *Acta Biomater.* **2011**, *7* (11), 3946–3954.

(107) Laskar, A.; Ghosh, M.; Khattak, S. I.; Li, W.; Yuan, X. M. Degradation of Superparamagnetic Iron Oxide Nanoparticle-Induced Ferritin by Lysosomal Cathepsins and Related Immune Response. *Nanomedicine* **2012**, *7* (5), 705–717.

(108) Karovic, O.; Tonazzini, I.; Rebola, N.; Edström, E.; Lövdahl, C.; Fredholm, B. B.; Daré, E. Toxic Effects of Cobalt in Primary Cultures of Mouse Astrocytes. Similarities with Hypoxia and Role of HIF-1 $\alpha$ . *Biochem. Pharmacol.* **2007**, *73* (5), 694–708.

(109) Horie, M.; Nishio, K.; Fujita, K.; Kato, H.; Nakamura, A.; Kinugasa, S.; Endoh, S.; Miyauchi, A.; Yamamoto, K.; Murayama, H.; Niki, E.; Iwahashi, H.; Yoshida, Y.; Nakanishi, J. Ultrafine NiO Particles Induce Cytotoxicity *in Vitro* by Cellular Uptake and Subsequent Ni(II) Release. *Chem. Res. Toxicol.* **2009**, *22* (8), 1415–1426.

(110) Buyukhatipoglu, K.; Clyne, A. M. Superparamagnetic Iron Oxide Nanoparticles Change Endothelial Cell Morphology and Mechanics via Reactive Oxygen Species Formation. *J. Biomed. Mater. Res., Part A* **2011**, *96* (1), 186–195.

(111) Chimene, D.; Kaunas, R.; Gaharwar, A. K. Hydrogel Bioink Reinforcement for Additive Manufacturing: A Focused Review of Emerging Strategies. *Adv. Mater.* **2020**, *32* (1), 1902026.

(112) Polo, E.; del Pino, P.; Pardo, A.; Taboada, P.; Pelaz, B. Magnetic Nanoparticles for Cancer Therapy and Bioimaging. In *Nanooncology - Engineering Nanomaterials for Cancer Therapy and Diagnosis*; Gonçalves, G., Tobias, G., Eds.; Springer International: Cham, Switzerland, 2018; pp 239–279, DOI: 10.1007/978-3-319-89878-0\_7.

(113) Pelaz, B.; Charron, G.; Pfeiffer, C.; Zhao, Y.; De La Fuente, J. M.; Liang, X. J.; Parak, W. J.; Del Pino, P. Interfacing Engineered Nanoparticles with Biological Systems: Anticipating Adverse Nano-Bio Interactions. *Small* **2013**, *9* (9–10), 1573–1584.

(114) Palui, G.; Aldeek, F.; Wang, W.; Mattoussi, H. Strategies for Interfacing Inorganic Nanocrystals with Biological Systems Based on Polymer-Coating. *Chem. Soc. Rev.* **2015**, *44* (1), 193–227.

(115) Ruiz, A.; Morais, P. C.; Bentes de Azevedo, R.; Lacava, Z. G. M.; Villanueva, A.; del Puerto Morales, M. Magnetic Nanoparticles Coated with Dimercaptosuccinic Acid: Development, Characterization, and Application in Biomedicine. *J. Nanopart. Res.* **2014**, *16* (11), 2589.

(116) Valdepérez, D.; del Pino, P.; Sánchez, L.; Parak, W. J.; Pelaz, B. Highly Active Antibody-Modified Magnetic Polyelectrolyte Capsules. *J. Colloid Interface Sci.* **2016**, *474*, 1–8.

(117) Kim, H. M.; Kim, D. M.; Jeong, C.; Park, S. Y.; Cha, M. G.; Ha, Y.; Jang, D.; Kyeong, S.; Pham, X. H.; Hahm, E.; Lee, S. H.; Jeong, D. H.; Lee, Y. S.; Kim, D. E.; Jun, B. H. Assembly of Plasmonic and Magnetic Nanoparticles with Fluorescent Silica Shell Layer for Tri-Functional SERS-Magnetic-Fluorescence Probes and Its Bioapplications. *Sci. Rep.* **2018**, *8* (1), 13938.

(118) Liu, R.; Zhao, J.; Han, Q.; Hu, X.; Wang, D.; Zhang, X.; Yang, P. One-Step Assembly of a Biomimetic Biopolymer Coating for Particle Surface Engineering. *Adv. Mater.* **2018**, *30* (38), 1802851.

(119) Ejima, H.; Richardson, J. J.; Liang, K.; Best, J. P.; Van Koeverden, M. P.; Such, G. K.; Cui, J.; Caruso, F. One-Step Assembly of Coordination Complexes for Versatile Film and Particle Engineering. *Science (Washington, DC, U. S.)* **2013**, *341* (6142), 154–157.

(120) Testa-Anta, M.; Liébana-Viñas, S.; Rivas-Murias, B.; Rodríguez González, B.; Farle, M.; Salgueiriño, V. Shaping Iron Oxide Nanocrystals for Magnetic Separation Applications. *Nanoscale* **2018**, *10* (43), 20462–20467.

(121) Barrow, M.; Taylor, A.; Fuentes-Caparrós, A. M.; Sharkey, J.; Daniels, L. M.; Mandal, P.; Park, B. K.; Murray, P.; Rosseinsky, M. J.; Adams, D. J. SPIONs for Cell Labelling and Tracking Using MRI: Magnetite or Maghemite? *Biomater. Sci.* **2018**, *6* (1), 101–106.

(122) Pardo, A.; Pujales, R.; Blanco, M.; Villar-Alvarez, E. M.; Barbosa, S.; Taboada, P.; Mosquera, V. Analysis of the Influence of Synthetic Parameters on the Structure and Physico-Chemical Properties of Non-Spherical Iron Oxide Nanocrystals and Their Biological Stability and Compatibility. *Dalt. Trans.* **2016**, *45* (2), 797–810.

(123) Khot, V. M.; Salunkhe, A. B.; Ruso, J. M.; Pawar, S. H. Improved Magnetic Induction Heating of Nanoferrites for Hyperthermia

Applications: Correlation with Colloidal Stability and Magneto-Structural Properties. *J. Magn. Magn. Mater.* **2015**, *384*, 335–343.

(124) Salunkhe, A. B.; Khot, V. M.; Ruso, J. M.; Patil, S. I. Water Dispersible Superparamagnetic Cobalt Iron Oxide Nanoparticles for Magnetic Fluid Hyperthermia. *J. Magn. Magn. Mater.* **2016**, *419*, 533–542.

(125) Múzquiz-Ramos, E. M.; Guerrero-Chávez, V.; Macías-Martínez, B. I.; López-Badillo, C. M.; García-Cerda, L. A. Synthesis and Characterization of Maghemite Nanoparticles for Hyperthermia Applications. *Ceram. Int.* **2015**, *41* (1), 397–402.

(126) Datta, P.; Vyas, V.; Dhara, S.; Chowdhury, A. R.; Barui, A. Anisotropy Properties of Tissues: A Basis for Fabrication of Biomimetic Anisotropic Scaffolds for Tissue Engineering. *J. Bionic Eng.* **2019**, *16* (5), 842–868.

(127) Kim, B. S.; Mooney, D. J. Development of Biocompatible Synthetic Extracellular Matrices for Tissue Engineering. *Trends Biotechnol.* **1998**, *16* (5), 224–230.

(128) Saul, J. M.; Williams, D. F. Hydrogels in Regenerative Medicine. In *Handbook of Polymer Applications in Medicine and Medical Devices*; Modjarrad, K., Ebnesajjad, S., Eds.; Elsevier: Amsterdam, The Netherlands, 2011; pp 279–302, DOI: 10.1016/B978-0-323-22805-3.00012-8.

(129) Varaprasad, K.; Raghavendra, G. M.; Jayaramudu, T.; Yallapu, M. M.; Sadiku, R. A Mini Review on Hydrogels Classification and Recent Developments in Miscellaneous Applications. *Mater. Sci. Eng., C* **2017**, *79*, 958–971.

(130) Kim, H. N.; Jiao, A.; Hwang, N. S.; Kim, M. S.; Kang, D. H.; Kim, D. H.; Suh, K. Y. Nanotopography-Guided Tissue Engineering and Regenerative Medicine. *Adv. Drug Delivery Rev.* **2013**, *65* (4), 536–558.

(131) Sano, K.; Ishida, Y.; Aida, T. Synthesis of Anisotropic Hydrogels and Their Applications. *Angew. Chem., Int. Ed.* **2018**, *57* (10), 2532–2543.

(132) Chau, M.; De France, K. J.; Kopera, B.; Machado, V. R.; Rosenfeldt, S.; Reyes, L.; Chan, K. J. W.; Förster, S.; Cranston, E. D.; Hoare, T.; Kumacheva, E. Composite Hydrogels with Tunable Anisotropic Morphologies and Mechanical Properties. *Chem. Mater.* **2016**, *28* (10), 3406–3415.

(133) Wang, N.; Ma, M.; Luo, Y.; Liu, T.; Zhou, P.; Qi, S.; Xu, Y.; Chen, H. Mesoporous Silica Nanoparticles-Reinforced Hydrogel Scaffold Together with Pinacidil Loading to Improve Stem Cell Adhesion. *ChemNanoMat* **2018**, *4* (7), 631–641.

(134) Lin, X. Y.; Wang, Z. J.; Pan, P.; Wu, Z. L.; Zheng, Q. Monodomain Hydrogels Prepared by Shear-Induced Orientation and Subsequent Gelation. *RSC Adv.* **2016**, *6* (97), 95239–95245.

(135) Lu, Q.; Bai, S.; Ding, Z.; Guo, H.; Shao, Z.; Zhu, H.; Kaplan, D. L. Hydrogel Assembly with Hierarchical Alignment by Balancing Electrostatic Forces. *Adv. Mater. Interfaces* **2016**, *3* (8), 1500687.

(136) Di Meo, C.; Coviello, T.; Matricardi, P.; Alhaique, F.; Capitani, D.; Lamanna, R. Anisotropic Enhanced Water Diffusion in Scleroglucan Gel Tablets. *Soft Matter* **2011**, *7* (13), 6068–6075.

(137) Wu, Z. L.; Kurokawa, T.; Sawada, D.; Hu, J.; Furukawa, H.; Gong, J. P. Anisotropic Hydrogel from Complexation-Driven Reorientation of Semirigid Polyanion at Ca<sup>2+</sup> Diffusion Flux Front. *Macromolecules* **2011**, *44* (9), 3535–3541.

(138) Dinh, N. D.; Luo, R.; Christine, M. T. A.; Lin, W. N.; Shih, W. C.; Goh, J. C. H.; Chen, C. H. Effective Light Directed Assembly of Building Blocks with Microscale Control. *Small* **2017**, *13* (24), 1700684.

(139) Shi, W.; Huang, J.; Fang, R.; Liu, M. Imparting Functionality to the Hydrogel by Magnetic-Field-Induced Nano-Assembly and Macro-Response. *ACS Appl. Mater. Interfaces* **2020**, *12* (5), 5177–5194.

(140) Matos, A. M.; Gonçalves, A. I.; El Haj, A. J.; Gomes, M. E. Magnetic Biomaterials and Nano-Instructive Tools as Mediators of Tendon Mechanotransduction. *Nanoscale Adv.* **2020**, *2* (1), 140–148.

(141) Tomás, A. R.; Gonçalves, A. I.; Paz, E.; Freitas, P.; Domingues, R. M. A.; Gomes, M. E. Magneto-Mechanical Actuation of Magnetic Responsive Fibrous Scaffolds Boosts Tenogenesis of Human Adipose Stem Cells. *Nanoscale* **2019**, *11* (39), 18255–18271.

(142) Ansoorge, R.; Graves, M. Magnetic Field Generation. *The Physics and Mathematics of MRI*; Morgan & Claypool: San Rafael, CA, USA, 2016; DOI: 10.1088/978-1-6817-4068-3ch2.

(143) Liu, Y. L.; Chen, D.; Shang, P.; Yin, D. C. A Review of Magnet Systems for Targeted Drug Delivery. *J. Controlled Release* **2019**, *302*, 90–104.

(144) Johnson, C. D. L.; Ganguly, D.; Zuidema, J. M.; Cardinal, T. J.; Ziemba, A. M.; Kearns, K. R.; McCarthy, S. M.; Thompson, D. M.; Ramanath, G.; Borca-Tasciuc, D. A.; Dutz, S.; Gilbert, R. J. Injectable, Magnetically Orienting Electrospun Fiber Conduits for Neuron Guidance. *ACS Appl. Mater. Interfaces* **2019**, *11* (1), 356–372.

(145) Tognato, R.; Armiento, A. R.; Bonfrate, V.; Levato, R.; Malda, J.; Alini, M.; Eglín, D.; Giancane, G.; Serra, T. A Stimuli-Responsive Nanocomposite for 3D Anisotropic Cell-Guidance and Magnetic Soft Robotics. *Adv. Funct. Mater.* **2019**, *29* (9), 1804647.

(146) Gonçalves, A. I.; Rodrigues, M. T.; Carvalho, P. P.; Bañobre-López, M.; Paz, E.; Freitas, P.; Gomes, M. E. Exploring the Potential of Starch/Polycaprolactone Aligned Magnetic Responsive Scaffolds for Tendon Regeneration. *Adv. Healthcare Mater.* **2016**, *5* (2), 213–222.

(147) Kokkinis, D.; Schaffner, M.; Studart, A. R. Multimaterial Magnetically Assisted 3D Printing of Composite Materials. *Nat. Commun.* **2015**, *6*, 8643.

(148) Betsch, M.; Cristian, C.; Lin, Y. Y.; Blaeser, A.; Schöneberg, J.; Vogt, M.; Buhl, E. M.; Fischer, H.; Duarte Campos, D. F. Incorporating 4D into Bioprinting: Real-Time Magnetically Directed Collagen Fiber Alignment for Generating Complex Multilayered Tissues. *Adv. Healthcare Mater.* **2018**, *7* (21), 1800894.

(149) Haghnegahdar, A.; Khosrovpanah, H.; Andisheh-Tadbir, A.; Mortazavi, G.; Saeedi Moghadam, M.; Mortazavi, S.; Zamani, A.; Haghani, M.; Shojaei Fard, M.; Parsaei, H.; Koochi, O. Design and Fabrication of Helmholtz Coils to Study the Effects of Pulsed Electromagnetic Fields on the Healing Process in Periodontitis: Preliminary Animal Results. *J. Biomed. Phys. Eng.* **2014**, *4* (3), 83–90.

(150) Fuhrer, R.; Athanassiou, E. K.; Luechinger, N. A.; Stark, W. J. Crosslinking Metal Nanoparticles into the Polymer Backbone of Hydrogels Enables Preparation of Soft, Magnetic Field-Driven Actuators with Muscle-Like Flexibility. *Small* **2009**, *5* (3), 383–388.

(151) Sapir, Y.; Cohen, S.; Friedman, G.; Polyak, B. The Promotion of *in Vitro* Vessel-Like Organization of Endothelial Cells in Magnetically Responsive Alginate Scaffolds. *Biomaterials* **2012**, *33* (16), 4100–4109.

(152) Wang, H.; Tang, X.; Li, W.; Chen, J.; Li, H.; Yan, J.; Yuan, X.; Wu, H.; Liu, C. Enhanced Osteogenesis of Bone Marrow Stem Cells Cultured on Hydroxyapatite/Collagen I Scaffold in the Presence of Low-Frequency Magnetic Field. *J. Mater. Sci.: Mater. Med.* **2019**, *30* (8), 89.

(153) Nelson, I.; Gardner, L.; Carlson, K.; Naleway, S. E. Freeze Casting of Iron Oxide Subject to a Tri-Axial Nested Helmholtz-Coils Driven Uniform Magnetic Field for Tailored Porous Scaffolds. *Acta Mater.* **2019**, *173*, 106–116.

(154) Tokarev, A.; Yatvin, J.; Trotsenko, O.; Locklin, J.; Minko, S. Nanostructured Soft Matter with Magnetic Nanoparticles. *Adv. Funct. Mater.* **2016**, *26* (22), 3761–3782.

(155) Zhao, W.; Li, X.; Liu, X.; Zhang, N.; Wen, X. Effects of Substrate Stiffness on Adipogenic and Osteogenic Differentiation of Human Mesenchymal Stem Cells. *Mater. Sci. Eng., C* **2014**, *40*, 316–323.

(156) Peng, Y.; Liu, Q. J.; He, T.; Ye, K.; Yao, X.; Ding, J. Degradation Rate Affords a Dynamic Cue to Regulate Stem Cells beyond Varied Matrix Stiffness. *Biomaterials* **2018**, *178*, 467–480.

(157) Park, H. J.; Jin, Y.; Shin, J.; Yang, K.; Lee, C.; Yang, H. S.; Cho, S. W. Catechol-Functionalized Hyaluronic Acid Hydrogels Enhance Angiogenesis and Osteogenesis of Human Adipose-Derived Stem Cells in Critical Tissue Defects. *Biomacromolecules* **2016**, *17* (6), 1939–1948.

(158) Whang, M.; Kim, J. Synthetic Hydrogels with Stiffness Gradients for Durotaxis Study and Tissue Engineering Scaffolds. *Tissue Eng. Regen. Med.* **2016**, *13* (2), 126–139.

(159) Pesqueira, T.; Costa-Almeida, R.; Gomes, M. E. Magneto-therapy: The Quest for Tendon Regeneration. *J. Cell. Physiol.* **2018**, *233* (10), 6395–6405.



- (160) Vinhas, A.; Rodrigues, M. T.; Gonçalves, A. I.; Reis, R. L.; Gomes, M. E. Pulsed Electromagnetic Field Modulates Tendon Cells Response in IL-1 $\beta$ -Conditioned Environment. *J. Orthop. Res.* **2020**, *38*, 160–172.
- (161) Van Huizen, A. V.; Morton, J. M.; Kinsey, L. J.; Von Kannon, D. G.; Saad, M. A.; Birkholz, T. R.; Czajka, J. M.; Cyrus, J.; Barnes, F. S.; Beane, W. S. Weak Magnetic Fields Alter Stem Cell–Mediated Growth. *Sci. Adv.* **2019**, *5* (1), eaau7201.
- (162) Shuai, C.; Yang, W.; He, C.; Peng, S.; Gao, C.; Yang, Y.; Qi, F.; Feng, P. A Magnetic Micro-Environment in Scaffolds for Stimulating Bone Regeneration. *Mater. Des.* **2020**, *185*, 108275.
- (163) Xia, Y.; Sun, J.; Zhao, L.; Zhang, F.; Liang, X. J.; Guo, Y.; Weir, M. D.; Reynolds, M. A.; Gu, N.; Xu, H. H. K. Magnetic Field and Nano-Scaffolds with Stem Cells to Enhance Bone Regeneration. *Biomaterials*; Elsevier **2018**; pp 151–170, DOI: 10.1016/j.biomaterials.2018.08.040.
- (164) de Abreu, M. C.; Ponzoni, D.; Langje, R.; Artuzi, F. E.; Puricelli, E. Effects of a Buried Magnetic Field on Cranial Bone Reconstruction in Rats. *J. Appl. Oral Sci.* **2016**, *24* (2), 162–170.
- (165) Tay, A.; Sohrabi, A.; Poole, K.; Seidlits, S.; Di Carlo, D. A 3D Magnetic Hyaluronic Acid Hydrogel for Magnetomechanical Neuromodulation of Primary Dorsal Root Ganglion Neurons. *Adv. Mater.* **2018**, *30* (29), 1800927.
- (166) Kim, E. C.; Park, J.; Kwon, I. K.; Lee, S. W.; Park, S. J.; Ahn, S. J. Static Magnetic Fields Promote Osteoblastic/Cementoblastic Differentiation in Osteoblasts, Cementoblasts, and Periodontal Ligament Cells. *J. Periodontal Implant Sci.* **2017**, *47* (5), 273–291.
- (167) Yang, J.; Zhang, J.; Ding, C.; Dong, D.; Shang, P. Regulation of Osteoblast Differentiation and Iron Content in MC3T3-E1 Cells by Static Magnetic Field with Different Intensities. *Biol. Trace Elem. Res.* **2018**, *184* (1), 214–225.
- (168) Essen, H.; Fiolhais, M. C. N. Meissner Effect, Diamagnetism, and Classical Physics - a Review. *Am. J. Phys.* **2012**, *80* (2), 164–169.
- (169) Frka-Petesic, B.; Sugiyama, J.; Kimura, S.; Chanzy, H.; Maret, G. Negative Diamagnetic Anisotropy and Birefringence of Cellulose Nanocrystals. *Macromolecules* **2015**, *48* (24), 8844–8857.
- (170) Tian, B.; Lin, W.; Zhuang, P.; Li, J.; Shih, T. mo; Cai, W. Magnetically-Induced Alignment of Graphene *via* Landau Diamagnetism. *Carbon* **2018**, *131*, 66–71.
- (171) Petrov, D. A.; Zakhlevnykh, A. N. Statistical Theory of Magnetic Field Induced Phase Transitions in Negative Diamagnetic Anisotropy Liquid Crystals Doped with Carbon Nanotubes. *J. Mol. Liq.* **2019**, *287*, 110901.
- (172) Eguchi, Y.; Ohtori, S.; Sekino, M.; Ueno, S. Effectiveness of Magnetically Aligned Collagen for Neural Regeneration *in Vitro* and *in Vivo*. *Bioelectromagnetics* **2015**, *36* (3), 233–243.
- (173) Dubey, N.; Letourneau, P. C.; Tranquillo, R. T. Neuronal Contact Guidance in Magnetically Aligned Fibrin Gels: Effect of Variation in Gel Mechano-Structural Properties. *Biomaterials* **2001**, *22* (10), 1065–1075.
- (174) Torbet, J.; Malbouyres, M.; Builles, N.; Justin, V.; Roulet, M.; Damour, O.; Oldberg, Å.; Ruggiero, F.; Hulmes, D. J. S. Orthogonal Scaffold of Magnetically Aligned Collagen Lamellae for Corneal Stroma Reconstruction. *Biomaterials* **2007**, *28* (29), 4268–4276.
- (175) Maggini, L.; Liu, M.; Ishida, Y.; Bonifazi, D. Anisotropically Luminescent Hydrogels Containing Magnetically-Aligned MWCNTs-Eu(III) Hybrids. *Adv. Mater.* **2013**, *25* (17), 2462–2467.
- (176) Wu, L.; Ohtani, M.; Takata, M.; Saeki, A.; Seki, S.; Ishida, Y.; Aida, T. Magnetically Induced Anisotropic Orientation of Graphene Oxide Locked by *in Situ* Hydrogelation. *ACS Nano* **2014**, *8* (5), 4640–4649.
- (177) De France, K. J.; Yager, K. G.; Chan, K. J. W.; Corbett, B.; Cranston, E. D.; Hoare, T. Injectable Anisotropic Nanocomposite Hydrogels Direct *in Situ* Growth and Alignment of Myotubes. *Nano Lett.* **2017**, *17* (10), 6487–6495.
- (178) Echave, M. C.; Domingues, R. M. A.; Gómez-Florit, M.; Pedraz, J. L.; Reis, R. L.; Orive, G.; Gomes, M. E. Biphasic Hydrogels Integrating Mineralized and Anisotropic Features for Interfacial Tissue Engineering. *ACS Appl. Mater. Interfaces* **2019**, *11* (51), 47771–47784.
- (179) Jalili, N. A.; Muscarello, M.; Gaharwar, A. K. Nanoengineered Thermoresponsive Magnetic Hydrogels for Biomedical Applications. *Bioeng. Transl. Med.* **2016**, *1* (3), 297–305.
- (180) Tang, J.; Qiao, Y.; Chu, Y.; Tong, Z.; Zhou, Y.; Zhang, W.; Xie, S.; Hu, J.; Wang, T. Magnetic Double-Network Hydrogels for Tissue Hyperthermia and Drug Release. *J. Mater. Chem. B* **2019**, *7* (8), 1311–1321.
- (181) Samal, S. K.; Dash, M.; Shelyakova, T.; Declercq, H. A.; Uhlarz, M.; Bañobre-López, M.; Dubruel, P.; Cornelissen, M.; Herrmannsdörfer, T.; Rivas, J.; Padeletti, G.; De Smedt, S.; Braeckmans, K.; Kaplan, D. L.; Dediu, V. A. Biomimetic Magnetic Silk Scaffolds. *ACS Appl. Mater. Interfaces* **2015**, *7* (11), 6282–6292.
- (182) Su, H.; Han, X.; He, L.; Deng, L.; Yu, K.; Jiang, H.; Wu, C.; Jia, Q.; Shan, S. Synthesis and Characterization of Magnetic Dextran Nanogel Doped with Iron Oxide Nanoparticles as Magnetic Resonance Imaging Probe. *Int. J. Biol. Macromol.* **2019**, *128*, 768–774.
- (183) Gao, F.; Xie, W.; Miao, Y.; Wang, D.; Guo, Z.; Ghosal, A.; Li, Y.; Wei, Y.; Feng, S. S.; Zhao, L.; Fan, H. M. Magnetic Hydrogel with Optimally Adaptive Functions for Breast Cancer Recurrence Prevention. *Adv. Healthcare Mater.* **2019**, *8* (14), 1900203.
- (184) Daniel-Da-Silva, A. L.; Moreira, J.; Neto, R.; Estrada, A. C.; Gil, A. M.; Trindade, T. Impact of Magnetic Nanofillers in the Swelling and Release Properties of  $\kappa$ -Carrageenan Hydrogel Nanocomposites. *Carbohydr. Polym.* **2012**, *87* (1), 328–335.
- (185) Fuhrer, R.; Hofmann, S.; Hild, N.; Vetsch, J. R.; Herrmann, I. K.; Grass, R. N.; Stark, W. J. Pressureless Mechanical Induction of Stem Cell Differentiation Is Dose and Frequency Dependent. *PLoS One* **2013**, *8* (11), e81362.
- (186) Sakai, R.; Teramoto, Y.; Nishio, Y. Producing a Magnetically Anisotropic Soft Material: Synthesis of Iron Oxide Nanoparticles in a Carrageenan/PVA Matrix and Stretching of the Hybrid Gelatinous Bulk. *Polym. J.* **2018**, *50* (3), 251–260.
- (187) Roeder, L.; Bender, P.; Kundt, M.; Tschöpe, A.; Schmidt, A. M. Magnetic and Geometric Anisotropy in Particle-Crosslinked Ferrogels. *Phys. Chem. Chem. Phys.* **2015**, *17* (2), 1290–1298.
- (188) Bender, P.; Günther, A.; Tschöpe, A.; Birringer, R. Synthesis and Characterization of Uniaxial Ferrogels with Ni as magnetic phase. *J. Magn. Mater.* **2011**, *323* (15), 2055–2063.
- (189) Diaz-Bleis, D.; Vales-Pinzón, C.; Freile-Pelegrín, Y.; Alvarado-Gil, J. J. Thermal Characterization of Magnetically Aligned Carbonyl Iron/Agar Composites. *Carbohydr. Polym.* **2014**, *99*, 84–90.
- (190) Mohapatra, J.; Zeng, F.; Elkins, K.; Xing, M.; Ghimire, M.; Yoon, S.; Mishra, S. R.; Liu, J. P. Size-Dependent Magnetic and Inductive Heating Properties of Fe<sub>3</sub>O<sub>4</sub> Nanoparticles: Scaling Laws across the Superparamagnetic Size. *Phys. Chem. Chem. Phys.* **2018**, *20* (18), 12879–12887.
- (191) Pei, B.; Wang, W.; Fan, Y.; Wang, X.; Watari, F.; Li, X. Fiber-Reinforced Scaffolds in Soft Tissue Engineering. *Regen. Biomater.* **2017**, *4* (4), 257–268.
- (192) Huang, S.; Zhao, Z.; Feng, C.; Mayes, E.; Yang, J. Nanocellulose Reinforced P(AAm-Co-AAc) Hydrogels with Improved Mechanical Properties and Biocompatibility. *Composites, Part A* **2018**, *112*, 395–404.
- (193) Markides, H.; Rotherham, M.; El Haj, A. J. Biocompatibility and Toxicity of Magnetic Nanoparticles in Regenerative Medicine. *J. Nanomater.* **2012**, *2012*, 614094.
- (194) Jiang, Z.; Shan, K.; Song, J.; Liu, J.; Rajendran, S.; Pugazhendhi, A.; Jacob, J. A.; Chen, B. Toxic Effects of Magnetic Nanoparticles on Normal Cells and Organs. *Life Sci.* **2019**, *220*, 156–161.
- (195) Khan, I.; Saeed, K.; Khan, I. Nanoparticles: Properties, Applications and Toxicities. *Arabian J. Chem.* **2019**, *12* (7), 908–931.
- (196) Rose, J. C.; Cámara-Torres, M.; Rahimi, K.; Köhler, J.; Möller, M.; De Laporte, L. Nerve Cells Decide to Orient inside an Injectable Hydrogel with Minimal Structural Guidance. *Nano Lett.* **2017**, *17* (6), 3782–3791.
- (197) Helgeson, M. E.; Chapin, S. C.; Doyle, P. S. Hydrogel Microparticles from Lithographic Processes: Novel Materials for Fundamental and Applied Colloid Science. *Curr. Opin. Colloid Interface Sci.* **2011**, *16* (2), 106–117.



- (198) Yang, G.; Li, X.; He, Y.; Ma, J.; Ni, G.; Zhou, S. From Nano to Micro to Macro: Electrospun Hierarchically Structured Polymeric Fibers for Biomedical Applications. *Prog. Polym. Sci.* **2018**, *81*, 80–113.
- (199) Chen, R.; Chen, X.; Jin, X.; Zhu, X. Morphology Design and Control of Polymer Particles by Regulating the Droplet Flowing Mode in Microfluidic Chips. *Polym. Chem.* **2017**, *8* (19), 2953–2958.
- (200) Smoukov, S. K.; Tian, T.; Vitichuli, N.; Gangwal, S.; Geisen, P.; Wright, M.; Shim, E.; Marquez, M.; Fowler, J.; Velev, O. D. Scalable Liquid Shear-Driven Fabrication of Polymer Nanofibers. *Adv. Mater.* **2015**, *27* (16), 2642–2647.
- (201) Sommer, M. R.; Erb, R. M.; Studart, A. R. Injectable Materials with Magnetically Controlled Anisotropic Porosity. *ACS Appl. Mater. Interfaces* **2012**, *4* (10), 5086–5091.
- (202) Liu, W.; Li, Y.; Feng, S.; Ning, J.; Wang, J.; Gou, M.; Chen, H.; Xu, F.; Du, Y. Magnetically Controllable 3D Microtissues Based on Magnetic Microcryogels. *Lab Chip* **2014**, *14* (15), 2614–2625.
- (203) Xu, F.; Wu, C. A. M.; Rengarajan, V.; Finley, T. D.; Keles, H. O.; Sung, Y.; Li, B.; Gurkan, U. A.; Demirci, U. Three-Dimensional Magnetic Assembly of Microscale Hydrogels. *Adv. Mater.* **2011**, *23* (37), 4254–4260.
- (204) Omidinia-Anarkoli, A.; Boesveld, S.; Tuvshindorj, U.; Rose, J. C.; Haraszti, T.; De Laporte, L. An Injectable Hybrid Hydrogel with Oriented Short Fibers Induces Unidirectional Growth of Functional Nerve Cells. *Small* **2017**, *13* (36), 1702207.
- (205) Corr, D. T.; Hart, D. A. Biomechanics of Scar Tissue and Uninjured Skin. *Adv. Wound Care* **2013**, *2* (2), 37–43.
- (206) Li, Y.; Xiao, Y.; Liu, C. The Horizon of Materiobiology: A Perspective on Material-Guided Cell Behaviors and Tissue Engineering. *Chem. Rev.* **2017**, *117* (5), 4376–4421.
- (207) Tadsen, M.; Friedrich, R. P.; Riedel, S.; Alexiou, C.; Mayr, S. G. Contact Guidance by Microstructured Gelatin Hydrogels for Prospective Tissue Engineering Applications. *ACS Appl. Mater. Interfaces* **2019**, *11* (7), 7450–7458.
- (208) Laranjeira, M.; Domingues, R. M. A.; Costa-Almeida, R.; Reis, R. L.; Gomes, M. E. 3D Mimicry of Native-Tissue-Fiber Architecture Guides Tendon-Derived Cells and Adipose Stem Cells into Artificial Tendon Constructs. *Small* **2017**, *13* (31), 1700689.
- (209) Chklovskii, D. B. Synaptic Connectivity and Neuronal Morphology: Two Sides of the Same Coin. *Neuron* **2004**, *43* (5), 609–617.
- (210) Font Tellado, S.; Bonani, W.; Balmayor, E. R.; Foehr, P.; Motta, A.; Migliaresi, C.; Van Griensven, M. Fabrication and Characterization of Biphasic Silk Fibroin Scaffolds for Tendon/Ligament-to-Bone Tissue Engineering. *Tissue Eng., Part A* **2017**, *23* (15–16), 859–872.
- (211) Radhakrishnan, J.; Subramanian, A.; Krishnan, U. M.; Sethuraman, S. Injectable and 3D Bioprinted Polysaccharide Hydrogels: From Cartilage to Osteochondral Tissue Engineering. *Biomacromolecules* **2017**, *18* (1), 1–26.
- (212) Guimarães, C. F.; Gasperini, L.; Marques, A. P.; Reis, R. L. The Stiffness of Living Tissues and Its Implications for Tissue Engineering. *Nat. Rev. Mater.* **2020**, *5* (5), 351–370.
- (213) Wolfenson, H.; Yang, B.; Sheetz, M. P. Steps in Mechano-transduction Pathways That Control Cell Morphology. *Annu. Rev. Physiol.* **2019**, *81* (1), 585–605.
- (214) Dupont, S. Role of YAP/TAZ in Cell-Matrix Adhesion-Mediated Signalling and Mechanotransduction. *Exp. Cell Res.* **2016**, *343* (1), 42–53.
- (215) Fahy, N.; Alini, M.; Stoddart, M. J. Mechanical Stimulation of Mesenchymal Stem Cells: Implications for Cartilage Tissue Engineering. *J. Orthop. Res.* **2017**, *36* (1), 52–63.
- (216) Dan, P.; Velot, E.; Decot, V.; Menu, P. The Role of Mechanical Stimuli in the Vascular Differentiation of Mesenchymal Stem Cells. *J. Cell Sci.* **2015**, *128* (14), 2415–2422.
- (217) Zhuo, Y.; Choi, J. S.; Marin, T.; Yu, H.; Harley, B. A.; Cunningham, B. T. Quantitative Analysis of Focal Adhesion Dynamics Using Photonic Resonator Outcoupler Microscopy (PROM). *Light: Sci. Appl.* **2018**, *7* (1), 9.
- (218) Rienks, M.; Papageorgiou, A. P.; Frangogiannis, N. G.; Heymans, S. Myocardial Extracellular Matrix: An Ever-Changing and Diverse Entity. *Circ. Res.* **2014**, *114*, 872–888.
- (219) Abdeen, A. A.; Lee, J.; Bharadwaj, N. A.; Ewoldt, R. H.; Kilian, K. A. Temporal Modulation of Stem Cell Activity Using Magnetoactive Hydrogels. *Adv. Healthcare Mater.* **2016**, *5* (19), 2536–2544.
- (220) Armiento, A. R.; Stoddart, M. J.; Alini, M.; Eglin, D. Biomaterials for Articular Cartilage Tissue Engineering: Learning from Biology. *Acta Biomater.* **2018**, *65*, 1–20.
- (221) Malda, J.; Benders, K. E. M.; Klein, T. J.; de Grauw, J. C.; Kik, M. J. L.; Huttmacher, D. W.; Saris, D. B. F.; van Weeren, P. R.; Dhert, W. J. A. Comparative Study of Depth-Dependent Characteristics of Equine and Human Osteochondral Tissue from the Medial and Lateral Femoral Condyles. *Osteoarthr. Cartil.* **2012**, *20* (10), 1147–1151.
- (222) Clark, J. M. Variation of Collagen Fiber Alignment in a Joint Surface: A Scanning Electron Microscope Study of the Tibial Plateau in Dog, Rabbit, and Man. *J. Orthop. Res.* **1991**, *9* (2), 246–257.
- (223) Levato, R.; Webb, W. R.; Otto, I. A.; Mensinga, A.; Zhang, Y.; van Rijen, M.; van Weeren, R.; Khan, I. M.; Malda, J. The Bio in the Ink: Cartilage Regeneration with Bioprintable Hydrogels and Articular Cartilage-Derived Progenitor Cells. *Acta Biomater.* **2017**, *61*, 41–53.
- (224) Lin, S.; Lee, W. Y. W.; Feng, Q.; Xu, L.; Wang, B.; Man, G. C. W.; Chen, Y.; Jiang, X.; Bian, L.; Cui, L.; Wei, B.; Li, G. Synergistic Effects on Mesenchymal Stem Cell-Based Cartilage Regeneration by Chondrogenic Preconditioning and Mechanical Stimulation. *Stem Cell Res. Ther.* **2017**, *8* (1), 221.
- (225) Yang, J.; Zhang, Y. S.; Yue, K.; Khademhosseini, A. Cell-Laden Hydrogels for Osteochondral and Cartilage Tissue Engineering. *Acta Biomater.* **2017**, *57*, 1–25.
- (226) Salinas, E. Y.; Hu, J. C.; Athanasiou, K. A Guide for Using Mechanical Stimulation to Enhance Tissue-Engineered Articular Cartilage Properties. *Tissue Eng., Part B* **2018**, *24* (5), 345–358.
- (227) Bonhome-Espinosa, A. B.; Campos, F.; Durand-Herrera, D.; Sánchez-López, J. D.; Schaub, S.; Durán, J. D. G.; Lopez-Lopez, M. T.; Carriel, V. *In Vitro* Characterization of a Novel Magnetic Fibrin-Agarose Hydrogel for Cartilage Tissue Engineering. *J. Mech. Behav. Biomed. Mater.* **2020**, *104*, 103619.
- (228) Brady, M. A.; Talvard, L.; Vella, A.; Ethier, C. R. Bio-Inspired Design of a Magnetically Active Trilayered Scaffold for Cartilage Tissue Engineering. *J. Tissue Eng. Regen. Med.* **2017**, *11* (4), 1298–1302.
- (229) Gong, T.; Xie, J.; Liao, J.; Zhang, T.; Lin, S.; Lin, Y. Nanomaterials and Bone Regeneration. *Bone Res.* **2015**, *3*, 15029.
- (230) Alford, A. I.; Kozloff, K. M.; Hankenson, K. D. Extracellular Matrix Networks in Bone Remodeling. *Int. J. Biochem. Cell Biol.* **2015**, *65*, 20–31.
- (231) Katsamenis, O. L.; Chong, H. M. H.; Andriotis, O. G.; Thurner, P. J. Load-Bearing in Cortical Bone Microstructure: Selective Stiffening and Heterogeneous Strain Distribution at the Lamellar Level. *J. Mech. Behav. Biomed. Mater.* **2013**, *17*, 152–165.
- (232) Fernandez-Yague, M. A.; Abbah, S. A.; McNamara, L.; Zeugolis, D. I.; Pandit, A.; Biggs, M. J. Biomimetic Approaches in Bone Tissue Engineering: Integrating Biological and Physicomechanical Strategies. *Adv. Drug Delivery Rev.* **2015**, *84*, 1–29.
- (233) Short, A. R.; Koralla, D.; Deshmukh, A.; Wissel, B.; Stocker, B.; Calhoun, M.; Dean, D.; Winter, J. O. Hydrogels That Allow and Facilitate Bone Repair, Remodeling, and Regeneration. *J. Mater. Chem. B* **2015**, *3* (40), 7818–7830.
- (234) Kumar, A.; Rao, K. M.; Han, S. S. Synthesis of Mechanically Stiff and Bioactive Hybrid Hydrogels for Bone Tissue Engineering Applications. *Chem. Eng. J.* **2017**, *317*, 119–131.
- (235) De Lima, G. G.; Elter, J. K.; Chee, B. S.; Magalhães, W. L. E.; Devine, D. M.; Nugent, M. J. D.; De Sá, M. J. C. A Tough and Novel Dual-Response PAA/P(NiPAAM-Co-PEGDMA) IPN Hydrogels with Ceramics by Photopolymerization for Consolidation of Bone Fragments Following Fracture. *Biomed. Mater.* **2019**, *14* (5), No. 054101.
- (236) Turnbull, G.; Clarke, J.; Picard, F.; Riches, P.; Jia, L.; Han, F.; Li, B.; Shu, W. 3D Bioactive Composite Scaffolds for Bone Tissue Engineering. *Bioact. Mater.* **2018**, *3* (3), 278–314.

- (237) Nikpour, P.; Salimi-Kenari, H.; Fahimipour, F.; Rabiee, S. M.; Imani, M.; Dashtimoghadam, E.; Tayebi, L. Dextran Hydrogels Incorporated with Bioactive Glass-Ceramic: Nanocomposite Scaffolds for Bone Tissue Engineering. *Carbohydr. Polym.* **2018**, *190*, 281–294.
- (238) Wenz, A.; Borchers, K.; Tovar, G. E. M.; Kluger, P. J. Bone Matrix Production in Hydroxyapatite-Modified Hydrogels Suitable for Bone Bioprinting. *Biofabrication* **2017**, *9* (4), No. 044103.
- (239) Paul, A.; Manoharan, V.; Krafft, D.; Assmann, A.; Uquillas, J. A.; Shin, S. R.; Hasan, A.; Hussain, M. A.; Memic, A.; Gaharwar, A. K.; Khademhosseini, A. Nanoengineered Biomimetic Hydrogels for Guiding Human Stem Cell Osteogenesis in Three Dimensional Microenvironments. *J. Mater. Chem. B* **2016**, *4* (20), 3544–3554.
- (240) Yun, H. M.; Lee, E. S.; Kim, M. J.; Kim, J. J.; Lee, J. H.; Lee, H. H.; Park, K. R.; Yi, J. K.; Kim, H. W.; Kim, E. C. Magnetic Nanocomposite Scaffold-Induced Stimulation of Migration and Odontogenesis of Human Dental Pulp Cells through Integrin Signaling Pathways. *PLoS One* **2015**, *10* (9), No. e0138614.
- (241) Arjmand, M.; Ardeshirylajimi, A.; Maghsoudi, H.; Azadian, E. Osteogenic Differentiation Potential of Mesenchymal Stem Cells Cultured on Nanofibrous Scaffold Improved in the Presence of Pulsed Electromagnetic Field. *J. Cell. Physiol.* **2018**, *233* (2), 1061–1070.
- (242) Ganesh, N.; Ashokan, A.; Rajeshkannan, R.; Chennazhi, K.; Koyakutty, M.; Nair, S. V. Magnetic Resonance Functional Nano-Hydroxyapatite Incorporated Poly(caprolactone) Composite Scaffolds for *in Situ* Monitoring of Bone Tissue Regeneration by MRI. *Tissue Eng., Part A* **2014**, *20* (19–20), 2783–2794.
- (243) Yun, H. M.; Ahn, S. J.; Park, K. R.; Kim, M. J.; Kim, J. J.; Jin, G. Z.; Kim, H. W.; Kim, E. C. Magnetic Nanocomposite Scaffolds Combined with Static Magnetic Field in the Stimulation of Osteoblastic Differentiation and Bone Formation. *Biomaterials* **2016**, *85*, 88–98.
- (244) Li, Q.; Ge, L.; Wan, W.; Jiang, J.; Zhong, W.; Ouyang, J.; Xing, M. Magnetically Guided Fabrication of Multilayered Iron Oxide/Polycaprolactone/Gelatin Nanofibrous Structures for Tissue Engineering and Theranostic Application. *Tissue Eng., Part C* **2015**, *21* (10), 1015–1024.
- (245) Chen, H.; Sun, J.; Wang, Z.; Zhou, Y.; Lou, Z.; Chen, B.; Wang, P.; Guo, Z.; Tang, H.; Ma, J.; Xia, Y.; Gu, N.; Zhang, F. Magnetic Cell-Scaffold Interface Constructed by Superparamagnetic IONP Enhanced Osteogenesis of Adipose-Derived Stem Cells. *ACS Appl. Mater. Interfaces* **2018**, *10* (S1), 44279–44289.
- (246) Karahaliloglu, Z.; Yalçın, E.; Demirbilek, M.; Denkbaz, E. B. Magnetic Silk Fibroin e-Gel Scaffolds for Bone Tissue Engineering Applications. *J. Bioact. Compat. Polym.* **2017**, *32* (6), 596–614.
- (247) Filippi, M.; Dasen, B.; Guerrero, J.; Garelo, F.; Isu, G.; Born, G.; Ehrbar, M.; Martin, I.; Scherberich, A. Magnetic Nanocomposite Hydrogels and Static Magnetic Field Stimulate the Osteoblastic and Vasculogenic Profile of Adipose-Derived Cells. *Biomaterials* **2019**, *223*, 119468.
- (248) Koons, G. L.; Diba, M.; Mikos, A. G. Materials Design for Bone-Tissue Engineering. *Nat. Rev. Mater.* **2020**, *5* (8), 584–603.
- (249) Huang, W.-S.; Chu, I.-M. Injectable Polypeptide Hydrogel/Inorganic Nanoparticle Composites for Bone Tissue Engineering. *PLoS One* **2019**, *14* (1), e0210285.
- (250) Hou, R.; Zhang, G.; Du, G.; Zhan, D.; Cong, Y.; Cheng, Y.; Fu, J. Magnetic Nanohydroxyapatite/PVA Composite Hydrogels for Promoted Osteoblast Adhesion and Proliferation. *Colloids Surf., B* **2013**, *103*, 318–325.
- (251) Liu, Y.; Luo, D.; Wang, T. Hierarchical Structures of Bone and Bioinspired Bone Tissue Engineering. *Small* **2016**, *12* (34), 4611–4632.
- (252) Johnson, G. A.; Tramaglino, D. M.; Levine, R. E.; Ohno, K.; Choi, N.-Y.; Woo, S. L.-Y. Tensile and Viscoelastic Properties of Human Patellar Tendon. *J. Orthop. Res.* **1994**, *12* (6), 796–803.
- (253) Thorpe, C. T.; Birch, H. L.; Clegg, P. D.; Screen, H. R. C. Tendon Physiology and Mechanical Behavior: Structure-Function Relationships. In *Tendon Regeneration: Understanding Tissue Physiology and Development to Engineer Functional Substitutes*; Gomes, M. E., Reis, R. L., Rodrigues, M. T., Eds.; Elsevier: San Diego, CA, USA, 2015; pp 3–39. DOI: 10.1016/B978-0-12-801590-2.00001-6.
- (254) Thorpe, C. T.; Screen, H. R. C. Tendon Structure and Composition. *Adv. Exp. Med. Biol.* **2016**, *920*, 3–10.
- (255) Smith, L.; Xia, Y.; Galatz, L. M.; Genin, G. M.; Thomopoulos, S. Tissue-Engineering Strategies for the Tendon/Ligament-to-Bone Insertion. *Connect. Tissue Res.* **2012**, *53* (2), 95–105.
- (256) Laternser, S.; Keller, H.; Leupin, O.; Rausch, M.; Graf-Hausner, U.; Rimann, M. A Novel Microplate 3D Bioprinting Platform for the Engineering of Muscle and Tendon Tissues. *SLAS Technol.* **2018**, *23* (6), 599–613.
- (257) Yin, H.; Yan, Z.; Bauer, R. J.; Peng, J.; Schieker, M.; Nerlich, M.; Docheva, D. Functionalized Thermosensitive Hydrogel Combined with Tendon Stem/Progenitor Cells as Injectable Cell Delivery Carrier for Tendon Tissue Engineering. *Biomed. Mater.* **2018**, *13* (3), No. 034107.
- (258) Domingues, R. M. A.; Chiera, S.; Gershovich, P.; Motta, A.; Reis, R. L.; Gomes, M. E. Enhancing the Biomechanical Performance of Anisotropic Nanofibrous Scaffolds in Tendon Tissue Engineering: Reinforcement with Cellulose Nanocrystals. *Adv. Healthcare Mater.* **2016**, *5* (11), 1364–1375.
- (259) Yang, G.; Lin, H.; Rothrauff, B. B.; Yu, S.; Tuan, R. S. Multilayered Polycaprolactone/Gelatin Fiber-Hydrogel Composite for Tendon Tissue Engineering. *Acta Biomater.* **2016**, *35*, 68–76.
- (260) Rinoldi, C.; Costantini, M.; Kijeńska-Gawrońska, E.; Testa, S.; Fornetti, E.; Heljak, M.; Ćwiklińska, M.; Buda, R.; Baldi, J.; Cannata, S.; Guzowski, J.; Gargioli, C.; Khademhosseini, A.; Swieszkowski, W. Tendon Tissue Engineering: Effects of Mechanical and Biochemical Stimulation on Stem Cell Alignment on Cell-Laden Hydrogel Yarns. *Adv. Healthcare Mater.* **2019**, *8* (7), 1801218.
- (261) Pesqueira, T.; Costa-Almeida, R.; Mithieux, S. M.; Babo, P. S.; Franco, A. R.; Mendes, B. B.; Domingues, R. M. A.; Freitas, P.; Reis, R. L.; Gomes, M. E.; Weiss, A. S. Engineering Magnetically Responsive Tropeolastin Spongy-Like Hydrogels for Soft Tissue Regeneration. *J. Mater. Chem. B* **2018**, *6* (7), 1066–1075.
- (262) Calejo, I.; Costa-Almeida, R.; Reis, R. L.; Gomes, M. E. A Textile Platform Using Continuous Aligned and Textured Composite Microfibers to Engineer Tendon-to-Bone Interface Gradient Scaffolds. *Adv. Healthcare Mater.* **2019**, *8* (15), 1900200.
- (263) Lin, Z.; Zhao, X.; Chen, S.; Du, C. Osteogenic and Tenogenic Induction of HBMSCs by an Integrated Nanofibrous Scaffold with Chemical and Structural Mimicry of the Bone-Ligament Connection. *J. Mater. Chem. B* **2017**, *5* (5), 1015–1027.
- (264) Kim, B. S.; Kim, E. J.; Choi, J. S.; Jeong, J. H.; Jo, C. H.; Cho, Y. W. Human Collagen-Based Multilayer Scaffolds for Tendon-to-Bone Interface Tissue Engineering. *J. Biomed. Mater. Res., Part A* **2014**, *102* (11), 4044–4054.
- (265) Sensini, A.; Cristofolini, L. Biofabrication of Electrospun Scaffolds for the Regeneration of Tendons and Ligaments. *Materials* **2018**, *11* (10), 1963.
- (266) Jana, S.; Levensgood, S. K. L.; Zhang, M. Anisotropic Materials for Skeletal-Muscle-Tissue Engineering. *Adv. Mater.* **2016**, *28* (48), 10588–10612.
- (267) Qazi, T. H.; Mooney, D. J.; Pumberger, M.; Geißler, S.; Duda, G. N. Biomaterials Based Strategies for Skeletal Muscle Tissue Engineering: Existing Technologies and Future Trends. *Biomaterials* **2015**, *53*, 502–521.
- (268) Jhala, D.; Vasita, R. A Review on Extracellular Matrix Mimicking Strategies for an Artificial Stem Cell Niche. *Polym. Rev.* **2015**, *55* (4), 561–595.
- (269) Eskandari, M.; Arvayo, A. L.; Levenston, M. E. Mechanical Properties of the Airway Tree: Heterogeneous and Anisotropic Pseudoelastic and Viscoelastic Tissue Responses. *J. Appl. Physiol.* **2018**, *125* (3), 878–888.
- (270) Kwon, H.; Guasch, M.; Nagy, J. A.; Rutkove, S. B.; Sanchez, B. New Electrical Impedance Methods for the *in Situ* Measurement of the Complex Permittivity of Anisotropic Skeletal Muscle Using Multipolar Needles. *Sci. Rep.* **2019**, *9* (1), 1–16.
- (271) Ostrovidov, S.; Shi, X.; Zhang, L.; Liang, X.; Kim, S. B.; Fujie, T.; Ramalingam, M.; Chen, M.; Nakajima, K.; Al-Hazmi, F.; Bae, H.; Memic, A.; Khademhosseini, A. Myotube Formation on Gelatin



Nanofibers - Multi-Walled Carbon Nanotubes Hybrid Scaffolds. *Biomaterials* **2014**, *35* (24), 6268–6277.

(272) Chen, M. C.; Sun, Y. C.; Chen, Y. H. Electrically Conductive Nanofibers with Highly Oriented Structures and Their Potential Application in Skeletal Muscle Tissue Engineering. *Acta Biomater.* **2013**, *9* (3), 5562–5572.

(273) Hu, X.; Nian, G.; Liang, X.; Wu, L.; Yin, T.; Lu, H.; Qu, S.; Yang, W. Adhesive Tough Magnetic Hydrogels with High Fe<sub>3</sub>O<sub>4</sub> Content. *ACS Appl. Mater. Interfaces* **2019**, *11* (10), 10292–10300.

(274) Cezar, C. A.; Roche, E. T.; Vandenburgh, H. H.; Duda, G. N.; Walsh, C. J.; Mooney, D. J. Biologic-Free Mechanically Induced Muscle Regeneration. *Proc. Natl. Acad. Sci. U. S. A.* **2016**, *113* (6), 1534–1539.

(275) Li, Y.; Poon, C. T.; Li, M.; Lu, T. J.; Pingguan-Murphy, B.; Xu, F. Chinese-Noodle-Inspired Muscle Myofiber Fabrication. *Adv. Funct. Mater.* **2015**, *25* (37), 5999–6008.

(276) Bonetto, A.; Bonewald, L. F. Bone and Muscle. In *Basic and Applied Bone Biology*, 2nd ed.; Burr, D. B., Allen, M. R., Eds.; Elsevier: London, U.K., 2019; pp 317–332. DOI: 10.1016/b978-0-12-813259-3.00016-6.

(277) Camelliti, P.; Borg, T. K.; Kohl, P. Structural and Functional Characterisation of Cardiac Fibroblasts. *Cardiovasc. Res.* **2005**, *65* (1), 40–51.

(278) Feiner, R.; Shapira, A.; Dvir, T. Scaffolds for Tissue Engineering of Functional Cardiac Muscle. In *Handbook of Tissue Engineering Scaffolds*; Mozafari, M., Sefat, F., Atala, A., Eds.; Elsevier: London, U.K., 2019; pp 685–703, DOI: 10.1016/b978-0-08-102563-5.00032-0.

(279) Tandon, N.; Cannizzaro, C.; Chao, P. H. G.; Maidhof, R.; Marsano, A.; Au, H. T. H.; Radisic, M.; Vunjak-Novakovic, G. Electrical Stimulation Systems for Cardiac Tissue Engineering. *Nat. Protoc.* **2009**, *4* (2), 155–173.

(280) Shin, S. R.; Zihlmann, C.; Akbari, M.; Assawes, P.; Cheung, L.; Zhang, K.; Manoharan, V.; Zhang, Y. S.; Yükksekaya, M.; Wan, K. T.; Nikkhah, M.; Dokmeci, M. R.; Tang, X. S.; Khademhosseini, A. Reduced Graphene Oxide-GelMA Hybrid Hydrogels as Scaffolds for Cardiac Tissue Engineering. *Small* **2016**, *12* (27), 3677–3689.

(281) Qazi, T. H.; Rai, R.; Dippold, D.; Roether, J. E.; Schubert, D. W.; Rosellini, E.; Barbani, N.; Boccaccini, A. R. Development and Characterization of Novel Electrically Conductive PANI-PGS Composites for Cardiac Tissue Engineering Applications. *Acta Biomater.* **2014**, *10* (6), 2434–2445.

(282) Kai, D.; Prabhakaran, M. P.; Jin, G.; Ramakrishna, S. Polypyrrole-Contained Electrospun Conductive Nanofibrous Membranes for Cardiac Tissue Engineering. *J. Biomed. Mater. Res., Part A* **2011**, *99* (3), 376–385.

(283) Zhu, K.; Shin, S. R.; van Kempen, T.; Li, Y. C.; Ponraj, V.; Nasajpour, A.; Mandla, S.; Hu, N.; Liu, X.; Leijten, J.; Lin, Y. D.; Hussain, M. A.; Zhang, Y. S.; Tamayol, A.; Khademhosseini, A. Gold Nanocomposite Bioink for Printing 3D Cardiac Constructs. *Adv. Funct. Mater.* **2017**, *27* (12), 1605352.

(284) Martins, A. M.; Eng, G.; Caridade, S. G.; Mano, J. F.; Reis, R. L.; Vunjak-Novakovic, G. Electrically Conductive Chitosan/Carbon Scaffolds for Cardiac Tissue Engineering. *Biomacromolecules* **2014**, *15* (2), 635–643.

(285) Shin, S. R.; Jung, S. M.; Zalabany, M.; Kim, K.; Zorlutuna, P.; Kim, S. B.; Nikkhah, M.; Khabiry, M.; Azize, M.; Kong, J.; Wan, K. T.; Palacios, T.; Dokmeci, M. R.; Bae, H.; Tang, X.; Khademhosseini, A. Carbon-Nanotube-Embedded Hydrogel Sheets for Engineering Cardiac Constructs and Bioactuators. *ACS Nano* **2013**, *7* (3), 2369–2380.

(286) Ahadian, S.; Yamada, S.; Ramón-Azcón, J.; Estili, M.; Liang, X.; Nakajima, K.; Shiku, H.; Khademhosseini, A.; Matsue, T. Hybrid Hydrogel-Aligned Carbon Nanotube Scaffolds to Enhance Cardiac Differentiation of Embryoid Bodies. *Acta Biomater.* **2016**, *31*, 134–143.

(287) Naseer, S. M.; Manbachi, A.; Samandari, M.; Walch, P.; Gao, Y.; Zhang, Y. S.; Davoudi, F.; Wang, W.; Abrinia, K.; Cooper, J. M.; Khademhosseini, A.; Shin, S. R. Surface Acoustic Waves Induced Micropatterning of Cells in Gelatin Methacryloyl (GelMA) Hydrogels. *Biofabrication* **2017**, *9* (1), No. 015020.

(288) Sun, T.; Shi, Q.; Huang, Q.; Wang, H.; Xiong, X.; Hu, C.; Fukuda, T. Magnetic Alginate Microfibers as Scaffolding Elements for the Fabrication of Microvascular-Like Structures. *Acta Biomater.* **2018**, *66*, 272–281.

(289) Ito, A.; Ino, K.; Hayashida, M.; Kobayashi, T.; Matsunuma, H.; Kagami, H.; Ueda, M.; Honda, H. Novel Methodology for Fabrication of Tissue-Engineered Tubular Constructs Using Magnetite Nanoparticles and Magnetic Force. *Tissue Eng.* **2005**, *11* (9–10), 1553–1561.

(290) Bonfrate, V.; Manno, D.; Serra, A.; Salvatore, L.; Sannino, A.; Buccolieri, A.; Serra, T.; Giancane, G. Enhanced Electrical Conductivity of Collagen Films through Long-Range Aligned Iron Oxide Nanoparticles. *J. Colloid Interface Sci.* **2017**, *501*, 185–191.

(291) Vannozzi, L.; Yasa, I. C.; Ceylan, H.; Menciassi, A.; Ricotti, L.; Sitti, M. Self-Folded Hydrogel Tubes for Implantable Muscular Tissue Scaffolds. *Macromol. Biosci.* **2018**, *18* (4), 1700377.

(292) Liu, Y.; Xu, K.; Chang, Q.; Darabi, M. A.; Lin, B.; Zhong, W.; Xing, M. Highly Flexible and Resilient Elastin Hybrid Cryogels with Shape Memory, Injectability, Conductivity, and Magnetic Responsive Properties. *Adv. Mater.* **2016**, *28* (35), 7758–7767.

(293) Golob, M.; Moss, R. L.; Chesler, N. C. Cardiac Tissue Structure, Properties, and Performance: A Materials Science Perspective. *Ann. Biomed. Eng.* **2014**, *42* (10), 2003–2013.

(294) Leipzig, N. D.; Shoichet, M. S. The Effect of Substrate Stiffness on Adult Neural Stem Cell Behavior. *Biomaterials* **2009**, *30* (36), 6867–6878.

(295) Madhusudanan, P.; Raju, G.; Shankarappa, S. Hydrogel Systems and Their Role in Neural Tissue Engineering. *J. R. Soc., Interface* **2020**, *17* (162), 20190505.

(296) Antman-Passig, M.; Shefi, O. Remote Magnetic Orientation of 3D Collagen Hydrogels for Directed Neuronal Regeneration. *Nano Lett.* **2016**, *16* (4), 2567–2573.

(297) Pisanic, T. R.; Blackwell, J. D.; Shubayev, V. I.; Fiñones, R. R.; Jin, S. Nanotoxicity of Iron Oxide Nanoparticle Internalization in Growing Neurons. *Biomaterials* **2007**, *28* (16), 2572–2581.

(298) Vijayavenkataraman, S. Nerve Guide Conduits for Peripheral Nerve Injury Repair: A Review on Design, Materials and Fabrication Methods. *Acta Biomater.* **2020**, *106*, 54–69.

(299) Santos, L.; Silva, M.; Gonçalves, A. I.; Pesqueira, T.; Rodrigues, M. T.; Gomes, M. E. *In Vitro* and *In Vivo* Assessment of Magnetically Actuated Biomaterials and Prospects in Tendon Healing. *Nanomedicine* **2016**, *11* (9), 1107–1122.

(300) Pavón, J. J.; Allain, J. P.; Verma, D.; Echeverry-Rendón, M.; Cooper, C. L.; Reece, L. M.; Shetty, A. R.; Tomar, V. *In Situ* Study Unravels Bio-Nanomechanical Behavior in a Magnetic Bacterial Nanocellulose (MBNC) Hydrogel for Neuro-Endovascular Reconstruction. *Macromol. Biosci.* **2019**, *19* (2), 1800225.

(301) Skaat, H.; Ziv-Polat, O.; Shahar, A.; Last, D.; Mardor, Y.; Margel, S. Magnetic Scaffolds Enriched with Bioactive Nanoparticles for Tissue Engineering. *Adv. Healthcare Mater.* **2012**, *1* (2), 168–171.

(302) Panda, R. K.; Muduli, R.; Behera, D. Electric and Magnetic Properties of Bi Substituted Cobalt Ferrite Nanoparticles: Evolution of Grain Effect. *J. Alloys Compd.* **2015**, *634*, 239–245.

(303) Ramírez-acosta, C. M.; Cifuentes, J.; Castellanos, M. C.; Moreno, R. J.; Muñoz-camargo, C.; Cruz, J. C.; Reyes, L. H. Ph-Responsive, Cell-Penetrating, Core/Shell Magnetite/Silver Nanoparticles for the Delivery of Plasmids: Preparation, Characterization, and Preliminary *In Vitro* Evaluation. *Pharmaceutics* **2020**, *12* (6), 561.

(304) Goudou, S. R.; Yasa, I. C.; Hu, X.; Ceylan, H.; Hu, W.; Sitti, M. Biodegradable Untethered Magnetic Hydrogel Milli-Grippers. *Adv. Funct. Mater.* **2020**, *30*, 2004975.